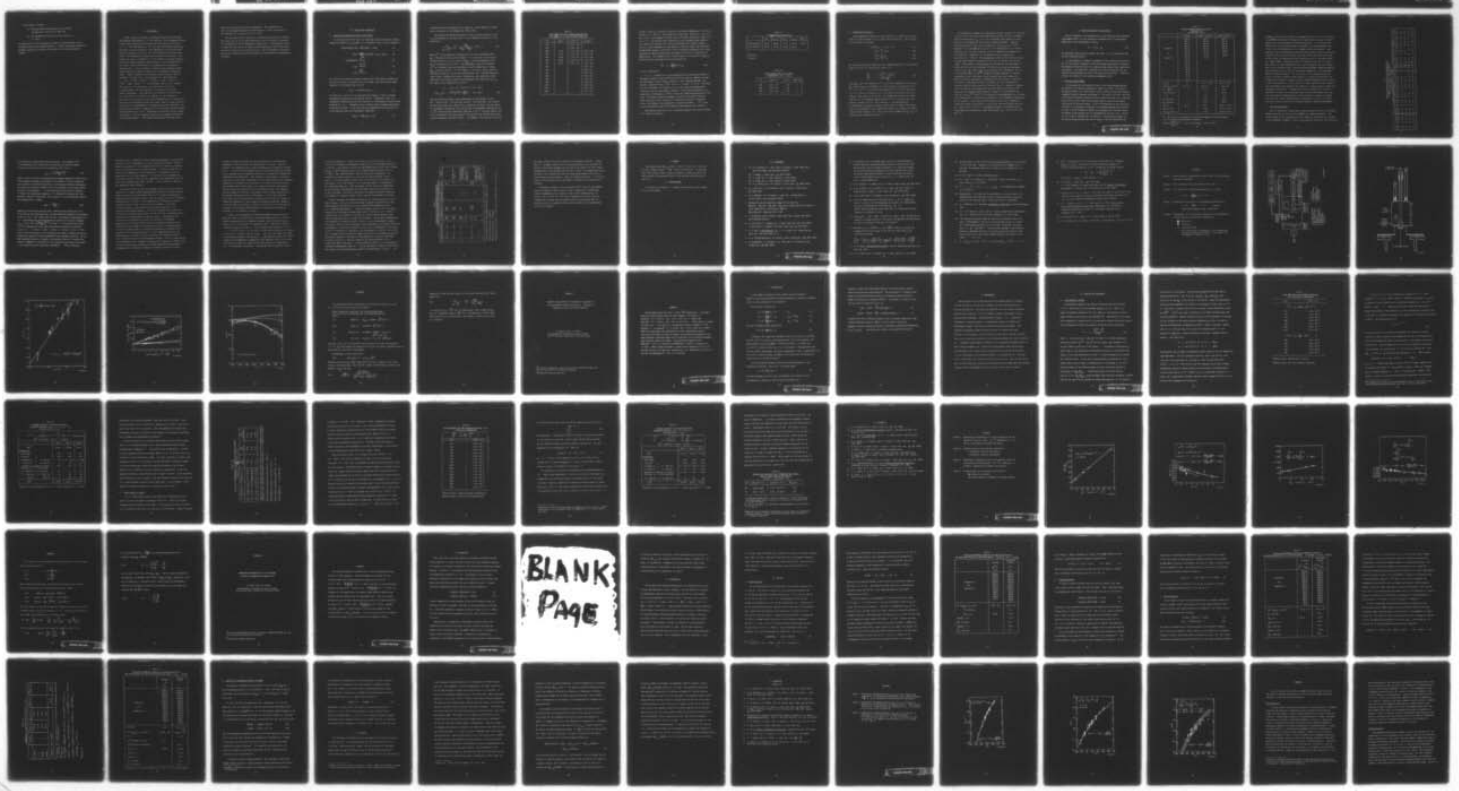
AD-A056 022 SRI INTERNATIONAL MENLO PARK CA F/G 7/4
THE ABSOLUTE MEASUREMENT OF RATE CONSTANTS FOR SOME KEY REACTIO--ETC(U)
APR 78 D M GOLDEN, M ROSSI, G P SMITH F44620-75-C-0067
UNCLASSIFIED AFOSR-TR-78-1068 NL

1 OF 2
AD
A056022





AD A056022

AD No.
DDC FILE COPY

-1068

LEVEL II

Approved for public release;
distribution unlimited.

Final Report
Covering the Period 1 January 1975 through 28 February 1978

April 1978

THE ABSOLUTE MEASUREMENT OF RATE CONSTANTS FOR SOME KEY REACTIONS INVOLVING FREE RADICALS

DDC
RECEIVED
JUL 6 1976
F

By: DAVID M. GOLDEN, MICHEL ROSSI, GREGORY P. SMITH, KARAN E. LEWIS, SIDNEY W. BENSON, MIRIAM LEV-ON, STEPHEN E. STEIN, and FRIEDHELM ZABEL

Prepared for:

Air Force Office of Scientific Research
Building 410
Bolling Air Force Base
Washington, D.C. 20332

Attention: Dr. Robert A. Osteryoung

AFOSR Contract F44620-75-C-0067

SRI Project PYU-4039

This document has been approved for public release and sale; its distribution is unlimited.

STANFORD RESEARCH INSTITUTE
Menlo Park, California 94025 · U.S.A.

78 06 27 099

STANFORD RESEARCH INSTITUTE
Menlo Park California 94025 · U S A

Final Report
Covering the Period 1 January 1975 through 28 February 1978

(11) April 78

(18) AFOSR (19) TR-78-1068

(6)

THE ABSOLUTE MEASUREMENT OF RATE CONSTANTS FOR SOME KEY REACTIONS INVOLVING FREE RADICALS,

(9) Final rept. 1 Jan 75-28 Feb 78,

(10) By: DAVID M. GOLDEN, MICHEL ROSSI, GREGORY P. SMITH, KARAN E. LEWIS, SIDNEY W. BENSON, MIRIAM LEV-ON, STEPHEN E. STEIN, and FRIEDHELM ZABEL

DDC
RECEIVED
JUL 6 1978
F

(12) 165 p.

Prepared for:

Air Force Office of Scientific Research
Building 410
Bolling Air Force Base
Washington, D.C. 20332

Attention: Dr. Robert A. Osteryoung

(15) AFOSR Contract F44620-75-C-0067

SRI Project PYU-4039

Approved by:

MARION E. HILL, *Director*
Chemistry Laboratory

P. J. JORGENSEN, *Vice President*
Physical and Life Sciences

78 06 27 099
410 281 slt

INTRODUCTION

This final report is part of a continuing effort to study and understand free radical processes of importance in combustion and other chemical systems.

We include two preprints of papers, Chapters 1 and 2, submitted to the Journal of the American Chemical Society. These papers describe our recent work on combination reactions and heats of formation of stabilized radicals.

Chapter 3 is a preprint of a paper submitted to the International Journal of Chemical Kinetics. This paper is complementary to our initial work on multiphoton dissociation, which was published (J. Amer. Chem. Soc., 99, 8063 (1977)) and is included as Chapter 4).

Chapter 5 represents work of both practical importance for stratospheric modeling, as well as theoretical importance with respect to understanding the details of radical-radical interactions. This paper recently appeared in the International Journal of Chemical Kinetics, 10, 489 (1978).

Chapter 6 has been submitted to the Journal of Chemical Physics. This paper illustrates our radical combination model for the prototypical methyl radical combination.

ACCESSION for
NTIS White Section
DDC Buff Section
UNANNOUNCED
JUSTIFICATION
BY
DISTRIBUTION/AVAILABILITY CODES
Dist. AVAIL. and/or SPECIAL
A

PRECEDING PAGE BLANK

CONTENTS

INTRODUCTION iii

Chapter 1 THE EQUILIBRIUM CONSTANT AND RATE CONSTANT FOR ALLYL RADICAL RECOMBINATION IN THE GAS PHASE. . . . 1

Abstract 3
I Introduction 5
II Experimental 7
III Results and Discussion 9
A. Equilibrium and Kinetics (844 ≤ 1061). . . 9
B. Recombination Kinetics 10
IV RRKM CALCULATIONS AND DISCUSSION 17
1. Vibrational Model. 17
2. The Rotational Model 19
V Summary 27
VI Acknowledgment 27
VII References (Chapter 1) 29

Appendix 39

Chapter 2 ABSOLUTE RATE CONSTANTS FOR METATHESIS REACTIONS OF ALLYL AND BENZYL RADICALS WITH HI(DI). THE HEAT OF FORMATION OF ALLYL AND BENZYL RADICALS 41

Abstract 43
I Introduction 45
II Experimental 47
III Results and Discussion 49
A. Allyl Radical + HI(DI) 49
B. Benzyl Radical + HI(DI) 53
IV References (Chapter 2) 61

Appendix 69

Chapter 3 HOMOGENEOUS DECOMPOSITION OF VINYL ETHERS. THE HEAT OF FORMATION OF ETHANAL-2-YL 71

Abstract 73
I Introduction 75
II Experimental 76
III Results 77
A. Ethylvinylether 77
B. t-Butylvinylether 80
C. Benzylvinylether 81
D. Reactions of 2-Ethanalyl Radical ($\dot{C}H_2CHO$) 86
IV Discussion 87
V References (Chapter 3) 91

Appendix 97

PRECEDING PAGE BLANK

Chapter 4 INFRARED PHOTODECOMPOSITION OF ETHYL VINYL ETHER. A CHEMICAL PROBE OF MULTIPHOTON DYNAMICS 103

Chapter 5 APPLICATION OF RRKM THEORY OF THE REACTIONS $OH + NO_2 + N_2 \rightarrow HONO_2 + N_2$ (1) and $ClO + NO_2 + N_2 \rightarrow ClONO_2 + N_2$ (2); A Modified Gorin Model Transition State 105

Abstract 105
Introduction 107
Background 109
Details of the Calculation 110
Results 115
Extrapolation of the Model to $ClONO_2$ 119
Conclusions 123
Acknowledgments 123
References (Chapter 5). 125

Appendix: PARAMETERS FOR NITRIC ACID $G(E^+)$ AND $N(E^*)$ CALCULATION 133

Chapter 6 A MODIFIED GORIN TRANSITION STATE IN BOND SCISSION REACTIONS. AN APPLICATION TO ETHANE DISSOCIATION . 135

Abstract 137
I Introduction 139
II Background 140
III Details of the Calculations 143
The RRKM Model 143
The Transition State 144
Chemical Activation 147
IV Results and Discussion 148
High-Pressure Rate Constants (Hindrance) . . . 148
Pressure Dependence ($<\Delta E>$ 152
Chemical Activation 153
V Conclusions 156
Acknowledgments 159

References (Chapter 6). 161

FIGURES

Chapter 1

1 BLOCK DIAGRAM FOR EXPERIMENTAL SETUP OF VLPP (Very Low-Pressure Pyrolysis) EXPERIMENT . . . 34

2 VERY LOW-PRESSURE PYROLYSIS REACTOR (133.5 cm^3) . . 35

3 VAN'T HOFF PLOT OF EQUILIBRIUM CONSTANT $K_{r,d} = k_r/k_d$ 36

4 BRAUMAN PLOT FOR THE RECOMBINATION REACTION k_r AT 625 K 37

5 EXPERIMENTAL AND CALCULATED RATE CONSTANTS k_r FOR RECOMBINATION OF ALLYL RADICALS IN FUNCTION OF TEMPERATURE 38

Chapter 2

1 EXPERIMENTAL DETERMINATION OF k_3 FOR THE METATHESIS REACTION ALLYL$^{\cdot}$ + DI → PROPYLENE-d_1 + I$^{\cdot}$ AT 1014 K 64

2 ARRHENIUS PLOT OF RATE CONSTANTS FROM TABLE I . . . 65

3 EXPERIMENTAL DETERMINATION OF k_3 FOR THE METATHESIS REACTION BENZYL$^{\cdot}$ + DI → TOLUENE-d_1 + I$^{\cdot}$ AT 989 K 66

4 ARRHENIUS PLOT OF RATE CONSTANTS FROM TABLE IV . . 67

Chapter 3

1 UNIMOLECULAR DECOMPOSITION RATES (k_{uni}/s^{-1}) AS A FUNCTION OF TEMPERATURE FOR THE MOLECULAR ELIMINATION MODE OF ETHYLVINYLETHER 94

2 UNIMOLECULAR DECOMPOSITION RATE (k_{uni}/s^{-1}) AS A FUNCTION OF TEMPERATURE FOR THE MOLECULAR ELIMINATION MODE OF t-BUTYLVINYLETHER 95

3 UNIMOLECULAR DECOMPOSITION RATES (k_{uni}/s^{-1}) AS A FUNCTION OF TEMPERATURE FOR THE BOND FISSION IN BENZYLVINYLETHER 96

Chapter 5

1 EFFECTIVE BIMOLECULAR RATE CONSTANTS FOR NITRIC ACID RECOMBINATION VERSUS PRESSURE AT 296 K. . . . 128

2 PLOTS SIMILAR TO FIGURE 1 FOR OTHER TEMPERATURES. . 129

3 RATES FOR REACTIONS (1) AND (2) AS A FUNCTION OF THE ATMOSPHERIC TEMPERATURE AND PRESSURE PROFILE. . 130

4 PERCENTAGE DECLINE OF THE PREDICTED RRKM RATE CONSTANT FROM A VALUE EXTRAPOLATED FROM THE LOW-PRESSURE LIMIT FOR THREE CALCULATIONS DESCRIBED IN TABLE I 131

Chapter 6

1 HIGH-PRESSURE METHYL RADICAL RECOMBINATION RATE CONSTANTS AT VARIOUS TEMPERATURES 166

2 PRESSURE DEPENDENCE OF RATE CONSTANTS 167

3 ETHANE DECOMPOSITION RATE $k(E)$ AS A FUNCTION OF EXCESS MOLECULAR ENERGY $E-E_0$. 168

4 PRESSURE DEPENDENCE OF THE RELATIVE YIELDS FOR REACTIONS (1) DECOMPOSITION AND (2) STABILIZATION FOR CHEMICAL ACTIVATION 169

TABLES

Chapter 1

I EQUILIBRIUM AND RATE CONSTANT MEASUREMENTS $2C_3H_5\cdot \underset{k_d}{\overset{k_r}{\rightleftarrows}} C_6H_{10}$ IN THE GAS-PHASE USING VLPP 11

II THERMOCHEMICAL QUANTITIES 13

III RATE CONSTANTS FOR ALLYL RADICAL RECOMBINATION AT T = 625 K 13

IV MOLECULAR PARAMETERS FOR RRKM-CALCULATIONS: 1,5-HEXADIENE (BA) 18

V RESULTS OF RRKM CALCULATIONS FOR THE BOND-BREAKING PROCESS 1,5-HEXADIENE → 2 ALLYL RADICAL AT SELECTED TEMPERATURES 20

VI EXPERIMENTAL AND CALCULATED RECOMBINATION RATE CONSTANTS FOR RADICAL RECOMBINATION REACTIONS INVOLVING STABILIZED RADICALS 25

Chapter 2

I RATE CONSTANTS FOR METATHESIS REACTIONS AS A FUNCTION OF TEMPERATURE 51

II ESTIMATED ENTROPY OF ACTIVATION FOR THE METATHESIS REACTION, $C_3H_6 + I\cdot \rightarrow C_3H_5\cdot + HI$ 53

III KINETIC AND THERMOCHEMICAL PARAMETERS FOR THE EQUILIBRIUM, PROPYLENE + $I\cdot \underset{k_3}{\overset{k_4}{\rightleftarrows}}$ ALLYL$\cdot$ + HI 55

IV RATE CONSTANTS FOR THE METATHESIS REACTION AS A FUNCTION OF TEMPERATURE 57

V ESTIMATED ENTROPY OF ACTIVATION FOR THE METATHESIS REACTION, $C_7H_7\cdot + DI \rightarrow C_7H_7D + I\cdot$ 59

VI MEASURED AND CALCULATED RATE PARAMETERS AND OVERALL ENTROPY CHANGE FOR THE EQUILIBRIUM, TOLUENE + $I\cdot \underset{k_3}{\overset{k_4}{\rightleftarrows}}$ BENZYL$\cdot$ + HI 60

Chapter 3

I MOLECULAR PARAMETERS ENTERING THE RRKM-CALCULATION OF THE TRETRO-ENE REACTION OF ETHYLVINYLETHER 79

II MOLECULAR PARAMETERS ENTERING THE RRKM-CALCULATION OF RETRO-ENE REACTION OF t-BUTYLVINYLETHER. 82

III THERMOCHEMICAL QUANTITIES 84

IV MOLECULAR PARAMETERS ENTERING THE RRKM-CALCULATION OF THE RATE CONSTANT FOR THE REACTION BENZYLVINYLETHER → $C_7H_7\cdot$ + $\cdot CH_2CHO$ 85

Chapter 5

I RRKM HINDERED GORIN MODEL PARAMETERS 116

Chapter 6

I PARAMETERS 145

II MODEL PARAMETERS FOR ETHANE DECOMPOSITION 152

Chapter 1

THE EQUILIBRIUM CONSTANT AND RATE CONSTANT FOR ALLYL RADICAL RECOMBINATION IN THE GAS PHASE[†]

M. Rossi,[‡] K. D. King,[‡‡] and D. M. Golden

Thermochemistry and Chemical Kinetics Group

SRI INTERNATIONAL

Menlo Park, California 94025

[†] This work was supported, in part, by contract F44620-75-C-0067 with the Air Force Office of Scientific Research.

[‡] Postdoctoral Research Associate.

[‡‡] On leave from: Department of Chemical Engineering, University of Adelaide, N.S.W. 5001, Australia.

ABSTRACT

The equilibrium and recombination 2 allyl $\rightleftarrows$ 1,5-hexadiene at $\langle T \rangle$ = 950 K, and the recombination reaction at T = 625 K have been studied in a VLPP (very low-pressure pyrolysis) apparatus. The van't Hoff plot yields $\ln(K_{r,d}/M^{-1}) = \frac{-33.50 + 10.71}{R} + \frac{54540}{RT}$, which gives ΔH_f^0(allyl) = 38.3 ± 1.5 kcal/mol, a bond dissociation energy BDE(C_3H_5–H) = 85.5 ± 1.5 kcal/mol and an allyl resonance energy ARE = 12.5 ± 2.0 kcal/mol. The recombination rate constant k_r at $\langle T \rangle$ = 900 K is found to be (1.90 ± .80) * 10^9 M^{-1} s^{-1}, and at T = 625 K, k_r is (6.50 ± 1.0) * 10^9 M^{-1} s^{-1}. RRKM calculations indicate a degree of fall-off k_r/k_r^∞ = .56 at 625 K and .078 at 900 K.

PRECEDING PAGE BLANK

I INTRODUCTION

Allyl radical is the prototype of a resonance stabilized radical whose thermochemistry and reactivity in the gas phase has been the subject of numerous investigations.[1-3] There has been considerable controversy[1a] about the correct value of the heat of formation and the allyl resonance energy (ARE).[4] Quoted values for ARE range from 10 to 25 kcal/mol, but recent experimental values for ARE now seem to fall around 11 $\pm$ 2 kcal/mol. The correct value for ARE is certainly fundamental for a thorough understanding of chemical bonding and ground state properties of conjugated radicals. Theoretical calculations on open-shell species, such as allyl radical, are hampered somewhat by intrinsic difficulties,[5] but despite this problem, the Generalized Valence-Bond (GVB) concept appears to be quite successful.[6]

Furthermore, the need for the accurate determination of radical-radical recombination rate constants has been clearly pointed out.[7] *Absolute rate* constants for many disproportionation reactions and radical-molecule reactions are critically dependent on the rates for combination of the radicals, since many rate constants have been measured relative to the radical combination rate constants. Thermochemical parameters of free radicals can also be obtained from the Arrhenius parameters of free radical combination in cases where the reverse reaction (dissociation) has been studied. Radical recombination rate studies in the case of resonance stabilized radicals are sparse and the rates for allyl and 2-methallyl recombination have only been measured at ambient temperature by flash photolysis.[8,9] It seemed appropriate to extend the rate measurements in order to get a reliable set of Arrhenius parameters for allyl recombination at higher temperatures where this reaction is the prototype for important chain terminations.

PRECEDING PAGE BLANK

In this paper, we report:

(A) The equilibrium and kinetics of allyl radical recombination at $844 \leq T/K \leq 1061$, and

(B) The recombination kinetics of allyl radical at $T = 625$ K.

The method used is Very Low-Pressure Pyrolysis (VLPP) employing a newly designed molecular beam sampling apparatus thereby eliminating complicated secondary reactions of radicals on the walls of the mass spectrometry chamber.[10]

II EXPERIMENTAL

Figure 1 depicts the general experimental design of the molecular beam-sampling VLPP apparatus. A valve-capillary tube arrangement delivers a controlled, steady flow of reactant gas to the reactor (typically, 10^{13} - 5 * 10^{16} molecules/sec). In cases where the reactant gas had an unsuitably low vapor pressure at room temperature, the whole gas inlet system was placed in a hot box. The flow then enters the low-pressure reactor, and subsequently effuses from the reactor exit aperture. The product gas flux is collimated (< 1 cm in diameter) on passing through a differential pumping chamber, modulated with a rotating chopper wheel, and finally ionized and detected by a quadrupole mass spectrometer (Finnigan 400). A lock-in amplifier (Princeton Applied Research Model 1284) separates the modulated signal from the unmodulated background signal. Figure 2 displays the two-aperture reactor design. Reactor parameters are given by (B = large aperture, S = small aperture): $V = .134\ \ell$, $\omega = 4982 * (T/M)^{1/2}\ s^{-1}$, $k_e^M(B) = 2.5571 * (T/M)^{1/2}\ s^{-1}$, $k_e^M(S) = .2088 * (T/M)^{1/2}\ s^{-1}$. The all-quartz reactor (i.e., Knudsen cell) encased in a nickel block was heated with an electrical clam-shell heater, and the temperature was measured by a chromel-alumel thermocouple. The experiments were carried out by monitoring mass spectrometric intensities as a function of the temperature, the flow rate of the gas into the reactor (F_M^i/molecules s^{-1}) and the residence time of the molecules within the reactor (small or large aperture).[11] Diallyloxalate ($C_3H_5OCOCOOC_3H_5$) was purchased from Pfaltz and Bauer, Inc., and was purified simply by pumping off all lower boiling fractions (mainly CH_2=CH-CH_2-CHO) at 10^{-3} torr. GC-MS-analysis revealed no further impurities present. 3,3′-azo-1-propene ($C_3H_5N_2C_3H_5$) was prepared according to literature procedures.[12] (The samples contained H_2O and diethylether

which did not interfere with our measurements. The concentration of 3,3′-azo-1-propene was measured by monitoring m/e = 28 in the absence of the molecular ion of $C_3H_5N_2C_3H_5$ at m/e = 110.)

The reactions were all studied in a reaction vessel which was "cleaned" after every set of two or three experiments (flow rate studies) by passing air through the vessel at temperatures around 1100 K. This procedure served to remove the soot which was formed at high temperatures (1100 K) and could be seen on the walls of the reaction vessel. Such a procedure was necessary because the carbon coating greatly enhanced the interference by heterogeneous reactions.

III RESULTS AND DISCUSSION

A. Equilibrium and Kinetics ($844 \leq T/K \leq 1061$)

In the range $844 \leq T/K \leq 1061$, the following reaction system was studied using diallyloxalate, $C_8H_{10}O_4$(DAO), as a convenient source of allyl radicals:[13]

$$C_3H_5OCOCOOC_3H_5(DAO) \xrightarrow{k_1} 2C_3H_5\cdot + 2CO_2 \qquad (1)$$

$$2C_3H_5\cdot \underset{k_d}{\overset{k_r}{\rightleftharpoons}} C_6H_{10}(BA); \quad K_{r,d} = k_r/k_d \qquad (2)$$

$$C_3H_5OCOCOOC_3H_5 \xrightarrow{k_e^{DAO}} \qquad (3)$$

$$C_3H_5\cdot \xrightarrow{k_e^{C_3H_5\cdot}} \qquad (4)$$

$$C_6H_{10} \xrightarrow{k_e^{BA}} \qquad (5)$$

CO_2 served as an internal standard or monitor for allyl radical, because for every allyl radical, a molecule of CO_2 was formed. This was verified experimentally by "titrating" $C_3H_5\cdot$ with DI:

$$C_3H_5\cdot + DI \xrightarrow{k_3} C_3H_5D + I\cdot \qquad (6)$$

For $[DI]_{ss} \geq 5 * 10^{-8}$ M, it was verified that $[C_3H_5D]_{ss} = [CO_2]_{ss}$ through independent calibrations with propylene and CO_2. Furthermore, this is an experimental demonstration that the formation of 1,5-hexadiene proceeds through recombination of intermediate allyl radicals and not through unimolecular elimination from DAO. It was found that the disproportionation reaction (7) is not important under our experimental conditions:

$$2C_3H_5\cdot \xrightarrow{k_7} C_3H_4 + C_3H_6 \qquad (7)$$

a conclusion further confirmed by the absence of sizable amounts of allene[7] and by the results of the Brauman plot (Vide infra).

The steady-state kinetic expression for the reaction system (1) to (5) in a low-pressure stirred flow reactor is (see Appendix for details of the derivation):

$$\frac{k_r}{k_d + k_e^{BA}} = k_e^{BA} * \frac{2R^0_{BA}}{(R^0_{CO_2} - 2R^0_{BA})^2} \equiv k_e^{BA} * y \qquad (8)$$

where k_e^{BA} is the escape rate constant (in s^{-1}) for 1,5-hexadiene (BA), R^0_{BA} is the specific flow rate (in moles s^{-1} l^{-1}) of BA out of the reactor (as monitored by m/e = 67 or 54)[14] and $R^0_{CO_2}$ is the corresponding flow of CO_2 (as monitored by m/e = 44).[14] Two experiments, each with different k_e^{BA} (or residence time) were performed at a given temperature, varying F^I_{DAO} typically from 10^{15} - 4 * 10^{16} molec s^{-1}, so that k_r and k_d could be determined separately, but this was possible only over a limited temperature range. Table I displays the results obtained over the temperature range (844-1061 K) and Figure 3 shows the corresponding van't Hoff plot for $K_{r,d}$. The results can be summarized as follows:

$$k_r = (1.9 \pm .8) * 10^9 \ M^{-1} \ s^{-1}; \ \langle T \rangle = 880 \ K$$

$$\ln(K_{r,d}/M^{-1}) = \frac{-33.5 + 10.71}{R} + \frac{54540}{RT}; \qquad \langle T \rangle = 950 \ K \qquad (9)[15]$$

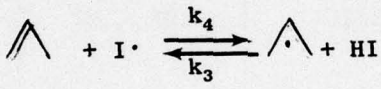
Thus this method provides a direct measurement of equilibrium (2) with ΔS^0 = -33.5 eu, ΔE^0 = -54.5 kcal/mol and ΔH^0 = -56.4 kcal/mol. The variable and sometimes large error limits of $K_{r,d}$ displayed in Figure 3 are the result of the algebraic separation of k_r and k_d from two independent experimental sets of k_e^{BA} (large and small apertures) according to (8).[16] The heat capacity data for 1,5-hexadiene[17] and allyl radical[18] are such that ΔS^0 and ΔH^0 show no temperature dependence from 300 to 950 K. With ΔH^0_f(BA) = 20.2 kcal/mol (Table II),

Table I

EQUILIBRIUM AND RATE CONSTANT MEASUREMENTS
$2C_3H_5 \underset{k_d}{\overset{k_r}{\rightleftharpoons}} C_6H_{10}$ IN THE GAS-PHASE USING VLPP

T/K	k_d/s^{-1}	$k_r/M^{-1}\ s^{-1}$	$K_{r,d}/M^{-1}$
844		$2.17 * 10^9$	
845		$2.05 * 10^9$	
858	2.72	$1.04 * 10^9$	$3.83 * 10^8$
888	3.33	$1.06 * 10^9$	$3.19 * 10^8$
895	18.40	$2.40 * 10^9$	$1.31 * 10^8$
900	18.55	$3.24 * 10^9$	$1.75 * 10^8$
922	13.75	$1.53 * 10^9$	$1.11 * 10^8$
927			$7.30 * 10^7$
946			$6.81 * 10^7$
975			$2.63 * 10^7$
988			$1.94 * 10^7$
988			$1.42 * 10^7$
990			$1.63 * 10^7$
991			$1.60 * 10^7$
1057			$1.53 * 10^6$
1061			$9.51 * 10^5$

and $\Delta H^0 = -56.4 \pm 1.0$ kcal/mol (Figure 3), one obtains ΔH^0_f(allyl,g) = 38.3 ± 1.5 kcal/mol at T = 300 K.[19] The second law entropy, $\Delta S^0 = -33.50$ e.u. ((9), standard state: 1 atm) compares favorably with an a priori estimate of −34.80 ± 1.0 e.u..[17,18] The present result indicates an allyl resonance energy (ARE) of 12.5 kcal/mol on the basis of a value of 98.0 kcal/mol for BDE of propane. This is in good agreement with the reported literature values from shock-tube decomposition studies of olefins[1b,c,d] and in excellent agreement with a value determined by photoionization mass spectrometry[2] of 38.4 ± 1.7 kcal/mol for ΔH^0_f(allyl,g). The agreement with a value of 39.10 ± 1.0 kcal/mol for $\Delta H^0_{f,300}$ derived from the measurement of the equilibrium (10)



(10)

is also noteworthy.[20]

It was pointed out in the Introduction that the earlier study[1a] of the present system (1)-(5) yielded values for $K_{r,d}$ and k_r, somewhat too high, thus providing a value of $\Delta H^0_{f,300}$(allyl,g) = 41.2 kcal/mol and ARE = 9.6 kcal/mol, together with $k_r = 6.2 * 10^9$ M^{-1} s^{-1} at 913 K to 1063 K. The reason for this discrepancy was found to lie in a wall-catalyzed recombination reaction in the mass spectrometry chamber.[10] The present experimental configuration of the apparatus, however, rules out complicating reactions of this kind. The apparent excellent agreement with GVB calculations[6] should be taken "cum grano salis," because the "stabilization energy" is referred to the total energy of the hypothetical canonical structure  , which is not an observable species and therefore experimentally not accessible.

The measured value for k_r (9) is discussed together with values obtained at T = 625 K in section B.

Table II

THERMOCHEMICAL QUANTITIES

	S^{o}_{300} [a]	$C_{p,300}$ [a]	$C_{p,625}$ [a]	$C_{p,950}$ [a]	$\Delta H^{o}_{f,300}$ [b]
1,5-hexadiene[15]	89.40	28.80	50.10	62.44	20.20
allyl radical[17]	62.10	14.60	24.95	30.97	

[a] cal/K mol.

[b] kcal/mol.

Table III

RATE CONSTANTS FOR ALLYL RADICAL RECOMBINATION AT T = 625 K

T/K	$k_r/M^{-1}\ s^{-1}$	k_w/s^{-1}	Exp't No.
625	4.31×10^{9}	3.81	1
625	8.06×10^{9}	.58	2
625	7.12×10^{9}	.93	3

B. Recombination Kinetics

The recombination kinetics of allyl radical at T = 625 K were studied using 3,3′-azo-1-propene (Az) as a source of allyl radicals. The following reaction scheme was assumed:

$$C_3H_5N_2C_3H_5 \rightarrow 2C_3H_5\cdot + N_2 \quad (11)$$

$$2C_3H_5\cdot \xrightarrow{k_r} C_6H_{10} \quad (12)$$

$$C_3H_5\cdot \xrightarrow{k_w} \quad (13)$$

$$C_3H_5\cdot \xrightarrow{k_e} C_3H_5\cdot \quad (14)$$

The steady-state kinetic expression (the Brauman equation) for the reaction scheme (11)-(14) in a stirred-flow reactor is:[21]

$$\frac{F^i_{Az}}{F^o_{BA}} = 1 + \frac{(k_e^{C_3H_5\cdot} + k_w)V^{1/2}}{2k_r^{1/2}\, F^{o\,1/2}_{BA}} \quad (15)$$

where F^i_{AZ} is the flow (molecules s^{-1}) of 3,3′-azo-1-propene into the reactor, F^o_{BA} is the flow of 1,5-hexadiene out of the reactor (as monitored at m/e = 67 or 54), $k_e^{C_3H_5\cdot}$ is the escape rate constant (s^{-1}) of allyl radical and k_v (s^{-1}) is the rate constant for a first-order loss process of the allyl radicals (most likely on the walls). The temperature of 625 K was chosen such that Az was decomposed almost quantitatively, so that the mass spectrometric intensity of m/e = 28 (corrected for the contribution of 1,5-hexadiene) reflected the amount of allyl radicals found in the reactor (F^i_{Az}) after assessment of the calibration constant, α_{N_2} (using air), which relates the MS intensity (m/e = 28) to the rate of production ($F^i_{N_2} = F^o_{N_2}$) or (steady state) concentration of N_2.[22]

An alternative procedure for determination of F^i_{Az} consisted of "titration" of $C_3H_5\cdot$ with DI (6), while monitoring the MS intensity of m/e = 43 (C_3H_5D) under the condition $[DI]_{ss} \rightarrow \infty$, so that the amount C_3H_5D formed was representative of the amount of allyl radical originally present. However, the concentration of $C_3H_5\cdot$ had to be kept low ($[C_3H_5\cdot]_{ss} \cong 3.7 * 10^{13}$ molecules ℓ^{-1}, corresponding to $F^i_{Az} \cong 5 * 10^{13}$ molecules s^{-1} at T = 625 K), and $[DI]_{ss}$ had to be quite high in view of the smaller rate constant for D-transfer (k_3), compared to the recombination rate constant (k_r): $k_r/k_3 \cong 60$ at T = 625 K.[20] The disappearance of BA in favor of the increase in C_3H_5D could readily be observed at m/e = 62, 54 (for BA), and 43 (for C_3H_5D). Both methods of assessing F^i_{Az} gave essentially the same result to within 15%, but the first procedure was used for all reported experiments. A plot of F^i_{Az}/F^0_{BA} versus $1/F^{0\ 1/2}_{BA}$ gave straight lines according to (15) for two different values of $k_e^{C_3H_5\cdot}$ through the common intercept 1.0 (within experimental error, see Figure 4) and indicated that allyl radical was unable to abstract hydrogen in a disproportionation reaction, in line with the results of gas-phase pyrolysis experiments in static high-pressure reaction vessels[3,7] and the results of Section A (eqn. 7). However, it appears that allyl radical does undergo wall reactions, because the ratio of the slopes for the large and small aperture in Figure 4 is considerably less than the ratio $k_e^{C_3H_5\cdot}(B)/k_e^{C_3H_5\cdot}(S)$ indicating a non-negligible term k_w(first order loss process of allyl radical according to (13), presumably taking place on the walls[23]). The results of the pyrolysis of 3,3'-azo-1-propene are displayed in Table II from which it can be seen that the average value for $k_r = (6.50 \pm 1.0) * 10^9\ M^{-1}\ s^{-1}$ corresponds closely to the one derived at room temperature using kinetic flash spectroscopy[8] ($k_r = (8.50 \pm 3.0) * 10^9\ M^{-1}\ s^{-1}$).

IV RRKM CALCULATIONS AND DISCUSSION

The rate constants for recombination of allyl radicals were calculated using RRKM theory[24] for the unimolecular decomposition of 1,5-hexadiene making use of the thermodynamic relation:

$$k_r = K_{r,d} * k_d \qquad (16)$$

Two different transition-state models were used: (1) the vibrational and (2) the rotational model.[25]

In the absence of a complete assignment of the vibrational spectrum of BA, the vibrational frequencies of BA were deduced from those of propylene. The moments of inertia for BA were computed using standard bond lengths and bond angles. The vibrational frequencies were then adjusted so that the computed entropy matched the value from group additivity data.[17] Table IV displays the results of the frequency assignments for BA.

1. The Vibrational Model

In this model for the transition state of the bond-breaking process, the central $-C-C-$ bond was extended 2.5 times[26] to 3.85 Å. The torsion around the central $-C-C-$ bond becomes a free rotation of both allyl radical fragments in which resonance stiffening[18] of the former two $C-C=C$ (torsions) in BA took place, and the external rotation around the central $-C-C-$ bond was made active to allow these two rotational modes to share in the random distribution of molecular energy. Four C-C rocking modes of the C_3H_5-units in BA had to be replaced by unusually low frequency bending modes (42 cm^{-1}) in order to yield Arrhenius A-factors for decomposition of BA which would correspond to the measured rate of recombination[8] of $(8.50 \pm 3.0) * 10^9$ M^{-1} s^{-1} at T = 300 K through (16), see Table IV. The activation energy for the bond-breaking process (E_d) was set equal to $-\Delta H^0$ for equilibrium (2)

PRECEDING PAGE BLANK

Table IV

MOLECULAR PARAMETERS FOR RRKM-CALCULATIONS:
1,5-HEXADIENE (BA)
(Standard State: 1 Atm)

	Molecule	Complex: "Vibration"	Complex: "Rotation"
Frequencies and degeneracies	3000 (6)	3010 (2)	3010 (2)
	2960 (2)	3000 (8)	3000 (8)
	2850 (2)	1350 (6)	1350 (6)
	1650 (2)	1300 (6)	1300 (6)
	1470 (2)	1100 (6)	1100 (6)
	1420 (2)	950 (2)	950 (2)
	1400 (2)	400 (4)	400 (4)
	1300 (2)	350 (2)	350 (2)
	1220 (2)	42 (4)	
	1170 (2)		
	920 (3)		
	900 (2)		
	800 (2)		
	350 (2)		
	320 (6)		
	90 (1)		
	70 (1)		
	50 (1)		
$r_{C \perp\!\!\!\perp C} / \text{Å}$	1.54	3.85 ($\rho^{+} = 2.5$)[a]	3.85 ($\rho^{+} = 2.5$)[a]
$10^{120} I_A I_B I_C$ (gr cm^2)^3	$1.78 * 10^7$	$8.60 * 10^7$	$8.60 * 10^7$
10^{40} I_r / gr cm^2	- - -	21.20	21.20
$10^{80} I_1 I_2$ / (gr cm^2)^2	- - -	- - -	$(91.44)^2$
I^{+}/I	- - -	4.14	4.14
E^{o}_{300} / kcal/mole	- - -	55.70	56.70
$E_{d,300}$ / kcal/mole	- - -	56.40	56.40
S^{o}_{300} / e.u.	88.83	101.04	102.91: η = 90.0%
$\log(A_{d,300} / s^{-1})$	- - -	15.90	16.31: η = 90.0%
$\log(A_{r,300} / M^{-1} s^{-1})$	- - -	10.40[b]	10.81[b]: η = 90.0%

[a] $\rho^{+} = \frac{r^{+}}{r^{o}}$, where r^{+} is the distance of both allyl radical fragments in the activated complex and r^{o} is the central C-C bond length in the molecule.

[b] $2.303R \log \frac{\left(A_r / M^{-1} s^{-1}\right)}{\left(k_d / s^{-1}\right)} = -33.50 + 8.35$ with $\Delta S^{o}_{r,d} = -33.50$ e.u. (exp.)

assuming zero activation energy for recombination (E_r) at 0 K.[27] The results of the RRKM calculations are displayed in Figure 5 and are listed in Table V, together with the high-pressure Arrhenius parameters. It is obvious from Figure 5 that the vibrational model successfully fits the experimental data in this case of recombination of two resonance stabilized radicals. Past experience with the recombination of simple alkyl radicals such as tert-butyl, isopropyl, and ethyl has indicated that such a fixed transition state model was not suited to represent the loose transition state for the bond fission of a simple alkane. The model predicts a transition state with too large a heat capacity at high temperatures due to the loosening of the four rocking modes in the transition state, thus predicting increasing Arrhenius parameters and increasing values for k_r^∞ with increasing temperatures. The experiments indicate otherwise, however. In the present case of resonance-stabilized radicals, the above increase in heat capacity is essentially balanced by the resonance stiffening of internal rotations, thereby reducing the heat capacity of the transition state. The net result is a small decrease in heat capacity, and a concomitant small decrease in E_d and A_d or a slight negative temperature dependence (see Table V). Although k_r^∞ is seen to increase by a factor of 4 from 300 K to 1000 K, the vibrational model fits the experimental data (k_r) for allyl radical recombination quite satisfactorily in contrast to normal alkyl radicals, where the high-pressure experimental A-factors for recombination or bond scission have a pronounced negative temperature dependence.

2. The Rotational Model

This is essentially a Gorin model, which represents the four low-frequency bending vibrations of the two allyl fragments as hindered rotations. The internal modes of the transition state are simply the vibrations and rotations of the independent fragments. This is an alternative picture for the transition

Table V

RESULTS OF RRKM CALCULATIONS FOR THE BOND-BREAKING PROCESS
1,5-HEXADINE → 2 ALLYL RADICAL AT SELECTED TEMPERATURES.
(ΔS^0_r = + 33.50 e.u. from T ≈ 300 to 1000 K)
(collision frequency: $\omega \approx 4982 \left(\frac{T}{M}\right)^{1/2}$)

		VIBRATIONAL MODEL					ROTATIONAL MODEL				
T/°K	$K_{r,d}/M^{-1}$	$\lg(A_d/s^{-1})$	E_d	k_d/s^{-1}	$k_r/M^{-1}\ s^{-1}$	k/k^{∞}	$\lg(A_d/s^{-1})$	E_d	k_d/s^{-1}	$k_r/M^{-1}\ s^{-1}$	k/k^{∞}
300	$8.72 * 10^{34}$	15.90	56.40	$.55 * 10^{-25}$	$4.79 * 10^{9}$	.999	$\eta = 90.0$ 16.31	56.40	$.116 * 10^{-24}$	$1.01 * 10^{10}$	.9923
625	$1.07 * 10^{14}$	15.82	56.24	$.76 * 10^{-4}$	$8.16 * 10^{9}$	.555	$\eta = 91.5$ 15.42	54.96	$.688 * 10^{-4}$	$7.36 * 10^{9}$	.5430
800	$7.11 * 10^{9}$	15.79	56.14	.477	$3.39 * 10^{9}$	.173	$\eta = 92.5$ 15.085	54.17	.351	$2.50 * 10^{9}$	.2232
900	$1.59 * 10^{8}$	15.78	56.10	10.00	$1.59 * 10^{9}$	$.778 * 10^{-1}$	$\eta = 93.0$ 14.92	53.71	7.32	$1.16 * 10^{9}$	.1237
950	$3.23 * 10^{7}$	15.77	56.05	32.60	$1.05 * 10^{9}$	$.522 * 10^{-1}$	$\eta = 93.25$ 14.84	53.48	24.10	261.6	$.9222 * 10^{-1}$

state typical of simple bond scission reactions. The hindrance (η/%) is accomplished in the calculation by decreasing the effective moment of inertia of each of the two two-dimensional allyl rotors:

$$I_{eff} = I_1 I_2 \left(\frac{100 - \eta}{100} \right)^{1/2} \qquad (17)$$

where I_1 and I_2 are the two one-dimensional component moments of inertia of an allyl fragment excluding the component of the moment of inertia around the axis parallel to the bond being broken. The hindrance effectively decreases the number of available rotational states by confining the rotational motion of each of the fragments. As the centrifugal barrier moves to smaller r^+ values with increasing temperature, η is expected to increase with temperature, thereby[26] reducing k_r^∞. The relation of η to the Arrhenius A-factor for decomposition is simply:

$$A_H/A = \frac{100 - \eta}{100} \qquad (18)$$

where A_H is the A-factor derived from a transition state model with $\eta \neq 0$. In the case of the rotational model, the same molecular parameters were chosen as for (1), $E_d = -\Delta H^0$, except that the four low-frequency bending modes at 42 cm^{-1} were replaced by two two-dimensional rotations of the allyl fragments ($I_{eff} = 8.36 * 10^{83} * \left[\frac{(100 - \eta)}{100}\right]^{1/2}$ $(gr\ cm^2)^2$). It was found that a good fit to the experimental data could be obtained by choosing the following values for η: T = 300 K, η = 90%; T = 625 K, η = 91.5%; T = 900 K, η = 93%. Table V shows the results of the calculation and Figure 5 displays the corresponding plot together with the experimental rate constants k_r and k_r^∞. Not too much importance should be attached to the absolute value of η, because this number is dependent on the details of the transition state model with respect to its structure and the vibrational frequencies. Table V describes,

therefore, only a "reasonable" choice of molecular parameters for transition states (1) or (2). Furthermore, the exact relationship between η and the geometrical parameters of the fragments (rotational "freedom" or tightness) in the transition state are virtually unknown. It should be noted that in this case, the dependence of η on temperature is exceptionally weak in comparison with two recent examples.[25] For methyl radical recombination, η increases from 63% to 82% over the temperature range 300-1400 K and in the case of the recombination of $HO_2^{\cdot}$ with $NO_2^{\cdot}$, η varies from 92% to 98% over the temperature range 217-300 K.

An intuitive choice for the interfragment distance in the critical configuration of a normal alkane undergoing bond fission to two alkyl radicals would be the top of the centrifugal barrier.[17,26] Recent calculations on ethane dissociation suggest, however, that the application of the criterion of minimum density of states[29] is more appropriate in locating the critical configuration with respect to the reaction coordinate. If no other structural changes in the molecule occur during the bond split, the location of the minimum density of states will coincide with the location of the top of the centrifugal barrier. As the C-C bond is breaking, however, lowering of the rocking modes is expected to occur. Loosening of these vibrations in the molecule will shift the location of the minimum density of states towards smaller values of the reaction coordinate and alternatively, stiffening of internal modes will shift the minimum density of states to larger values of the reaction coordinate as compared to the location of the centrifugal barrier.[29] As the temperature goes up, the minimum density of states, as well as the top of the rotational barrier move to smaller values of the interfragment distance. The -C-C- bond scission in 1,5-hexadiene to two resonance stabilized allyl radicals is a special case in that the anticipated loosening of internal modes upon bond breaking is accompanied by a concomitant "resonance stiffening," mainly of the free

internal rotations, resulting in a near cancellation of the temperature dependence of the location of the minimum density of states. The near balance of two opposing effects, namely loosening and stiffening of internal modes in the critical configuration of 1,5-hexadiene upon bond breaking, and its apparent lack of temperature sensitivity, resembles the temperature independent vibrational model. This balance is thus thought to be the main reason for the very small "tightening" of the transition state with increasing temperature as reflected in the increase of η by only 3% from 300 to 900 K. The explanation put forward above is of a qualitative nature and warrants further detailed calculations on the 1,5-hexadiene system. The foregoing discussion makes it clear why a vibrational model is equally successful in describing the bond scission of 1,5-hexadiene. In this case, both the vibrational, and rotational models are characterized by the same (negative) temperature dependence of their respective Arrhenius parameters, though to a different degree (see Table V), whereas in the case of a C-C bond split in an alkane, the vibrational model predicts a strong positive temperature dependence of its Arrhenius parameters.

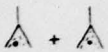
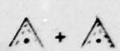
A glance at the high-pressure Arrhenius parameters E_d and log A_d for model (2), Table V, reveals that the rotational model has only $4 * R/2$ heat capacity associated with its hindered rotations, such that E_d and log A_d decrease by 2.7 kcal/mol and 1.24 logarithmic units, respectively, over the temperature range 300 to 900 K. Given the underlying assumption,[27] this is somewhat in disaccord with the result from the equilibrium study (vide supra), which predicts a constant value for E_d ($E_d = -\Delta H^0$) over this temperature range. With the present method of calculation (i.e., choosing an A-factor at T = 300 K to match the low-temperature recombination rate constant), one is led to conclude that the system has a negative activation energy for recombination ($E_r = -2.70$ kcal/mol), instead of + 1.80 kcal/mol (RT) as required by the

underlying assumption.[27] This is an artifact of the model, however, and is clearly the consequence of lacking heat capacity of the four hindered rotations. If conversely, one proceeds to match the high-temperature fall-off data at 900 K with E_d = + 56.40 kcal/mol, one is led to predict negative values for η at T = 300 K, (E_d = 59.34 kcal/mol), which is physically unreasonable. No attempt has been made, however, to associate an increased amount of heat capacity with these hindered internal rotations, knowing that the upper limit with respect to the heat capacity of the activated complex is represented in the vibrational model (1). With the present fall-off data for recombination of allyl radical, no unambiguous choice between transition state models (1) or (2) can be made. We favor at this point the simple vibrational transition state model (1), because it doesn't suffer from the shortcomings cited above.

Tsang[1c] estimated the Arrhenius parameters for the bond scission of BA at 1100 K (log A_d = 14.20, E_d = 59.3 kcal/mole), through the application of the usual geometric mean rule for the cross combination-to-combination ratio r($r = k_r(AB)/(k_r(AA)k_r(BB))^{1/2}$). Using the computed value of 14.20 for log A_d, together with the overall entropy change (ΔS^0) of −33.50 e.u. at T = 1000 K, yields log k_r = 8.79 (Table VI, reaction 4), which is one-to-one-and-a-half orders of magnitude too low in light of our results. The measured recombination rate constant k_r at 1000 K with ΔS^0 = −33.50 e.u. for equilibrium (2) results in log A_d of 15.75 or 15.26, according to the vibrational or rotational transition state model.[30] If the rate constant for allyl + CH_3· recombination is set equal to $10^{10.30}$ (see Table VI, reaction 2), one would predict a value of .95 or 1.68 for r, instead of 2.45 (as used by Tsang) on the basis of our measured value for k_r^{∞}, which is subject to the choice of the appropriate transition state model. We favor a value of r = 0.95 as a result of our preferred choice of the vibrational model (vide supra). A recent pyrolysis study of 1,1′-azoisobutane[32] provided an experimental value of r = .25 for the methyl + isobutyl radical pairs. The results of the flash photolysis study[9] of 2-methylbutene-1, where r = .09

Table VI

EXPERIMENTAL AND CALCULATED RECOMBINATION RATE CONSTANTS
FOR RADICAL RECOMBINATION REACTIONS INVOLVING STABILIZED RADICALS

No.	Recombination Reaction	T/°K	$\log(k_r(\text{exp.})/M^{-1}\ s^{-1})$	$\log(k_r(GM)^a/M^{-1}\ s^{-1})$	Ref.	Remarks
1	$CH_3^{\cdot} + CH_3^{\cdot} \rightarrow C_2H_6$	1000	10.30		31	
		300	10.38		31	
2	 $+ CH_3^{\cdot} \rightarrow C_5H_{10}$	1020	10.30		1d	Flash photolysis study
		300	9.35		9	
3	 $\rightarrow C_8H_{14}$	300	10.41		9	Flash photolysis
		1000		9.70		Shock-tube data[1d] for reaction (2)
		300		7.72		Data of ref. 9 for reaction (2)
4	 $\rightarrow C_6H_{10}$	1000	10.34[b] 9.85[c]		This work	
		1000		8.79	1c	Using A_d of ref. 1c and ΔS^o (refs. 17 and 18) for overall reaction to compete k_r [d]

[a] Value for $k_r(AB)/k_r^{1/2}(AA)k_r^{1/2}(BB)$ (geometric mean rule) is assumed to be 2.00[1c]

[b] Vibrational transition state. See Figure 5.

[c] Rotational transition state. See Figure 5.

[d] $2.303R \log[(A_r/M^{-1}\ s^{-1})/(A_d/s^{-1})] = -33.50 + 10.74$. At T = 1000 K, $k_r(\text{exp}) = A_r\ e^{-1}$ with $E_r = RT$

was found, seem too low and may indicate an experimental problem. Adjustment of r to higher values in this case would decrease k_r for reaction (3), Table VI, which seems somewhat high in view of the results for allyl radical recombination of van den Bergh and Callear[8] at 300 K, and concomitantly would increase k_r for reaction (2), Table VI, which seems unusually low for the cross-combination rate constant. These few examples show that r = 2.0 may not always be valid without prior experimental assessment of the involved rate constants.

We conclude, therefore, that the present "high" value for the recombination rate constant, which is quite similar in magnitude to common alkyl radical recombination rate constants (ethyl radical recombination, k_r = (7.80 ± 1.80) * 10^9 M^{-1} s^{-1}, ref. 33) is indicative of the fact that the recombination reaction shows no apparent activation energy and that the delocalization of the unpaired electron has no effect on the recombination rate of allyl radical.

V SUMMARY

This study yields $\Delta H^{o}_{f,300}$(allyl) = 38.3 ± 1.5 kcal mol^{-1}, and thus an allyl resonance energy ARE = 12.5 ± 2.0 kcal mol^{-1}. At the same time, these results yield a value for k_r^{∞} which is about the same as for alkyl radicals, indicating no effect of the electron delocalization on reactivity.

VI ACKNOWLEDGMENT

We would like to thank Dr. G. Manser who provided us with a sample of 3,3′-azo-1-propene.

VII REFERENCES

1. (a) D. M. Golden, N. A. Gac, and S. W. Benson, J. Amer. Chem. Soc., 91, 2136 (1969), and references therein;

   (b) W. Tsang, J. Chem. Phys., 46, 2817 (1967);

   (c) W. Tsang, Int. J. Chem. Kinetics, 1, 245 (1969);

   (d) W. Tsang, Int. J. Chem. Kinetics, 5, 929 (1973).

   (e) W. M. Marley and P. M. Jeffers, J. Phys. Chem., 79, 2085 (1975).

2. S. E. Buttrill, A. D. Williamson, and P. LeBreton, J. Chem. Phys., 62, 1586 (1975).

3. A. B. Trenwith, St. D. Wrigley, J. Chem. Soc., Faraday Trans. I, 73, 817 (1977), and references therein.

4. Defining the bond dissociation energy for any bond A-B, $DH^{o}_{T}(A\text{-}B) = \Delta H^{o}_{f,T}(A) + \Delta H^{o}_{f,T}(B) - \Delta H^{o}_{f,T}(A\text{—}B)$, we may define the stabilization energy in the allyl radical (ARE) as, $DH^{o}_{300}(nC_3H_7\text{—}H) - DH^{o}_{300}(\text{allyl—}H) \equiv \text{ARE}$.

5. J. M. McKelvey and G. Berthier, Chem. Phys. Lett., 41(3), 426 (1976), and references therein.

6. G. Levin and W. A. Goddard III, J. Amer. Chem. Soc., 97, 1649 (1975); G. Levin and W. A. Goddard III, Theor. Chim. Acta, 37, 253 (1975).

7. J. A. Kerr in Free Radicals, Vol. 1, J. K. Kochi, Ed., John Wiley and Sons, Inc., New York, 1973, Ch. 1.

8. H. E. Van den Bergh and A. B. Callear, Trans. Faraday Soc., 66, 2681 (1970).

9. F. Bayrakceken, J. H. Brophy, R. D. Fink, and J. E. Nicholas, Trans. Faraday Soc., 68, 228 (1972).

PRECEDING PAGE BLANK

10. In reference 1(a), a somewhat older version of the VLPP apparatus without molecular beam-sampling phase-sensitive detection was used. The different results obtained by Golden et al. could be accounted for by wall-catalyzed recombination of allyl radicals on the walls of the mass spectrometry chamber. We get essentially the results of 1(a) without phase-sensitive detection, i.e., a higher value for $K_{r,d}$ at these temperatures.

11. D. M. Golden, G. N. Spokes, and S. W. Benson, Angew. Chem., 85, 602 (1973).

12. B. H. Al-Sader, R. J. Crawford, Can. J. Chem., 48, 2745 (1970); R. J. Crawford and K. Takagi, J. Amer. Chem. Soc., 94, 7406 (1972).

13. D.G.L. James and S. M. Kambanis, Trans Faraday Soc., 65, 1350 (1969).

14. At every temperature the calibration factor α_j in $I^j = \alpha_j k_e^j [j]_{ss}$, where j is m/e 67, 54 (1,5-hexadiene) and 44 (CO_2) was determined by at least two different flow rates $k_e^j [j]_{ss} = F_j^i$. α_j relates mass spectrometric intensities (I^j) to steady-state concentrations of a molecule ($[j]_{ss}$).

15. $\ln(K_{r,d}/M^{-1}) = [\Delta S^o - \Delta nR(1 + \ln(R'T))]/R - \Delta E/RT$, where the superscript refers to a standard state of 1 Atm and R' distinguishes the gas constant in units of ℓ-atm/mol K from units of cal/mol K.

16. Defining $z_s = y_s * k_e^{BA}(S)$, $z_B = y_B * k_e^{BA}(B)$, and $K_{r,d} = k_r/k_d$, the propagation of errors yields for the relative error of $K_{r,d}$ the following expression:

$$\frac{\Delta K_{r,d}}{K_{r,d}} = \left(2\left(\frac{\Delta z_B + \Delta z_S}{z_B * k_e^{BA}(B) - z_s * k_e^{BA}(S)} \right)^2 + 2\left(\frac{\Delta z_B + \Delta z_S}{z_B - z_S} \right)^2 + \left(\frac{\Delta z_B}{z_B} \right)^2 \right)^{1/2}$$

17. S. W. Benson, Thermochemical Kinetics, 2nd Ed., John Wiley and Sons, Inc., New York, 1976.

18. H. E. O'Neal and S. W. Benson, Int. J. Chem. Kinetics, 1, 217 (1969).

19. The uncertainty in ΔH^o from the equilibrium measurements (2) is estimated to be ± 1 kcal/mol. Together with the uncertainty in ΔH_f^o(BA) of ± .5 kcal/mol, the combined uncertainty for ΔH_f^o(allyl, g) amounts to ± 1.5 kcal/mol.

20. M. Rossi and D. M. Golden, subsequent paper.

21. K. Y. Choo, P. C. Beadle, L. W. Piszkiewicz, and D. M. Golden, Int. J. Chem. Kinetics, 8, 45 (1976).

22. $I^{N_2} = \alpha_{N} + k_{a}^{N_2} * [N_2]_{ss} = \alpha_{N} + \alpha_{N_2} = \alpha_{N_2} F_{N_2}^{i}$. For explanation of symbols, see reference 14.

23. Experiment No. 1 in Table III was performed at an earlier stage of the recombination series than Nos. 2 and 3, indicating variable wall conditions of the reaction vessel within the series of experiments.

24. P. J. Robinson, K. A. Holbrook, Unimolecular Reactions, Wiley-Interscience, 1972.

25. (a) G. P. Smith, M. Lev-On, and D. M. Golden, submitted for publication.
(b) A. C. Baldwin and D. M. Golden, submitted to J. Phys. Chem.

26. The separation distance along the bond axis was chosen in such a way that it corresponded to the top of the centrifugal barrier in a model for a Lennard-Jones potential of the C-C bond connecting both C_3H_5 units: $\rho^+ = \frac{r^+}{r_0} = (6D_0/RT)^{1/6}$. This rotational maximum of the effective potential, including rotation, is not very sensitive to either T or the precise value of D_0, and for most common values of both occurs in the range: $\rho^+ \approx 2.5 - 3.0$

27. $E_r = \Delta E^{\ddagger}_{r,0\,K} + T\langle \Delta C_v^{\ddagger} \rangle + RT \equiv 0$ at 0 K and $\Delta E^{\ddagger}_{r,0\,K} + T\langle \Delta C_v^{\ddagger} \rangle > 0$ at T ≠ 0.

28. Given η and $I_A I_B I_C$ for a rotational model transition state. Changing $I_A I_B I_C$ to $I_A' I_B' I_C'$ results in a different hindrance parameter (η') to yield the same Arrhenius A-factor through the following relation:

$$\eta' = 100 - (100 - \eta) * \left(\frac{I_A' I_B' I_C'}{I_A I_B I_C} \right)^{1/2}$$

If $I_A' I_B' I_C' > I_A I_B I_C$, it then follows $\eta' < \eta$.

29. W. L. Hase, J. Chem. Phys., 64, 2442 (1975).
W. L. Hase, "Dynamics of Unimolecular Reactions" in Dynamics of Molecular Collisions, W. H. Miller (Ed.), Plenum Press, New York (1976).

30. $k_r(exp) = A_r e^{-1}$ at T = 1000 K. Note, that the values for A_d derived in this way do not correspond to the ones from Table V which have been derived by data fitting at 300 K and subsequent extrapolation to 1000 K.

31. See references in 22(a); S. W. Benson and H. E. O'Neal, Kinetic Data on Gas-Phase Unimolecular Reactions, NSRDS-NBS21, National Bureau of Standards Reference Data System, U.S. Government Printing Office, Washington, D.C., 1970.

32. G. McKay and I.M.C. Turner, Int. J. Chem. Kinetics, 10, 89 (1978).

33. D. A. Parkes and C. R. Quinn, J. Chem. Soc., Faraday Trans. I, 72, 1952 (1976).

CAPTIONS

Figure 1 Block diagram for experimental setup of VLPP (Very Low-Pressure Pyrolysis) experiment.

Figure 2 Very Low-Pressure Pyrolysis Reactor (133.5 cm^3)

Figure 3 Van't Hoff Plot of Equilibrium Constant $K_{r,d} = k_r/k_d$

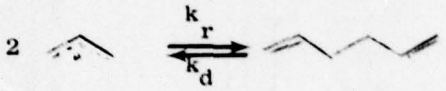


Figure 4 Brauman Plot (see text) for the Recombination Reaction k_r



at 625 K

(experiments numbers 2 and 3, Table III)

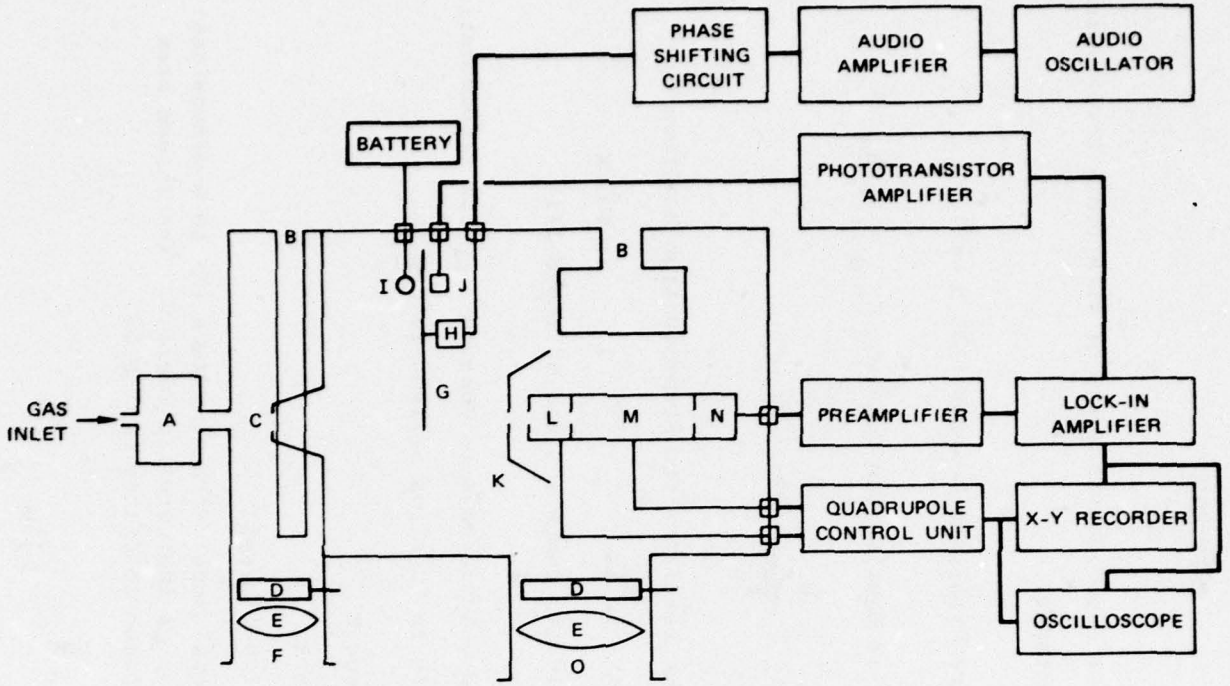
Figure 5 Experimental and Calculated Rate Constants k_r for Recombination of Allyl Radicals in Function of Temperature

■ Reference 8

● This work

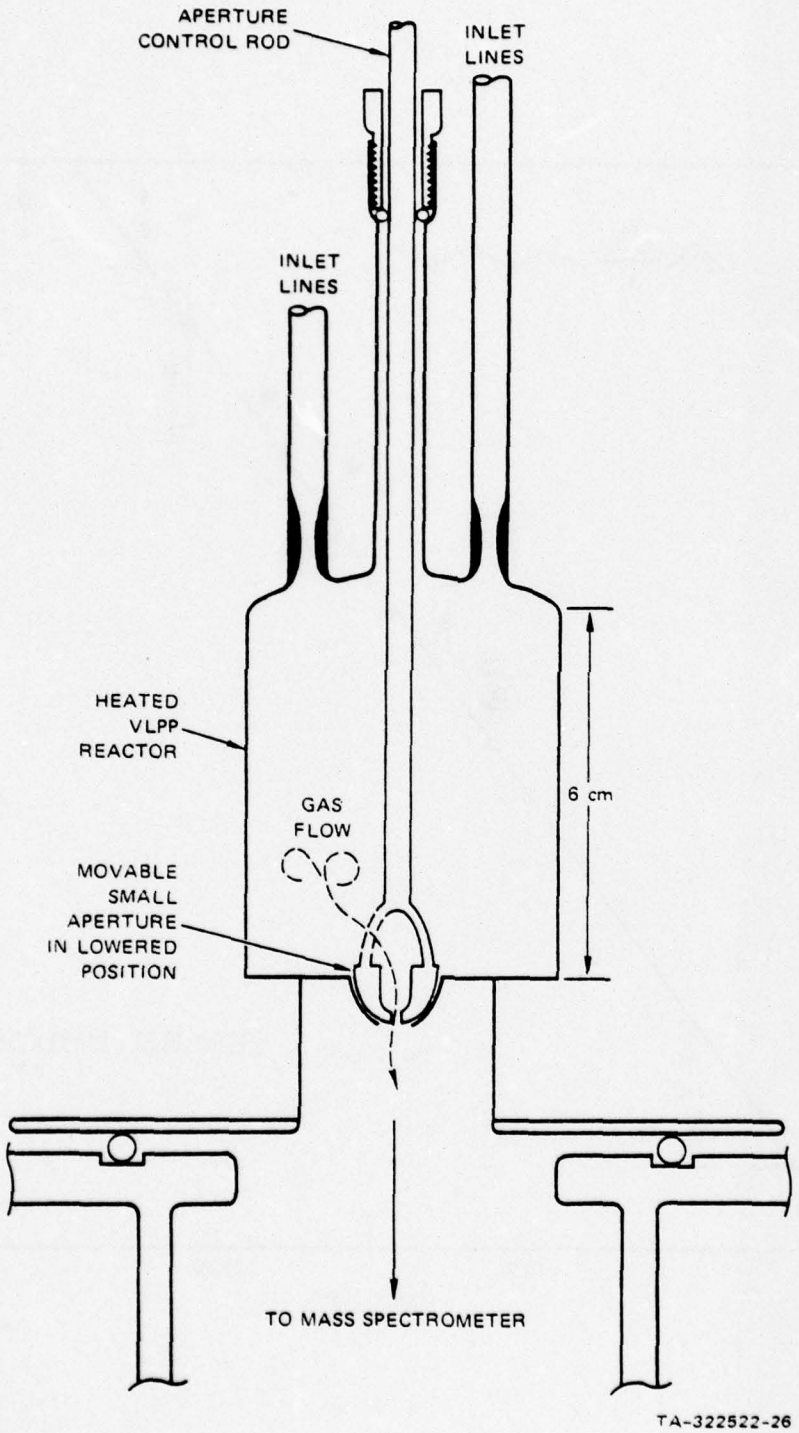
—— Vibrational Model

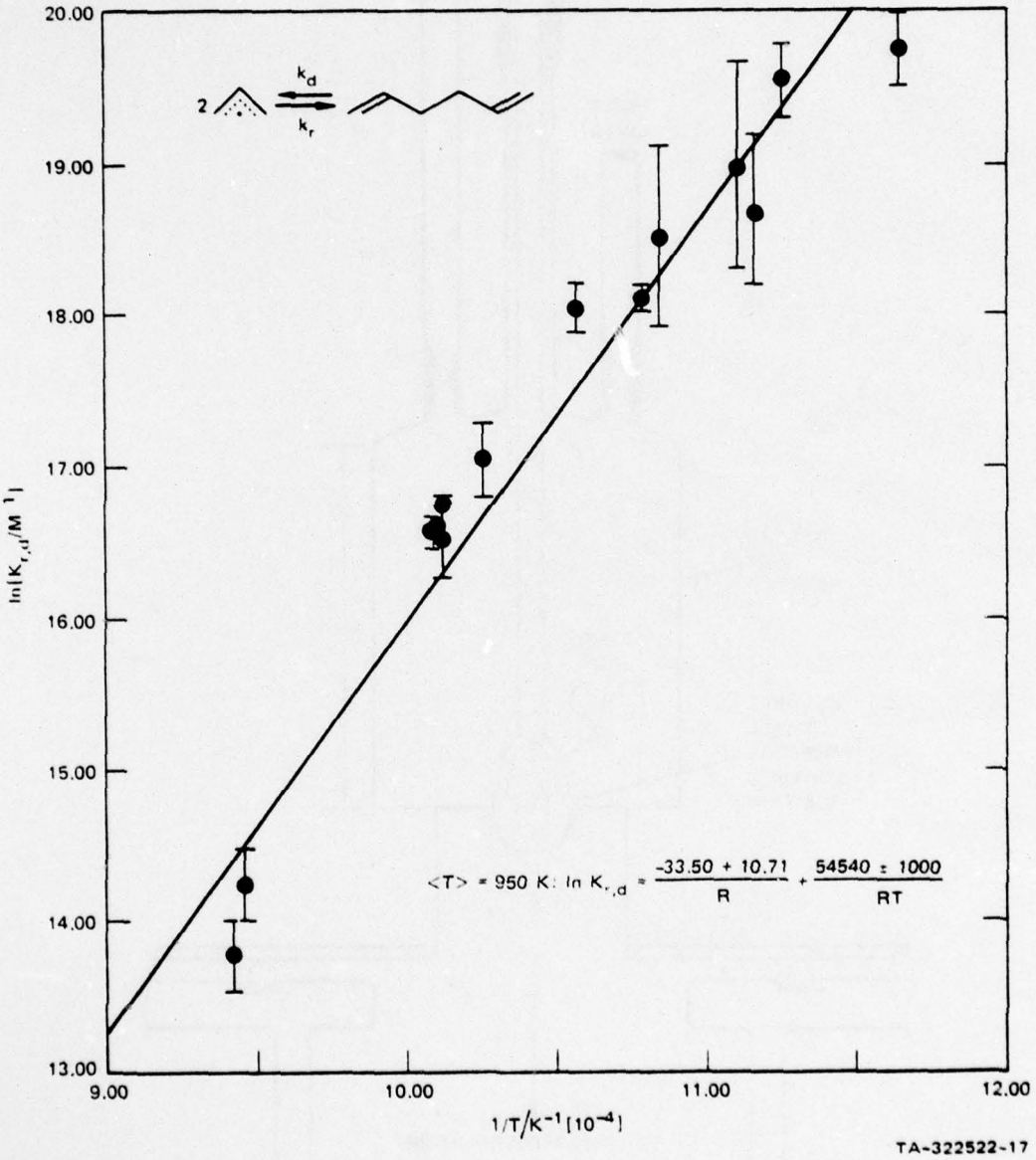
--- Rotational Model with Hindrance (η) to 2-dimensional rotation as indicated in Table V. The shaded area corresponds to values of $\eta \pm 5\%$

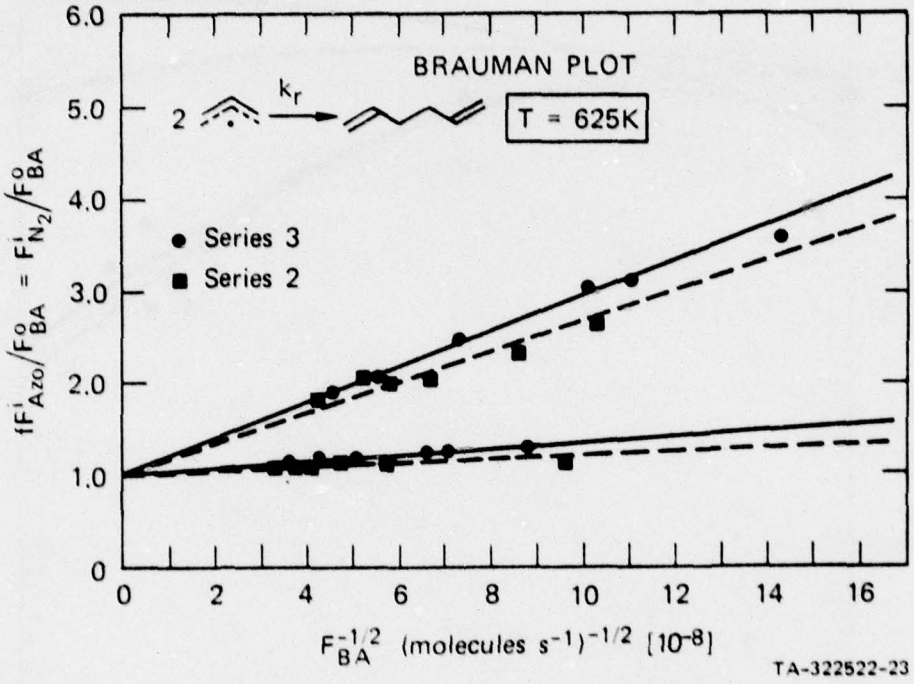


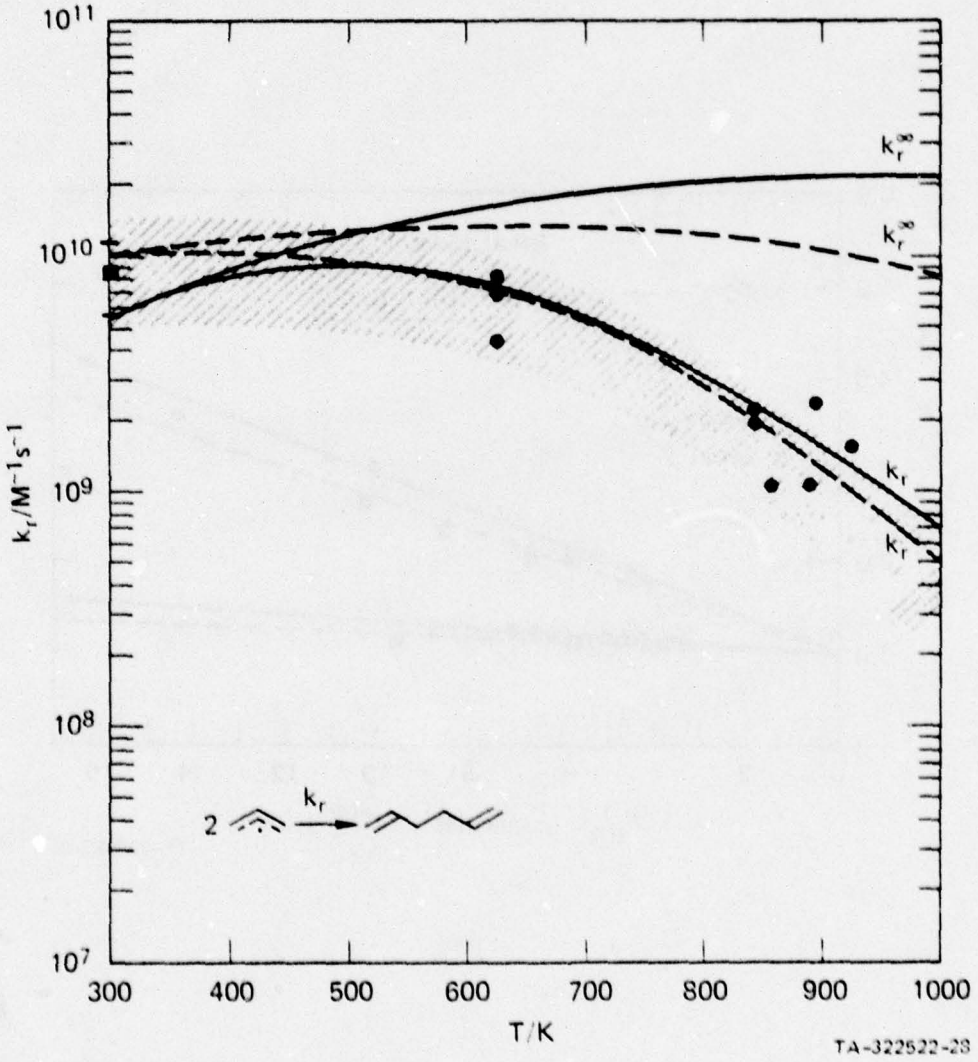
A Low-Pressure Flow Reactor
B Liquid N_2 Cryopump
C Beam Collimation Aperture
D Slide Valve
E Refrigerant Cooled Baffle
F 6-inch Oil Diffusion Pump
G Chopping Wheel
H Synchronous Motor
I Light Source
J Phototransistor
K Collimator and Shield
L Ion Source
M Quadrupole Mass Filter
N Electron Multiplier
O 4-inch Oil Pump

TA-322583-28R


APERTURE
CONTROL ROD
INLET
LINES
INLET
LINES
HEATED
VLPP
REACTOR
GAS
FLOW
6 cm
MOVABLE
SMALL
APERTURE
IN LOWERED
POSITION
TO MASS SPECTROMETER
TA-322522-26


20.00
19.00
18.00
17.00
16.00
15.00
14.00
13.00
9.00
10.00
11.00
12.00
$\ln[K_{r,d}/M^{-1}]$
$1/T/K^{-1}[10^{-4}]$
2
k_d
k_r
$\langle T \rangle$ = 950 K: $\ln K_{r,d} = \frac{-33.50 \pm 10.71}{R} + \frac{54540 \pm 1000}{RT}$
TA-322522-17


BRAUMAN PLOT
T = 625K
2
k_r
Series 3
Series 2
$fF^i_{Azo}/F^o_{BA} = F^i_{N_2}/F^o_{BA}$
$F^{-1/2}_{BA}$ (molecules $s^{-1})^{-1/2}$ [10^{-8}]
0
1.0
2.0
3.0
4.0
5.0
6.0
0
2
4
6
8
10
12
14
16
TA-322522-23


10^{11}
10^{10}
10^{9}
10^{8}
10^{7}
$k_r/M^{-1}s^{-1}$
k_r^∞
k_r^∞
k_r
k_r
2
k_r
300
400
500
600
700
800
900
1000
T/K
TA-322522-28

Appendix

The steady-state kinetic expressions for the reaction system (1) to (5) in a stirred flow reactor shall now be derived.

Under steady-state conditions, the following expressions (A1) to (A4) for the concentration of the involved species result:

$$(A1) \qquad d(DAO)/dt = R^{i}_{DAO} - k_1(DAO) - k_e^{DAO}(DAO) \equiv 0$$

$$(A2) \qquad d(CO_2)/dt = 2k_1(DAO) - k_e^{CO_2}(CO_2) \equiv 0$$

$$(A3) \qquad d(C_3H_5\cdot)/dt = 2k_1(DAO) + 2k_d(BA) - 2k_r(C_3H_5\cdot)^2 - k_e^{C_3H_5}(C_3H_5\cdot) \equiv 0$$

$$(A4) \qquad d(BA)/dt = k_r(C_3H_5\cdot)^2 - k_d(BA) - k_e^{BA}(BA) \equiv 0$$

where R^{i}_{P} is the flow of the species P into the reactor (in units of molecules $s^{-1}\ l^{-1}$), k_e^{P} is the escape rate constant of P out of the reactor, and DAO stands for diallyloxalate and BA for 1,5-hexadiene.

Rearrangement of (A4) yields (A5):

$$(A5) \qquad (BA)/(C_3H_5\cdot)^2 = k_r/(k_d + k_e^{BA})$$

Keeping in mind that $R^{o}_{P} = k_e^{P}(P)$, where R^{o}_{P} is the flow of species P out of the reactor, the combination of (A3) and (A4) results in (A6) using the substitution $2k_1(DAO) = R^{o}_{CO_2}$ from (A2):

$$(A6) \qquad \frac{(BA)}{(C_3H_5\cdot)^2} = \frac{\left(k_e^{C_3H_5\cdot}\right)^2 (BA)}{\left(k_e^{CO_2}(CO_2) - 2k_e^{BA}(BA)\right)^2}$$

Comparison of (A6) and (A5) results in the desired expression (A7), which enables one

$$\text{(A7)} \qquad \frac{k_r}{k_d + k_e^{BA}} = k_e^{BA} * \frac{2R^0_{BA}}{(R^0_{CO_2} - 2R^0_{BA})^2}$$

to establish $k_r/(k_d + k_e^{BA})$ with the experimental values of R^0_{BA} and $R^0_{CO_2}$. With two independent values of k_e^{BA} (e.g., corresponding to a large and a small aperture in the VLPP reactor), the algebraic separation of k_r and k_d is possible.

Chapter 2

ABSOLUTE RATE CONSTANTS FOR METATHESIS REACTIONS OF ALLYL AND BENZYL RADICALS WITH HI(DI). THE HEAT OF FORMATION OF ALLYL AND BENZYL RADICALS[†]

M. Rossi[‡] and D. M. Golden
Thermochemistry and Chemical Kinetics Group
SRI International, Menlo Park, California 94025

[†]This work was supported, in part, by contract F44620-75-C-0067 with the Air Force Office of Scientific Research.

[‡]Postdoctoral Research Associate.

ABSTRACT

The metathesis reaction, $C_3H_5^{\cdot} + HI(DI) \xrightarrow{k_3} C_3H_6(C_3H_5D) + I$, has been studied in the gas phase using the VLPP technique. The result is $\log(k_3/M^{-1}\ s^{-1}) = (9.73 \pm .21) - (4.0 \pm 1.0)/\theta$ at T = 1000 K and $\log(k_3/M^{-1}\ s^{-1}) = (9.58 \pm .35) - (3.0 \pm 1.0)/\theta$ at T = 635 K, where $\theta = 2.303$ RT in kcal mol^{-1}. The result for the metathesis reaction $C_6H_5CH_2^{\cdot} + DI \xrightarrow{k_3} C_6H_5CH_2D + I^{\cdot}$ is $\log(k_3/M^{-1}\ s^{-1}) = (9.93 \pm .22) - (4.0 \pm 1.0)/\theta$ at T = 965 K. These rate expressions were extrapolated to lower temperatures using a transition state model in order to compute the equilibrium constants for the above metathesis reactions using the rate constants for the reverse metathesis from classical iodination studies. The equilibrium constants yield ΔH_f^o(allyl) = 39.1 ± 1.0 kcal/mol and ΔH_f^o(benzyl) = 46.60 ± 1.5 kcal/mol at T = 300 K. These values correspond to stabilization energies of 11.7 ± 1.5 kcal/mol and 11.3 ± 2.0 kcal/mol, respectively (i.e., DH(allyl-H) = 86.3 ± 1.0 kcal/mol and DH($C_6H_5CH_2$–H) = 86.7 ± 1.5 kcal/mol).

PRECEDING PAGE BLANK

I INTRODUCTION

A large number of values for free radical heats of formation (ΔH_f^o (R·)) have been obtained by the spectrophotometric iodination technique which is well documented in the literature.[1]

The pertinent reactions are:

$$I_2 + M \rightleftharpoons 2I\cdot + M \quad ; \quad K_{I_2} \tag{1}$$

$$RI + I\cdot \underset{k_2}{\overset{k_1}{\rightleftharpoons}} R\cdot + I_2 \quad ; \quad K_{1,2} = k_1/k_2 \tag{2}$$

$$R\cdot + HI \underset{k_4}{\overset{k_3}{\rightleftharpoons}} RH + I\cdot \quad ; \quad K_{3,4} = k_3/k_4 \tag{3}$$

with the following overall equilibrium

$$RI + HI \rightleftharpoons RH + I_2 \tag{4}$$

In general, the temperature dependent values of k_1 and k_2/k_3 (starting with RI + HI) or k_4 and $K_{3,4}$ (starting with RH + I_2) can be obtained. The usual method of extracting ΔH_f^o(R·) from these studies is to assume that E_2 = 0.0 ± 1.0 kcal/mol and/or E_3 = 1.0 ± 1.0 kcal/mol. (The measured values of E_2-E_3 are not inconsistent with these assumptions.) Thus, a measurement of E_4 will yield a value for $\Delta H_{3,4}^o$ and ΔH_f^o(R·) will follow since the appropriate values for HI, I· and RH are known.[2]

Very low-pressure pyrolysis (VLPP) allows the measurement of fast bimolecular reactions — such as (5) in the gas phase.

$$R\cdot + HI \xrightarrow{k_3} RH + I\cdot \tag{5}$$

We take advantage of the fact that the measured rate constants k_3 are unencumbered by competitive radical-radical recombinations

PRECEDING PAGE BLANK

relative to which the overwhelming majority of fast bimolecular radical-molecule reactions have been measured.[3] The availability of Arrhenius parameters for forward and back reaction rate constants provides values for $\Delta H_f^o(R\cdot)$ and entropies of radicals ($S^o(R\cdot)$). Accordingly, we report in this work the rates of reactions (6) and (7)

$$C_3H_5\cdot + HI(DI) \xrightarrow{k_3} C_3H_6(C_3H_5D) + I\cdot \qquad (6)$$

$$C_6H_5\dot{C}H_2 + HI(DI) \xrightarrow{k_3} C_5H_5CH_3(C_6H_5CH_2D) + I\cdot \qquad (7)$$

together with their Arrhenius parameters over an extended temperature range, thereby obtaining values for $\Delta H_f^o(R\cdot)$ of allyl ($C_3H_5\cdot$) and benzyl ($C_6H_5\dot{C}H_2$) radicals by using the results of previously published determinations of k_4, A_4 and E_4 from iodination studies of propylene[4] and toluene.[5]

II EXPERIMENTAL

The description of the VLPP molecular beam sampling apparatus, together with the all-quartz reaction vessel (Knudsen cell) has been presented in a previous publication.[6] The source and purification of the radical precursors diallyloxalate ($C_8H_{10}O_4$), 3,3′-azo-1-propene ($C_6H_{10}N_2$) and bibenzyl ($C_{14}H_{14}$) have also been described.[6] Benzylvinylether ($C_9H_{10}O$) was synthesized according to literature methods.[7] GC-MS-analysis showed a 2% impurity of benzaldehyde (C_7H_6O), which did not interfere with our measurements. The standard gas-handling system was heated in order to increase the vapor pressure of diallyloxalate, bibenzyl and benzylvinyl ether, such that suitable flow rates of the radical precursors into the heated Knudsen cell could be obtained. Hydrogen iodide (Linde Air Products, Inc.) and deuterium iodide (99 atom %, Merck, Sharp and Dohme, Ltd., Canada) were used without further purification. The experiments were carried out by setting the flow of the radical precursor to a low and constant value and monitoring m/e = 43 (C_3H_5D) and m/e = 92 (C_7H_8) or m/e = 93 (C_7H_7D), as a function of flow rate of HI or DI. The reaction vessel had two inlet (capillary or needle valve) systems from two independent gas-handling systems so that the components met for the first time in the hot reactor.

III RESULTS AND DISCUSSION

A. Allyl Radical + HI(DI)

Diallyloxalate ($C_8H_{10}O_4$) was used as a precursor for allyl radicals at $<T>$ = 1000 K and 3,3′-azo-1-propene ($C_6H_{10}N_2$) at $<T>$ = 750 K. By using two different precursors for allyl radical it was possible to cover a range of 380 K in the study of the metathesis (6). Application of the steady state assumption to reaction (6) in a low-pressure stirred flow reactor results in the following relation[8] (see appendix for details of the derivation):

$$1/f = 1 + \frac{k_e^{C_3H_5\cdot} \cdot k_e^{HI}}{k_3(HI)} \qquad (8)$$

where f is the fraction of radicals "titrated" at a certain steady-state concentration (HI), $k_e^{C_3H_5\cdot}$, and k_e^{HI} are the escape rate constants (s^{-1}) of allyl radical and HI out of the reactor. f is defined as $(C_3H_6)/(C_3H_6)_\infty$, where (C_3H_6) is the steady-state concentration of C_3H_6 at a certain (HI), and $(C_3H_6)_\infty$ is the same concentration at (HI) = ∞, where essentially all radicals have reacted with HI. In the case of diallyloxalate as precursor for allyl radical, (CO_2) could be taken as representative of the amount of the allyl radicals present in the reaction system, so that 1/f could be equated to $(CO_2)/(C_3H_6)$ or $R^o_{CO_2}/R^o_{C_3H_6}$. This method proved to be valid because plots of 1/f vs. $R^o_{CO_2}/R^o_{C_3H_6}$ yielded straight lines with unit intercepts, confirming that the amount of CO_2 present was indeed representative of the amount of

PRECEDING PAGE BLANK

allyl radical in the system. The following assumptions have been made in deriving equation (8): (HI) >> ($C_3H_5\cdot$) and $F^i_{HI} = F^o_{HI}$, where F^o_{HI} is the flow of HI in, and F^o_{HI} is the flow out of the reactor. Under our experimental conditions both assumptions were found to be justified, so that a plot of 1/f vs. 1/(HI) gave a straight line with unit intercept (within experimental error) and $(k_e^{C_3H_5\cdot} \cdot k_e^{HI})/k_3$ as slope, from which k_3 was readily obtained given the reactor parameters.[6] Special attention was paid to the requirement of carrying out the titration at the lowest possible concentration of $C_3H_5\cdot$ in order to suppress the bimolecular recombination reaction. Figure 1 displays a typical plot 1/f vs. 1/(HI) and Table I lists the rate constants $k_3/M^{-1}\ s^{-1}$ as a function of temperature. These are plotted in the usual Arrhenius form in Figure 2. The results are:

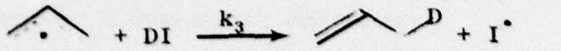
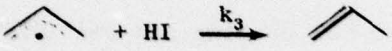
$$k_3 = 7.2 \times 10^8\ M^{-1}\ s^{-1} \quad \text{at} \quad \langle T \rangle = 1000\ K$$

$$k_3 = 3.6 \times 10^8\ M^{-1}\ s^{-1} \quad \text{at} \quad T = 635\ K$$

The Arrhenius plot of Figure 2 accommodates slight curvature over the temperature range 635-1000 K. For very exothermic reactions, such as (6) and (7), with very small activation energies, one expects a small isotope effect with $k_3^H/k_3^D = 1.5 \pm .5$.[9] This ratio of the rate constants can be seen at higher temperatures (Figure 2), where both HI and DI were used as titrating agents. It may be seen that E_3 at $\langle T \rangle$ = 1000 K is 4.0 ± 1.0 kcal/mol (log $A_3/M^{-1}\ s^{-1}$ = 9.58 ± .35), significantly different from the "usual" assumed value of 1.0 ± 1.0 kcal/mol used throughout the literature.[1]

Table I

RATE CONSTANTS FOR METATHESIS REACTIONS
AS A FUNCTION OF TEMPERATURE

T[K]	k_3[M^{-1} s^{-1}]
	
907	$4.80 * 10^8$ [a]
911	$4.90 * 10^8$ [a]
929	$6.68 * 10^8$ [a]
929	$6.99 * 10^8$ [a]
926	$6.37 * 10^8$ [a]
1007	$8.06 * 10^8$ [a]
1014	$6.76 * 10^8$ [a]
	
635	$3.57 * 10^8$ [b]
697	$5.50 * 10^8$ [b]
761	$4.83 * 10^8$ [b]
878	$7.24 * 10^8$ [b]
982	$8.54 * 10^8$ [b]

[a] Radical source: Diallyloxalate $C_8H_{10}O_4$

[b] Radical source: 3,3'-azo-1-propene $C_3H_5N_2C_3H_5$

Golden et al.[4] found the following rate expression at $\langle T \rangle$ = 530 K: $\log(k_4/M^{-1}\ s^{-1}) = 10.25 - 18.04/\theta$, where θ = 2.303 RT in kcal mol^{-1}. In order to provide a value at 1000 K for the equilibrium constant $K_{4,-3} = k_4/k_{-3}$ (3), where $R^{\cdot} = C_3H_5^{\cdot}$, a transition state model, which has been shown by Benson and coworkers to be appropriate[2] in cases of metathesis reactions, such as (6) and (7), was used to extrapolate the measured rate constant k_4 from 530 K to 1000 K. The transition state (9)



(9)

for reaction (6) or its reverse was approximated by taking allyl iodide (C_3H_5I) as a model, adding two CHI bending and one (CH)–I stretching mode to C_3H_5I and including other minor corrections due to the presence of the extra H-atom in (9). Table II demonstrates the method and summarizes the result for the entropy of activation $\Delta S_4^{\circ\ddagger}$ of the reverse of reaction (6). With $\Delta C_{p,4}^{\ddagger}$ = +3.94 e.u., the following rate expression at T = 1000 K results:

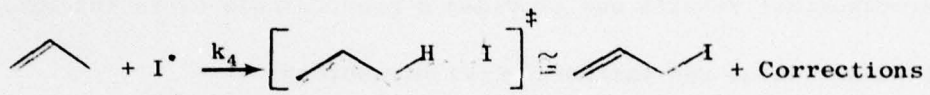
$$\log(k_4/M^{-1}\ s^{-1}) = 11.32 - 19.90/\theta, \qquad T = 1000\ K.$$

$K_{4,3}$ at T = 1000 K then turns out to be $1.39 * 10^{-2}$ which, together with an estimate for S°(allyl)[10] and C_p data[2,10] yields a "third law" standard heat of formation ΔH_f°(allyl) = 39.1 ± 1.0 kcal/mol at T = 300 K.[a] The "second law" heat of formation derived from the combination of the Arrhenius

[a] The combined error limits have been estimated to be ± 1.0 kcal/mol in view of the high precision determinations of k_4 (ref. 4) and k_3 (this work).

Table II

ESTIMATED ENTROPY OF ACTIVATION FOR THE
METATHESIS REACTION, $C_3H_6 + I^{\cdot} \rightarrow C_3H_5^{\cdot} + HI$
(Standard State: 1 atm)



$\Delta S_4^{o\ddagger'} = S^o(\cdot C_3H_5I) - S^o(I^{\cdot}) - S^o(C_3H_6)$

	300 K	530 K	1000 K
$\Delta S_4^{o\ddagger'}$	−29.31	−30.05	−31.17
Corrections:			
spin (Rln2)	1.39	1.39	1.39
rotation[a]	1.69	1.69	1.69
2 bending (C H I): 300 cm^{-1}	2 * 1.40	2 * 2.40	2 * 3.60
1 stretch (C H I):1000 cm^{-1}	.10	.50	1.40
resonance stiffening of internal rotation V_o = 4 → 13 kcal/mol	− 1.30	− 1.43	− 1.12
C=C, 1650 cm^{-1} → C ÷ C, 1400 cm^{-1}	0.0	0.0	+ .10
C − C, 1000 cm^{-1} → C ÷ C, 1400 cm^{-1}	− .10	− .30	− .50
420 cm^{-1} → 635 cm^{-1}	− .52	− 1.00	− .90
$\Delta S_4^{o\ddagger}$	−25.52	−24.40	−21.90

[a]Adjusted to give experimental A_4 at $\langle T \rangle$ = 530 K (log $A_4/M^{-1}\ s^{-1}$ = 10.25).

expressions is in excellent agreement, since the value of S^0(allyl) which is derived from A_3 and A_4 is 62.80 e.u., compared to the value[10] of 62.10 e.u. used in the "third law" calculations. Table III summarizes the kinetic and thermochemical results and provides a good example of an internally consistent set of Arrhenius and thermochemical parameters.

The allyl radical heat of formation derived above from two separate experiments is in excellent agreement with a recent equilibrium study and other determinations of ΔH_f^o(allyl).[6] The present value for ΔH_f^o(allyl) provides an allyl resonance stabilization energy (ARE) of 11.7 ± 1.5 kcal/mol (see, e.g., reference 11 for the definition of ARE). The large variation of A_3 and A_4 with temperature (Table III) is noteworthy; this brings about a concomitant change in E_3 and E_4 which tend to partially cancel the increase in the A-factor. Obviously, this cancellation of log A versus E is only partial, so that the suggested curvature in the Arrhenius plot in Figure 2 results. It has repeatedly been pointed out in the literature,[3] that the Arrhenius A-factor for the reaction of $I^{\cdot}$ with an alkane or olefin is quite high (log A_4 = 10.3 at 550 K). Such a behavior is obvious from Table III in the present case as well.

B. Benzyl Radical + HI(DI)

At $<T>$ = 880 K benzyl radicals were generated by unimolecular decomposition of benzylvinylether (C_7H_7–OC_2H_3) and at $<T>$ = 1060 K by the bond breaking process of bibenzyl (C_7H_7–C_7H_7). The evaluation of the rate constant k_3 (7) follows the same lines as in the case of allyl radical. Figure 3 displays

Table III

KINETIC AND THERMOCHEMICAL PARAMETERS FOR THE EQUILIBRIUM*

propylene + I· $\underset{k_3}{\overset{k_4}{\rightleftharpoons}}$ allyl· + HI

T/K	$\log(k_3/M^{-1}\ s^{-1})$	$\log(k_4/M^{-1}\ s^{-1})$	$\Delta S^0_{4,3}$ (e.u.) [a]	$\Delta S^0_{4,3}$ (e.u) [b]	$\Delta H^0_{4,3}$ (kcal mol^{-1}) [c]
1000	<u>9.73 − 4.0/θ</u>	11.32 − 19.90/θ	7.32	6.86	15.90
530	8.75 − 2.44/θ	<u>10.25 − 18.04/θ</u>	6.90	6.07	15.60
300	8.29 − 2.27/θ	9.47 − 17.55/θ	6.14	5.40	15.28 [d]

*Underlined values represent experimental results; others are extrapolated Arrhenius parameters using transition-state model (9) and Table II (θ = 2.303RT in kcal/mol).

[a] From Arrhenius expressions using $\ln(A_4/A_3) = \Delta S^0_{4,3}/R$

[b] Thermochemical estimate, references 2 and 10.

[c] From Arrhenius expression using $\Delta H^0_{4,3} = E_4 - E_3$

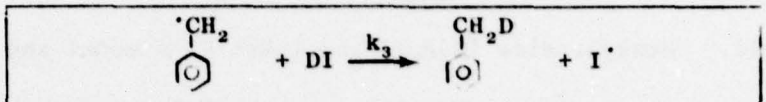
[d] Yields $\Delta H^0_f(\text{allyl}) = 39.13$ kcal/mol

a typical 1/f vs. 1/(HI) plot (equation 8), where f represents by analogy with the definition given in section A, the fraction of radicals titrated at a certain steady-state concentration of HI with respect to the total concentration of radicals present in the absence of HI; Table IV lists the resulting rate constants $k_3/M^{-1}\ s^{-1}$ as a function of temperature, and Figure 4 shows the corresponding Arrhenius plot. By using two different benzyl radical precursors, which decompose at different temperatures, it was possible to study the metathesis reaction (7) over a range of 315 K.

The rate constant $k_3/M^{-1}\ s^{-1}$ was found to be $1.08 * 10^9\ M^{-1}\ s^{-1}$ at $<T> = 965$ K. The activation energy E_3 at 965 K is 4.0 ± 1.0 kcal/mol ($\log A_3/M^{-1}\ s^{-1} = 9.93 \pm .22$) in remarkable agreement with the parameters found for allyl radical. The Arrhenius plot in Figure 4 suggests, by analogy with the allyl case, slight curvature at higher temperatures and a possible small systematic error between the two series of different precursors for benzyl radical, but it is obvious as well that the straight line, corresponding to $E_3 = 4.0 \pm 1.0$ kcal/mol does not do violence to the present data. Due to the more preliminary nature of the iodination study of toluene[5] the experimental rate of the reverse of reaction (7) at T = 500 K was assumed to be correct ($1.41 * 10^2\ M^{-1}\ s^{-1}$) rather than using the published Arrhenius parameters, since $A_4/M^{-1}\ s^{-1}$ seems to be too low by at least an order of magnitude. In order to derive a value for the equilibrium constant $K_{4,3} = k_4/k_3$ at T = 500 K (3), where $R^{\cdot} = C_7H_7^{\cdot}$,

Table IV

RATE CONSTANTS FOR THE METATHESIS REACTION AS A FUNCTION OF TEMPERATURE

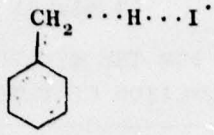


T/°K	k_3 [M^{-1} s^{-1}]
811	$7.08 * 10^8$ [a]
851	$5.78 * 10^8$ [a]
856	$9.03 * 10^8$ [a]
922	$6.99 * 10^8$ [a]
963	$9.35 * 10^8$ [a]
936	$1.35 * 10^9$ [b]
1004	$1.23 * 10^9$ [b]
1007	$1.40 * 10^9$ [b]
1038	$1.51 * 10^9$ [b]
1049	$1.27 * 10^9$ [b]
1050	$1.70 * 10^9$ [b]
1088	$1.37 * 10^9$ [b]
1090	$1.32 * 10^9$ [b]
1109	$1.72 * 10^9$ [b]
1126	$2.30 * 10^9$ [b]

[a] Radical Source: Benzylvinylether ($C_6H_5CH_2OC_2H_3$)

[b] Radical Source: Bibenzyl (1,2-Diphenylethane)

the transition state model (10) was used by analogy with the allyl case:



(10)

discussed above. Benzyliodide (C_7H_7I) was taken as a model and corrected for the transition state (10). Table V shows the detailed corrections and the computed entropy of activation $\Delta S_3^{0\ddagger}$ for reaction (7). The rate expression for k_3 extrapolated to T = 500 K is:

$$\log(k_3/M^{-1}\ s^{-1}) = 9.00 - 2.81/\theta \qquad (11)$$

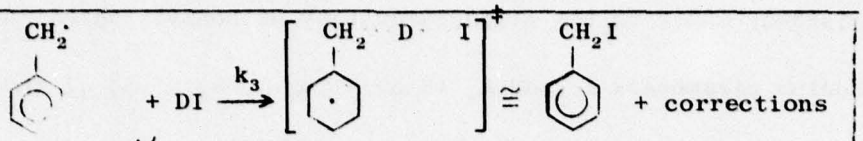
$K_{4,3}$ at T = 500 K is then computed to be 2.34×10^{-6}, which yields a standard heat of formation ΔH_f^0(benzyl) = 46.60 ± 1.50 kcal/mol at 300 K, using an estimate for S^0(benzyl)[10] and C_p data.[2,10]

The comparative rate shock-tube decomposition of isobutylbenzene[12] at $\langle T \rangle$ = 1100 K yields ΔH_f^0(benzyl) = 48.42 ± 2.0 kcal/mol at 300 K under the assumption of zero activation energy (in pressure units) for the reverse reaction at reaction temperature (Arrhenius activation energy for decomposition $E_d = \Delta H^0$), a value markedly higher than the currently accepted value from iodination studies and related evidence[1] of 45.00 ± 1.5 kcal/mol.[b] The

[b] Assumption of zero activation energy in concentration units at $\langle T \rangle$ = 1100 K would result in an even higher value for ΔH_f^0(benzyl) at T = 300 K (50.60 kcal/mol).

Table V

ESTIMATED ENTROPY OF ACTIVATION FOR THE METATHESIS REACTION, $C_7H_7\cdot + DI \rightarrow C_7H_7D + I\cdot$ (Standard State: 1 atm)



$\Delta S_3^{o\ddagger'} = S^o(C_7H_7I) - S^o(DI) - S^o(C_7H_7\cdot)$

	300 K	500 K	965 K
$\Delta S_3^{o\ddagger'}$	− 34.95	− 36.32	− 37.89
Corrections:			
spin (Rln2)	1.39	1.39	1.39
rotation[a]	1.98	1.98	1.98
2 bending (C(D)D I): 300 cm^{-1}	2 * 1.40	2 * 2.30	2 * 3.53
1 stretch (C(D)D I): 1000 cm^{-1}	.10	.50	1.33
Resonance stiffening of internal rotation, V_o = 3 → 15.5 kcal/mol	− 2.10	− 1.90	− 1.25
C–C, 1000 cm^{-1} → C ∴ C, 1200 cm^{-1}	− .10	− .20	− .38
$\Delta S_3^{o\ddagger}$	− 30.86	− 29.95	− 28.26

[a]Adjusted to give experimental A_3 at $\langle T \rangle$ = 965 K ($\log A_3/M^{-1}\ s^{-1}$ = 9.93).

discrepancy of the results of both experimental methods is not clear. Our value for ΔH_f^0(benzyl) lies right in between the two seemingly different results, and both seem compatible with our value from this study given our overall experimental error of ± 1.5 kcal/mol. This result is quite satisfactory, given that only the rate for the reverse of (7) was used. A consistency check on the standard entropy of benzyl radical using the Arrhenius parameters A_3 and A_4 (2.30 R log $A_4/A_3 = \Delta S^0_{4,3}$) could not be performed because of the lack of reliable Arrhenius parameters for the reverse of (7).[5] Instead, Arrhenius parameters were calculated for the reverse of (7) using an estimate for $\Delta S^0_{4,3}$[2,10] and the experimental A_3 together with the rate at T = 500 K. These results are listed in Table VI. The same observations can be made as in the allyl case when considering the magnitude of log A_4 and log A_3, respectively.

Table VI

MEASURED AND CALCULATED RATE PARAMETERS AND OVERALL ENTROPY CHANGE FOR THE EQUILIBRIUM*

Toluene + I· $\underset{\vec{k}_3}{\overset{k_4}{\rightleftharpoons}}$ benzyl· + HI

T/°K	$\log(k_3/M^{-1}\ s^{-1})$	$\log(k_4/M^{-1}\ s^{-1})$	$\Delta S^0_{4,3}$/e.u.
965	<u>9.93 − 4.0/θ</u>	11.42 − 20.51/θ [a]	6.84
500	9.00 − 2.81/θ	10.33 − 18.84/θ [b]	6.15

[a] E_4 obtained through $\Delta C^{\ddagger}_{p,4}$ = 3.60 e.u. and E_4 at T = 500 K (determined from experimental rate of reverse of (7) and A_4); A_4 calculated from A_4 at 500 K and $\Delta C^{\ddagger}_{p,4}$.

[b] A_4 from A_3 and $\Delta S^0_{4,3}$. E_4 determined from experimental rate of reverse of (7) and A_4.

* Underlined values represent experimental results; others are calculated Arrhenius parameters (using transition-state model (10) and Table V, θ = 2.303 RT in kcal/mol).

IV REFERENCES

1. D. M. Golden and S. W. Benson, Chem. Rev., 69, 125 (1969).
2. S. W. Benson, Thermochemical Kinetics, 2nd Ed., John Wiley and Sons, Inc., New York, 1976.
3. J. A. Kerr in Free Radicals, Vol. 1, J. K. Kochi, Editor, John Wiley and Sons, Inc., New York, 1973
4. D. M. Golden, A. S. Rodgers, and S. W. Benson, J. Amer. Chem. Soc., 88, 3196 (1966).
5. R. Walsh, D. M. Golden, and S. W. Benson, J. Amer. Chem. Soc., 88, 650 (1966).
6. M. Rossi, K. D. King, and D. M. Golden, preceeding paper.
7. W. H. Watanabe and L. E. Coulson, J. Amer. Chem. Soc., 79, 2828 (1956); H. Yuke, K. Hatada, K. Nagata, and K. Kajiyama, Bull. Chem. Soc. (Japan), 42, 3546 (1969).
8. N. A. Gac, D. M. Golden, and S. W. Benson, J. Amer. Chem. Soc., 91, 3091 (1969).
9. A. F. Trotman-Dickenson, G. S. Milne, Tables of Bimolecular Reactions, NSRDS-NBS9, National Bureau of Standards, Washington, D.C., 1967.
10. H. E. O'Neal and S. W. Benson, Int. J. Chem. Kinetics, 1, 217 (1969).
11. D. M. Golden, N. A. Gac, and S. W. Benson, J. Amer. Chem. Soc., 91, 2136 (1969).
12. W. Tsang, Int. J. Chem. Kinetics, 2, 311 (1970); W. Tsang, Int. J. Chem. Kinetics, 10, 41 (1978).

CAPTIONS

Figure 1 Experimental determination of k_3 (see equation 8) for the metathesis reaction allyl$^{\cdot}$ + DI $\xrightarrow{k_3}$ propylene-d_1 + I$^{\cdot}$ at 1014 K. Representative example from Table I.

Figure 2 Arrhenius plot of rate constants from Table I.

--- metathesis reaction involving DI

—— metathesis reaction involving HI

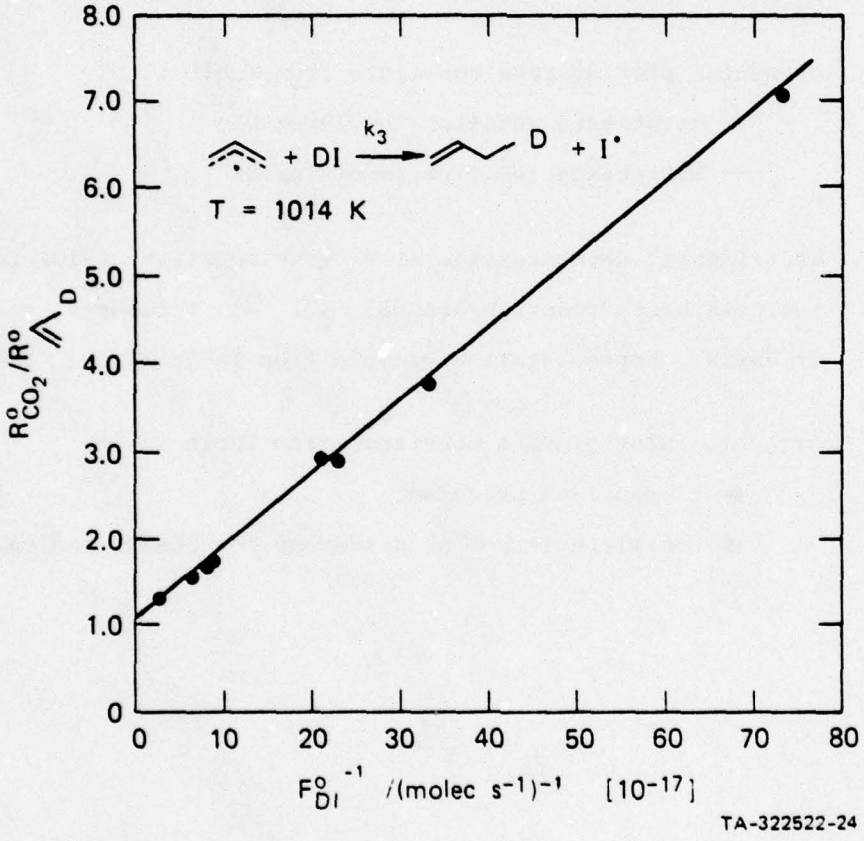
Figure 3 Experimental determination of k_3 (see equation A-10) for the metathesis reaction benzyl$^{\cdot}$ + DI $\xrightarrow{k_3}$ toluene-d_1 + I$^{\cdot}$ at 989 K. Representative example from Table IV.

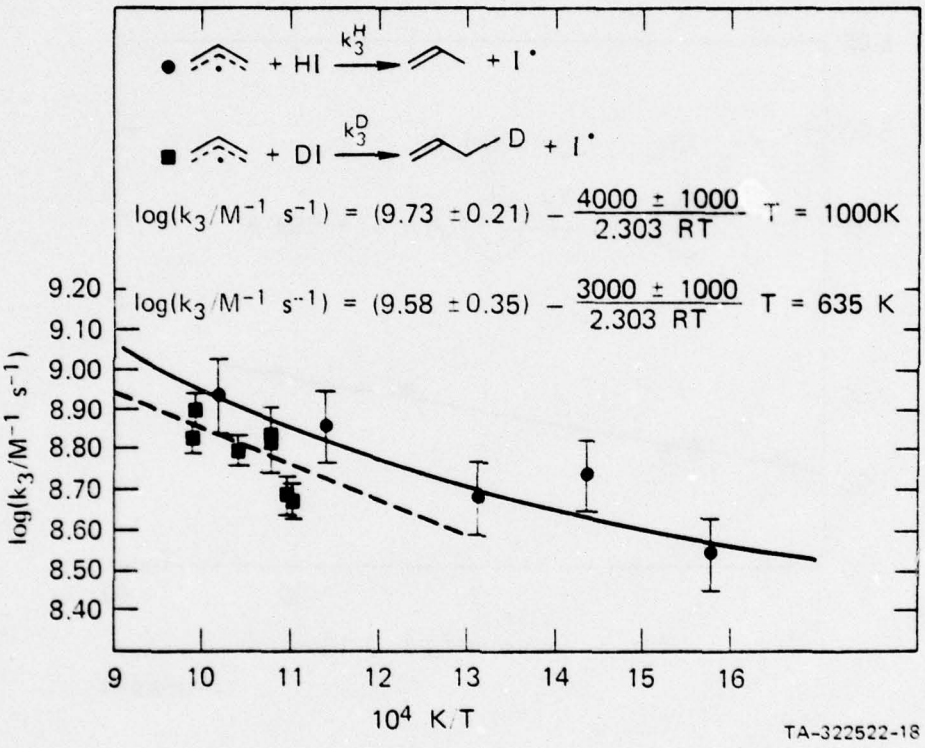
Figure 4 Arrhenius plot of rate constants from Table IV.

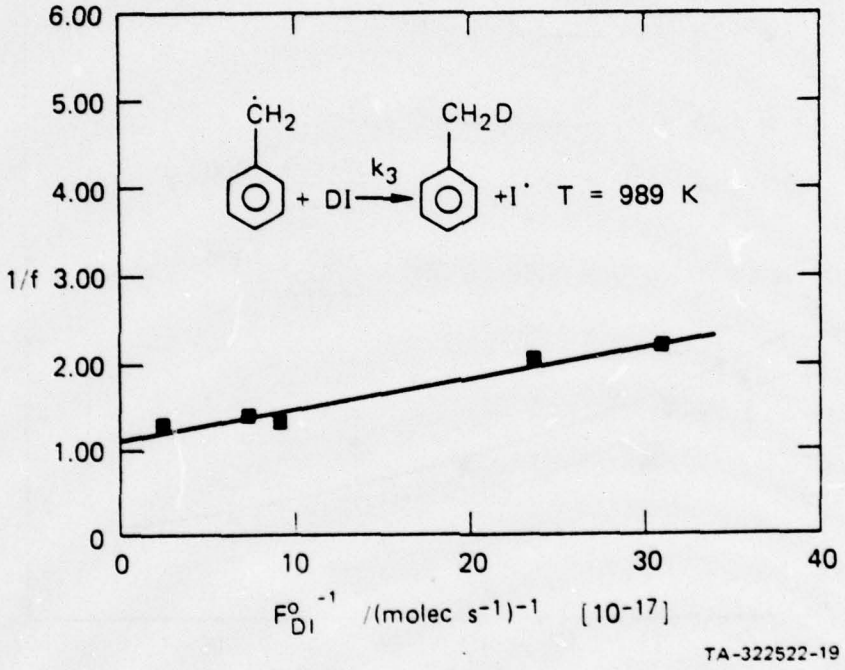
■ bibenzyl as precursor

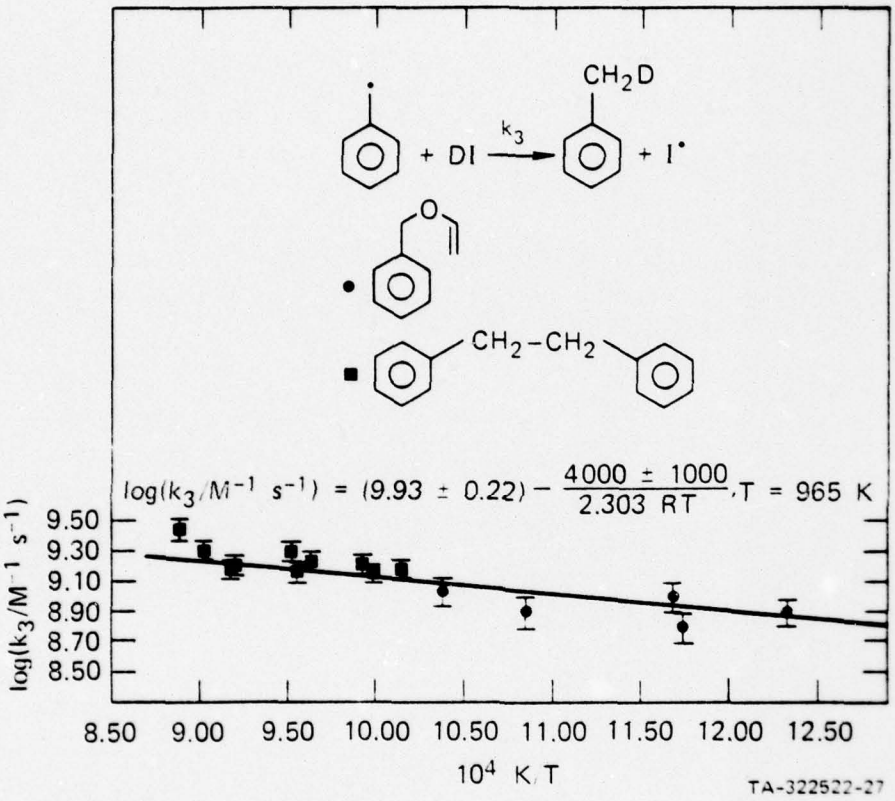
● benzylvinylether as precursor for benzyl radicals

PRECEDING PAGE BLANK


8.0
7.0
6.0
5.0
4.0
3.0
2.0
1.0
0
0
10
20
30
40
50
60
70
80
+ DI
k_3
D + I•
T = 1014 K
$R^o_{CO_2}/R^o_{\diagup\!\diagup\!\diagdown_D}$
$F^o_{DI}{}^{-1}$ /(molec s^{-1})$^{-1}$ [10^{-17}]
TA-322522-24


+ HI
k_3^H
+ I•
+ DI
k_3^D
D + I•
$\log(k_3/M^{-1}\ s^{-1}) = (9.73 \pm 0.21) - \frac{4000 \pm 1000}{2.303\ RT}$ T = 1000K
$\log(k_3/M^{-1}\ s^{-1}) = (9.58 \pm 0.35) - \frac{3000 \pm 1000}{2.303\ RT}$ T = 635 K
9.20
9.10
9.00
8.90
8.80
8.70
8.60
8.50
8.40
$\log(k_3/M^{-1}\ s^{-1})$
9
10
11
12
13
14
15
16
10^4 K/T
TA-322522-18


6.00
5.00
4.00
1/f 3.00
2.00
1.00
0
0
10
20
30
40
$\dot{C}H_2$
CH_2D
k_3
+ DI
+I˙
T = 989 K
$F^o_{DI}{}^{-1}$ /(molec s^{-1})$^{-1}$ [10^{-17}]
TA-322522-19


CH2D
+ DI
k3
+ I•
O
CH2–CH2
log(k3/M-1 s-1) = (9.93 ± 0.22) – 4000 ± 1000 / 2.303 RT, T = 965 K
log(k3/M-1 s-1)
9.50
9.30
9.10
8.90
8.70
8.50
8.50
9.00
9.50
10.00
10.50
11.00
11.50
12.00
12.50
10^4 K/T
TA-322522-27

Appendix

For a radical titration (metathesis) with HX, where X = I, Br, the pertinent reaction system is:

(A-1) $$R^{\cdot} + HX \xrightarrow{k_a} RH + X^{\cdot}$$

(A-2) $$R^{\cdot} \xrightarrow{k_e^{R^{\cdot}}}$$

(A-3) $$HX \xrightarrow{k_e^{HX}}$$

Under steady state conditions, the following expressions (A-4) to (A-6) for the concentration of the involved species result, where

(A-4) $$d(RH)/dt = k_a(R^{\cdot})(HX) - k_e^{RH}(RH) \equiv 0$$

(A-5) $$d(R^{\cdot})/dt = R_R^i - k_e^{R^{\cdot}}(R^{\cdot}) - k_a(R^{\cdot})(HX) \equiv 0$$

(A-6) $$d(HX)/dt = R_{HX}^i - k_e^{HX}(HX) - k_a(R^{\cdot})(HX) \equiv 0$$

k_e^P is the escape rate constant of species P and R_p^i is the flow rate of P into the VLPP reactor (in units of molecules s^{-1} ℓ^{-1}). With the use of (A-4) to (A-6), (RH) can be expressed as a function of (HX):

(-7) $$(RH) = \frac{k_a}{k_e^{RH}}(R^{\cdot})(HX) = \frac{k_a}{k_e^{RH}} * \frac{R_R^i}{k_e^{R^{\cdot}} + k_a(HX)} * \frac{R_{HX}^i}{k_e^{HX} + k_a(R^{\cdot})}$$

(A-7) is simplified to give (A-8) under the condition: (HX) >> (R·):

(A-8) $$(RH)_{\infty} = \frac{k_a}{k_e^{RH}} * \frac{R_R^i}{k_a(HX)} * \frac{R_{HX}^i}{k_e^{HX}}$$

PRECEDING PAGE BLANK

With the definition $1/f = \frac{(RH)_\infty}{(RH)}$, the following expression (A-9) is obtained, where $R^o_{HX} = k_e^{HX}(HX)$:

$$1/f = 1 + \frac{k_e^{R\cdot} k_e^{HX}}{k_a R^o_{HX}} + \frac{R^i_{R\cdot}}{R^o_{HX}} \qquad \text{(A-9)}$$

In the limit of high (HX), where $R^i_{HX} = R^o_{HX}$ holds to a good approximation and where R^i_R is negligible with respect to R^o_{HX} and R^i_{HX}, respectively; (A-9) can be simplified to expression (A-10), which relates the experimental quantities 1/f and R^i_{HX} to the desired rate constant k_a if the escape rate constants $k_e^{R\cdot}$ and k_e^{HX} are known.

$$1/f = 1 + \frac{k_e^{R\cdot} k_e^{HX}}{k_a R^i_{HX}} \qquad \text{(A-10)}$$

Chapter 3

HOMOGENEOUS DECOMPOSITION OF VINYL ETHERS. THE HEAT OF FORMATION OF ETHANAL-2-YL[†]

M. Rossi[‡] and D. M. Golden

Thermochemistry and Chemical Kinetics Group
SRI International - Menlo Park, California 94025

[†]This work was supported, in part, by contract F44620-75-C-0067 with the Air Force Office of Scientific Research.

[‡]Postdoctoral Research Associate.

ABSTRACT

The thermal unimolecular decomposition of three vinylethers has been studied in a VLPP apparatus. The high-pressure rate constant for the retro-ene reaction of ethylvinylether was found to be log (k/s^{-1}) = $(11.47 + .25) - \frac{43.4 \pm 1.0}{2.303\ RT}$ at $\langle T \rangle$ = 900 K and that of t-butylvinylether proved to be log $(k/s^{-1}) = (12.00 \pm .27) - \frac{38.4 \pm 1.0}{2.303\ RT}$ at $\langle T \rangle$ = 800 K. No evidence for the competition of the higher energy homolytic bond-fission process could be obtained from the experimental data. The rate constant obtained for the C-O bond scission reaction in the case of benzylvinylether was log $(k/s^{-1}) = (15.05 \pm .30) - \frac{49.3 \pm 1.0}{2.303\ RT}$ at $\langle T \rangle$ = 750 K. Together with $\Delta H^{o}_{f,300}$(benzyl·) = 46.6 kcal/mol, the activation energy for this reaction results in $\Delta H^{o}_{f,300}(\dot{C}H_2CHO)$ = +3.9 ± 2.0 kcal/mol and in a resonance stabilization energy of 3.2 ± 2.0 kcal/mol for 2-ethanalyl radical.

PRECEDING PAGE BLANK

I INTRODUCTION

Most vinyl ethers have been reported to decompose by molecular elimination mechanisms, and cyclic transition states have been frequently suggested as a result of the negative entropies of activation and low activation energies observed.[1] Recently, it was observed that ethylvinylether yielded not only acetaldehyde and ethylene (c.f., (1)) , the products of the retro-ene molecular elimination,[1] but also significant amounts of ketene, ethane, and butane upon multiphoton dissociation by an intense CO_2-laser.[2] A higher activation energy reaction path, the bond sicission process (2),

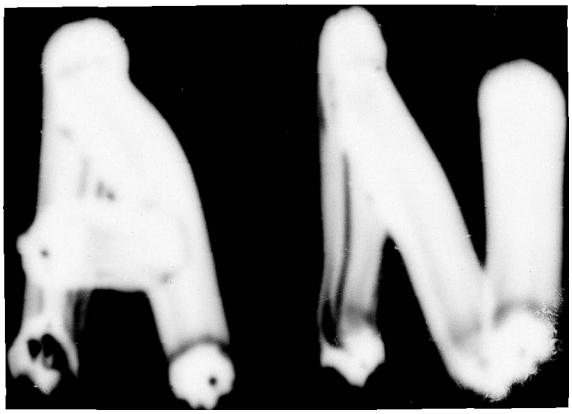
$$C_2H_5OC_2H_3 \xrightarrow{k_1} CH_3CHO + C_2H_4 \qquad (1)$$

$$C_2H_5OC_2H_3 \xrightarrow{k_2} C_2H_5\cdot + \dot{C}H_2CHO \qquad (2)$$

is held responsible for the occurrence of the latter products, which are believed to be due to secondary reactions of radicals produced in reaction (2). Using this assumption, an apparent reaction "temperature" of $\sim$ 1600 K could be inferred from the branching ratio k_1/k_2, when irradiated with the CO_2 laser.

Specifically, we embarked on a complementary thermal study of the decomposition of various vinyl ethers in order to detect and study the reactivity of the radicals $C_2H_5\cdot$ and $\dot{C}H_2CHO$ (ethanal-2-yl) with respect to ketene, ethane, and butane formation. In addition, the quantitative assessment of the Arrhenius parameters for the bond scission of benzylvinylether

PRECEDING PAGE BLANK



to benzyl and ethanal-2-yl radical at high temperatures gives the heat of formation ($\Delta H^{o}_{f,300}$) and resonance stabilization energy of ethanal-2-yl. We report the unimolecular decomposition of ethylvinylether (C_2H_5—O—C_2H_3), t-butylvinylether (t-C_4H_9—O—C_2H_3), and benzylvinylether ($C_6H_5CH_2OC_2H_3$) in a VLPP apparatus up to temperatures of 1300 K.

II EXPERIMENTAL

The molecular beam sampling VLPP apparatus with phase-sensitive detection has been described in detail elsewhere,[3] and the methods of assessing the unimolecular reaction rate constant k_{uni} from the mass spectroscopic data have been described in a review article.[4] The VLPP reactor parameters are: V = 133.4 ml, $\omega = 4982 * (T/M)^{1/2}$ s^{-1}, $k^{M}_{e}(B) = 2.5571 * (T/M)^{1/2}$ s^{-1}, $k^{M}_{e}(S) = .2088 * (T/M)^{1/2}$ s^{-1}. Ethylvinylether (Aldrich) and t-butylvinylether (Haven Chemicals) were used after trap-to-trap distillation. GC-MS analysis of t-butylvinylether revealed negligible amounts of isobutene, t-butanol, and t-butyl acetate. Benzylvinylether was synthesized following standard procedures.[5] GC-MS analysis revealed the presence of ~ 2% benzaldehyde, which was removed by distillation in vacuo. The low vapor pressure of benzylvinylether made necessary the use of a heated inlet system when higher flow rates were required. In all experiments with the vinylethers, except

for the case where the heated inlet system had to be used, an internal standard (CO_2, CHF_3) was used. Deuterium iodide (99 atom %) was purchased from Merck, Sharp, and Dohme and was used without further purification. The gas mixtures were prepared in a standard gas-handling vacuum line and stored in 5-ℓ darkened bulbs.

III RESULTS

A. Ethylvinylether

For the decomposition of ethylvinylether, the pertinent reactions are (1) and (2). The course of reaction (1) was followed by monitoring the first-order disappearance of ethylvinylether (m/e = 14, 15, 26, 27, 28, 29, 31, 42, 43, 44, 45, 72) at m/e = 72. The appearance of the reaction products acetaldehyde (m/e = 44, 43, 29) and ethylene (m/e = 28,27,26) could not be observed quantitatively, because the mass spectrum of ethylvinylether had a significant contribution to the intensities of almost all of the peaks of the reaction products. Ketene was not detected up to temperatures of 1270 K, although an RRK calculation with the Arrhenius parameters[6] $\log (k/s^{-1}) = 11.50 - 44.5/\theta$,* predicted detectable yields under our conditions ($k_1/k_2 \cong 5.5$ at T = 1300 K). Control experiments with acetic anhydride (3) at 1270 K confirmed that ketene (m/e = 42, 41,14) is

$$CH_3COOCOCH_3 \rightarrow CH_2CO + CH_3COOH \qquad (3)$$

* $\theta = 2.303\ RT$; $s = 22$, $\omega = 4982 * (T/M)^{1/2}\ s^{-1}$ (reference 7).

stable under our conditions, and also produced acetic acid (m/e = 60, 45, 15), as well as methane and CO_2, which apparently stem from the decomposition of acetic acid on the walls of the reactor. It is noteworthy that acetaldehyde decomposes at high temperatures to give CO and CH_4, probably according to (4), since the presence of methyl

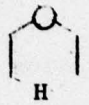
$$CH_3CHO \rightarrow CH_3^{\cdot} + CHO^{\cdot} \rightarrow CH_4 + CO \qquad (4)$$

radicals was established through titration with DI to give easily detected CH_3D (m/e = 17, 16, 15). The absence of ketene forces us to conclude that the bond fission reaction (2) is not competing under our experimental conditions up to 1270 K.

The rate constant k_1 was independent of the flow rate over the range $10^{14} \leq F^i_{EVE} \leq 5 * 10^{16}$ molecules s^{-1}, and the experimental values of k_{uni}/s^{-1} versus T/K are plotted in Figure 1. Moreover, no dependence of k_{uni} on the aperture size of the VLPP reactor was found, further confirming the absence of secondary reactions. RRK calculations indicated that k_1 is in the fall-off range in the temperature range studied (750-1050 K). In order to obtain the high-pressure Arrhenius parameters from the fall-off data of Figure 1, RRKM calculations were performed using a fixed transition state model (see Appendix and Table I) and varying the activation energy to match the data. The previously measured Arrhenius A-factor[1] log (A_1/s^{-1}) = 11.5 at T = 800 K for the six-membered transition state of the retro-ene reaction (1) was assumed

Table I

MOLECULAR PARAMETERS ENTERING THE RRKM-CALCULATION OF THE RETRO-ENE REACTION OF ETHYLVINYLETHER. $C_2H_5OC_2H_3 \rightarrow C_2H_4 + CH_3CHO$

	Molecule 	Activated Complex 
Frequencies and degeneracies	3080(3) 2910(5) 1640(1) 1430(3) 1320(3) 1170(1) 1070(4) 960(1) 800(3) 580(1) 350(4) 200(3) 100(1)	3080(3) 2910(5) 1640(1) 1430(3) 1320(3) 1170(1) 1070(3) 1050(1) 960(1) 800(2) 700(1) 600(2) 400(2) 350(4)
$10^{120} I_A I_B I_C$ / (gr cm²)³	3.93 * 10^6	3.93 * 10^6
E^0 / kcal/mol		44.1
S^0_{300} / e.u.	80.25	72.83
$\log(A^\infty_{900} / s^{-1})$		11.47
E^∞_{900} / kcal/mol		43.4
$\log(A^\infty_{300} / s^{-1})$		11.61
E^∞_{300} / kcal/mol		43.7

to be correct. Figure 1 displays the results of the RRKM calculation (for reaction 1) whose high-pressure Arrhenius parameters are:

$$\log (k_1/s^{-1}) = 11.5 - 43.4/\theta \qquad \langle T \rangle = 900 \text{ K} \qquad (5)$$

The activation energy is believed to match the data to within ± 1 kcal/mol with a concomitant uncertainty in log (A_1/s^{-1}) of ± .25.

B. t-Butylvinylether

In order to observe the bond sicission reaction, another vinyl ether with a lower activation energy than EVE was chosen. Thus, t-butylvinylether was decomposed in a VLPP reactor. The pertinent reactions are (6) and (7):

$$t\text{-}C_4H_9OC_2H_3 \xrightarrow{k_6} CH_3CHO + i\text{-}C_4H_8 \qquad (6)$$

$$t\text{-}C_4H_9OC_2H_3 \xrightarrow{k_7} \dot{C}H_2CHO + t\text{-}C_4H_9\cdot \qquad (7)$$

The extent of the unimolecular decomposition was observed by monitoring the disappearance of t-butylvinylether at m/e = 100 or 57 for reasons elucidated above. Again, no indication of the appearance of ketene which would be indicative of the occurrence of the higher energy reaction path (7), at m/e = 14 or 42 could be found up to temperatures of 1220 K, indicating that the bond scission reaction is too slow to compete with the retro-ene reaction.

Flow rate studies of the unimolecular reaction rate constant k_7 revealed no dependence in the range $8.5 * 10^{13} \leq F^i_{EVE} \leq 10 * 10^{16}$ molecules s^{-1}. The values obtained for k_{uni} are plotted versus temperature in Figure 2. At the

temperatures of decomposition (625-925 K), k_{uni} is in the fall-off range, so that the respective high-temperature Arrhenius parameters were obtained through RRKM calculations (see Appendix and Table II) using a transition-state model (six-membered ring). The calculation fits the data for the following high-pressure Arrhenius parameters (Figure 2):

$$\log (k_6/s^{-1}) = 1200 - 38.4/\theta \quad \langle T \rangle = 800 \text{ K} \qquad (8)$$

The activation energy is believed to fit the data to within ± 1 kcal/mol with a concomitant uncertainty of ± .27 in $\log (A_6/s^{-1})$.

C. Benzylvinylether

In an attempt to study the bond-breaking process to produce ethanal-2-yl radical ($\dot{C}H_2CHO$) without interference from a lower energy (molecular elimination) reaction path, benzylvinylether was decomposed. The reaction system under investigation was the following:

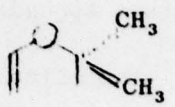
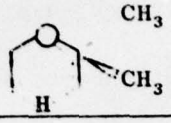
$$C_7H_7OC_2H_3 \xrightarrow{k_9} C_7H_7\cdot + CH_2\dot{C}HO \qquad (9)$$

$$C_7H_7\cdot + DI \xrightarrow{k_{10}} C_7H_7D + I\cdot \qquad (10)$$

The extent of decomposition of benzylvinylether was followed by trapping one of the reaction products, benzyl radical, with an excess of DI to produce toluene-d_1 (C_7H_7D), which could readily be monitored at m/e = 93. This method was necessary because benzylvinylether had only a very small intensity molecular

Table II

MOLECULAR PARAMETERS ENTERING THE RRKM-CALCULATION OF THE RETRO-ENE REACTION OF t-BUTYLVINYLETHER. $t\text{-}C_4H_9OC_2H_3 \rightarrow i\text{-}C_4H_8 + CH_3CHO$

	Molecule 	Activated Complex 
Frequencies and degeneracies	2940(6) 2900(3) 2870(3) 1640(1) 1430(3) 1380(5) 1220(4) 1000(4) 900(3) 650(4) 580(1) 450(4) 350(4) 250(1) 220(3) 80(1) 60(1)	2940(6) 2900(3) 2870(3) 1640(1) 1430(3) 1380(5) 1220(3) 1000(4) 900(3) 650(4) 580(1) 450(4) 350(4) 330(3) 250(1) 220(2)
$10^{120} I_A I_B I_C$ / (gr cm^2)^3	$2.05 * 10^7$	$2.05 * 10^7$
E^0 / kcal/mol		38.0
S^0_{300} / e.u.	93.40	85.80
$\log(A_{800} / s^{-1})$		12.00
E^∞_{800} / kcal/mol		38.4
$\log(A_{300} / s^{-1})$		11.83
E^∞_{300} / kcal/mol		38.0

ion peak m/e = 134 (< 1% of base peak at m/e = 91) and other minor fragmentation peaks, so that it proved to be impossible to monitor accurately the disappearance of the parent compound through its fragmentation pattern. The concentration of the excess component DI was chosen to give a yield >95% for reaction using the recently measured rate constant k_{10} at these temperatures.[8] Special attention was paid to the requirement of working at low concentrations of benzylvinylether ($F^i_{EVE} \leq 3 * 10^{14}$ molec s^{-1}) in order to suppress the recombination reaction of benzyl and ethanal-2-yl radicals to form 3-phenylpropanol, which was indeed identified by its mass spectrum (m/e = 134, 105, 92, 91) at flow rates of benzylvinylether higher than $3 * 10^{14}$ molecules s^{-1}. Figure 3 displays the results of the unimolecular decomposition of benzylvinylether at flow rates $\leq 3 * 10^{14}$ molec s^{-1} in the form k_{uni}/s^{-1} versus T/K.

In order to determine the high-pressure Arrhenius parameters for the bond scission process, RRKM calculations were performed using the well known vibrational model often mentioned in the literature.[9] (See Appendix and Tables III and IV). The results of these calculations are plotted in Figure 3, together with the experimentally determined rate constants k_{uni}. The calculation fits the data for the following high-pressure Arrhenius parameters:

$$\log(k_9/s^{-1}) = (15.05 \pm .30) - (49.30 \pm 1.00)/\theta \qquad <T> = 750\ K \qquad (11)$$

Table III

THERMOCHEMICAL QUANTITIES (Standard State: 1 atm)

	Footnote	S^0_{300} / e.u.	$C_{p,500}$/e.u.	ΔS^0_{300}/e.u.	ΔS^0_{750}/e.u.
$C_7H_7OC_2H_3$	a	103.60	61.60		
$C_7H_7^{\cdot}$	b	75.30	40.08		
$\dot{C}H_2CHO$	c	64.63	18.31		
CH_3CHO	d	67.50	18.20		
$C_7H_7OC_2H_3 \rightarrow C_7H_7^{\cdot} + \dot{C}H_2CHO$				36.33	33.12

[a] Reference 6. *This value could be ~ 3 e.u. too high given intramolecular interactions* in the ether (c.f., ethylvinyl ether).

[b] Reference 10.

[c] $S^0_{300}(\dot{C}H_2CHO) = S^{int}_{300}(CH_3CHO) + R\ln 2(\text{spin}) - R\ln 2(\text{symmetry}) - S^0(C{-}H)_{3100} -$

$-2S^0(H{-}C{<})_{1500} + 3\ R\ln 43/44(\text{transl + rot.}) + 1/2\ R\ln \frac{1.71}{2.76}(\text{int. rot.}) = 64.63$ e.u.

$C_p(\dot{C}H_2CHO) = C_p(CH_3CHO) - C_p(C{-}H)_{3100} - 2C_p(HCH)_{1500} - C_p(CH_3{-}CHO)_{V=1.2} +$

$+ C_p(\dot{C}H_2{-}CHO)_{V\cong 3} = 18.31$ e.u.

[d] Reference 6.

Table IV

MOLECULAR PARAMETERS ENTERING THE RRKM-CALCULATION OF THE RATE CONSTANT FOR THE REACTION BENZYLVINYL ETHER → $C_7H_7^{\cdot}$ + $^{\cdot}CH_2CHO$

	Molecule 	Activated Complex 
Frequencies and degeneracies	3080(7) 2930(3) 1590(5) 1360(5) 1170(5) 1100(1) 1020(3) 950(6) 830(3) 690(2) 610(1) 540(3) 340(2) 280(4) 200(2) 80(1)	3050(9) 2820(1) 1740(1) 1510(6) 1330(3) 1110(6) 990(5) 880(3) 760(1) 690(2) 610(2) 510(1) 420(4) 380(2) 250(1) 150(4) 100(1)
$r(C\text{-}O)/\mathring{A}$	1.33	1.33 * 2.5 = 3.32
$10^{120}I_A I_B I_C$ [a] / (gr cm²)³	3.055 * 10^8	8.056 * 10^8
I^+ / I		1.45
$10^{40}I_r$(phenyl) / gr cm²	73.0	
$10^{40}I_r$(benzyl-2-ethanalyl)		50.0
S^o_{300} / e.u.	99.80	105.62
log A_{300} / s^{-1}		14.50
log A_{750} / s^{-1}		15.05
E^o / kcal/mol		47.0
E_{750} / kcal/mol		49.3

[a] One external rotation was chosen to be active in the activated complex.

D. Reactions of 2-Ethanalyl Radical ($\dot{C}H_2CHO$)

Two groups of experiments were performed: (1) one in which F^i_{BVE} did not exceed approximately $8 * 10^{13}$ molecules s^{-1} ("low" flow rates of benzylvinylether) and (2) the other with $F^i_{BVE} \simeq 5 * 10^{15}$ molecules s^{-1} ("high" flow rates).

At "low" flow rates of benzylvinylether, CH_3CHO (m/e = 44, 43, 29), CH_2CO (m/e = 42, 14), and CO (m/e = 28) were detected mass spectrometrically. Upon addition of DI, CH_2DCHO (m/e = 45, 44, 29) appeared, CH_2CO disappeared, and CO formation was attenuated with respect to experiments without DI. Therefore, it is believed that at low flow rates, the reactions (12) and (13) are operative:

$$2\dot{C}H_2CHO \rightarrow CH_3CHO + CH_2{=}C{=}O \qquad (12)$$

$$\dot{C}H_2CHO \rightarrow CH_3\dot{C}O \rightarrow \dot{C}H_3 + CO \qquad (13)$$

The fast homogeneous disproportionation reaction (12) apparently takes place even at low flow rates, whereas the decomposition of $\dot{C}H_2CHO$ (13) is thought to take place on the walls of the reaction vessel, the first step being exothermic by about 10 kcal/mol.* We attempted direct detection of the radicals by using low electron voltage (LEV), but the intensities were below our limits of detectability.

At high flow rates of benzylvinylether, LEV experiments indicated no $\dot{C}H_2CHO$ radicals present; a finding which was further supported by the results

*Assuming a stabilization energy for 2-ethanalyl radical of 2.00 kcal/mol. See discussion.

of experiments of decomposition of benzylvinylether with DI, which gave indication of the presence of only small amounts of CH_2DCHO or CH_3DCO (m/e = 45). However, in the runs with DI, CH_3CHO and CH_2CO were found which means that at high levels of $\dot{C}H_2CHO$ the disproportionation reaction (12) is sufficiently fast to compete with reaction (14):

$$\dot{C}H_2CHO + DI \rightarrow CH_2DCHO + I^{\cdot} \qquad (14)$$

Furthermore, in runs with DI, $\dot{C}H_3$ radical was indirectly detected as CH_3D (m/e = 17, 16, 15) and CO occurrence was again attenuated due to removal of $\dot{C}H_2CHO$ radical. A series of fast secondary reactions, probably involving H-atoms, apparently takes place at higher flow rates as indicated by the appreciable intensities of the peaks at m/e = 78, 79, 104, 105, 106.

IV DISCUSSION

The high-pressure Arrhenius activation energy for the retro-ene reaction of ethylvinylether is in good agreement with the values reported in the literature.[1] RRK calculations* suggest that the occurrence of the higher energy reaction path of C-O bond fission at 1300 K may have escaped the present detection techniques due to the unfavorable ratio of the rate constants

---

*$\log(k_1/s^{-1}) = 11.5 - 44.5/\theta$, $\log(k_2/s^{-1}) = 15.0 - (65.0 \pm 2)/\theta$, where k_1 refers to the retro-ene reaction and k_2 refers to the C-O bond scission reaction.

of the molecular elimination mode (k_1) to the homolytic C-O bond-scission mode (k_2). This argument is further strengthened if one keeps in mind that the C-O bond strengths are known to be accurate only to $\pm$ 2 kcal/mol. In the case of the thermal decomposition of t-butylvinylether, RRK calculations indicate* a ratio k_1/k_2 = 220 at T = 900 K, which almost certainly rendered the detection of the higher energy reaction path with respect to the retro-ene reaction impossible using the present experimental technique. The Arrhenius activation energy for the retro-ene reaction of t-butylvinylether falls within the expected range. The present value is higher and believed to be more reliable than the one from the classical high-pressure static experiment[11] for reasons cited above (narrow range of temperatures). Since the attempt of studying the reactivity of ethanal-2-yl radical failed using ethylvinylether and t-butylvinylether as a source, we chose a compound whose lowest energy reaction path was a bond fission process to give the desired radical ($\dot{C}H_2CHO$). The bond fission of the C-O bond in benzylvinylether is the lowest energy reaction path and yields benzyl and ethanal-2-yl radicals unencumbered by the reaction products of the retro-ene reaction. The determination of the Arrhenius activation energy for the bond split reaction in BVE yields the heat of formation and the stabilization energy of ethanal-2-yl radical under the

---

* $\log(k_1/s^{-1}) = 11.85 - 38.0/\theta$, $\log(k_2/s^{-1}) = 15.0 - 60/\theta$.

constraint of the following assumptions: (1) known standard heats of formation of benzyl radical ($\Delta H^{o}_{f,300}(C_7H_7^{\cdot})$), (2) known C_p values for benzylvinyl ether, benzyl, and ethanal-2-yl radical as a function of temperature, (3) known overall entropy change for the bond fission reaction (ΔS^{o}), and (4) known rate of recombination of the radicals at the temperature of decomposition of benzylvinylether.

The Arrhenius activation energy for the homolytic C-O bond fission of benzylvinylether may be identified with ΔE^{o} for the reaction if the activation energy for the recombination reaction of benzyl and ethanal-2-yl radical is assumed to be zero at the temperature of decomposition. Accordingly, ΔH^{o} = 50.8 ± 1.0 kcal/mol at 750 K and with the $C_{p,500}$ values of Table III, one obtains the bond dissociation energy (= ΔH^{o}_{300}) at 300 K for reaction (9): (9): ΔH^{o}_{300} = 52.2 ± 1.0 kcal/mol. The heat of formation of the species involved in reaction (9) are related through relation (15):

$$BDE(C_7H_7\text{-}OC_2H_3) = \Delta H^{o}_{300} = \Delta H^{o}_{f,300}(C_7H_7^{\cdot}) + \Delta H^{o}_{f,300}(\dot{C}H_2CHO) - \Delta H^{o}_{f,300}(C_7H_7OC_2H_3) \quad (15)$$

With the group additivity value of −1.73 kcal/mol[6] for the standard heat of formation of benzylvinylether, and a recent value for the heat of formation fo benzyl radical (46.5 kcal/mol[8]), one obtains a value of 3.90 ± 2.0 kcal/mol for $\Delta H^{o}_{f,300}(\dot{C}H_2CHO)$. On the basis of a value of 98.0 kcal/mol for

the bond strength in $H\text{-}CH_2CHO$, corresponding to BDE of a bond in a normal alkane, $\Delta H^o_{f,300}(\dot{C}H_2CHO)$ would be 7.1 kcal/mol. The difference between the "hypothetical" standard heat of formation of $\dot{C}H_2CHO$ (7.1 kcal/mol) and the above experimental value of 3.9 ± 2.0 kcal/mol is the resonance stabilization energy (SE) due to delocalization of the unpaired electron over the 3-center π-system analogous to allyl radical and is computed to be 3.2 ± 2.0 kcal/mol. This value for the resonance stabilization energy compares well (within the uncertainties) with the values recently found for the closely related acetonyl radical ($CH_3C\dot{O}CH_2$)[12] and is significantly lower than the allyl resonance stabilization energy of 12.0 ± 1 kcal/mol.[3] If the activation energy for the C-O bond fission of benzylvinylether is identified with ΔH^o for the reaction (i.e., the activation energy for the recombination of benzyl and ethanal-2-yl radical is assumed to be zero at 0 K, and RT at the temperature of decomposition), one computes $\Delta H^o_{f,300}(\dot{C}H_2CHO)$ = 2.4 ± 2.0 kcal/mol and SE = 4.7 ± 2.0 kcal/mol.

V REFERENCES

(Chapter 3)

1. G. G. Smith and F. W. Kelley, Progr. Phys. Org. Chem., 8, 75-234 (1971).

2. R. N. Rosenfeld, J. I. Brauman, J. R. Barker, and D. M. Golden, J. Amer. Chem. Soc., 99, 8063 (1977).

3. M. Rossi, K. D. King, and D. M. Golden, submitted to J. Amer. Chem. Soc.

4. D. M. Golden, G. N. Spokes, and S. W. Benson, Angew. Chem., 84, 602 (1973).

5. W. H. Watanabe and L. E. Conlon, J. Amer. Chem. Soc., 79, 2828 (1957); H. Yuke, K. Hatada, K. Nagata, and K. Kajiyma, Bull. Chem. Soc. (Japan), 42, 3546 (1969).

6. Estimated rate expression following the methods outlined in S. W. Benson, Thermochemical Kinetics, 2nd Ed., John Wiley and Sons, Inc., New York (1976).

7. D. M. Golden, R. K. Solly, and S. W. Benson, J. Phys. Chem., 75, 1333 (1971).

8. M. Rossi and D. M. Golden, submitted to J. Amer. Chem. Soc.

9. W. Forst, Theory of Unimolecular Reactions, Academic Press, New York (1973).

10. H. E. O'Neal and S. W. Benson, Int. J. Chem. Kinetics, 1, 221 (1969).

11. T. O. Bamkole and E. U. Emovon, J. Chem. Soc., (B) 1968, 332.

12. F. Zabel, D. M. Golden, and S. W. Benson, Int. J. Chem. Kinetics, 10 295 (1978), and references therein.

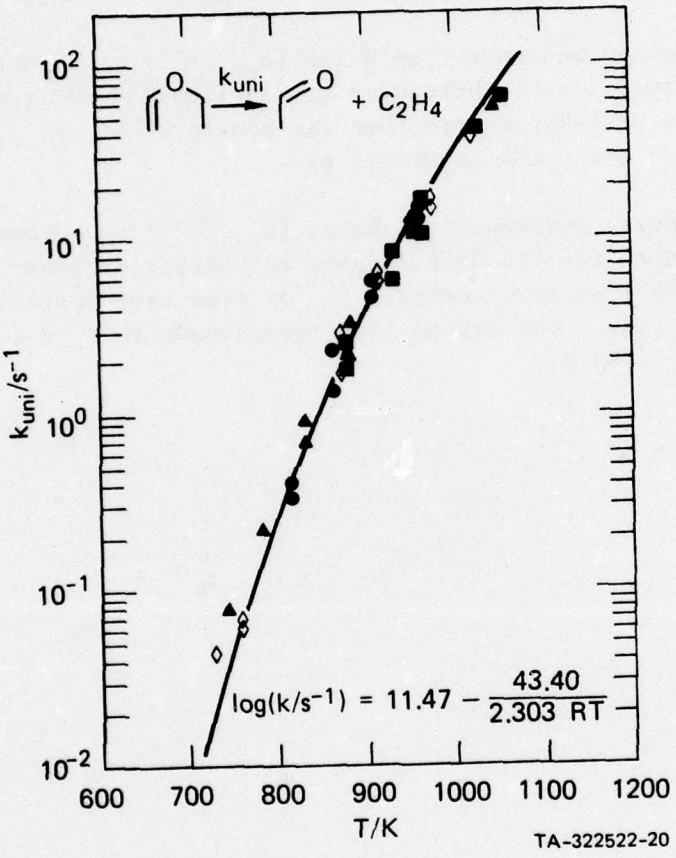
CAPTIONS

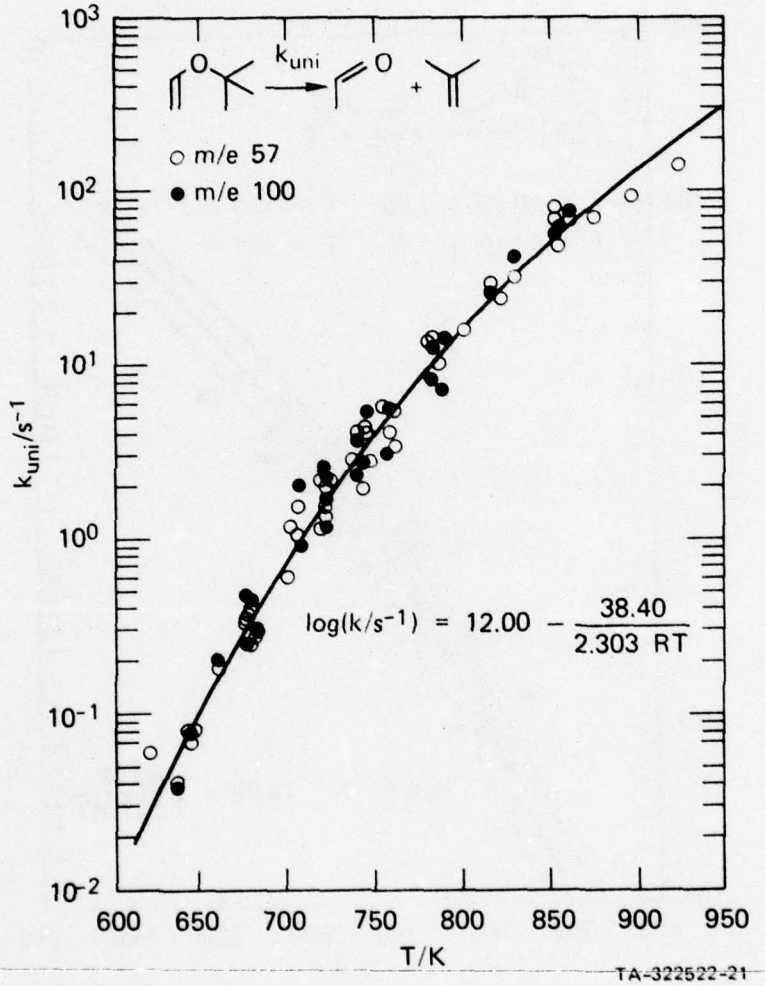
Figure 1 Unimolecular Decomposition Rates (k_{uni}/s^{-1}) as a Function of Temperature for the Molecular Elimination Mode of Ethylvinylether. (■, ▲, ●, ◇ represent different series of experiments)

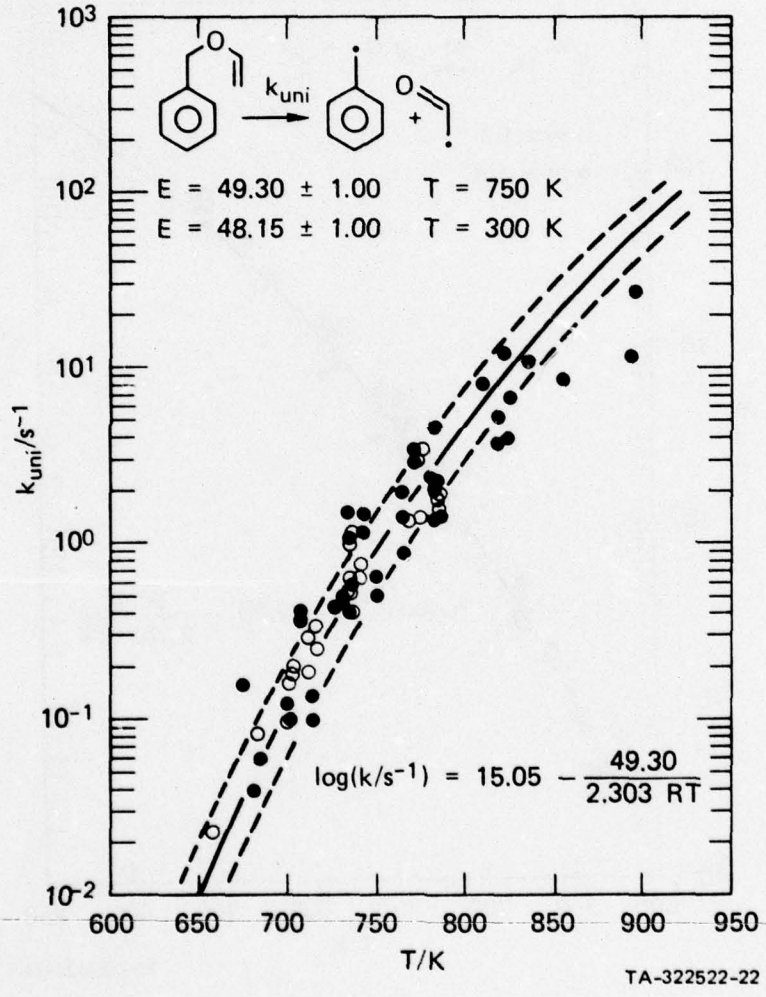
Figure 2 Unimolecular Decomposition Rates (k_{uni}/s^{-1}) as a Function of Temperature for the Molecular Elimination Mode of t-Butylvinyether. The loss of t-Butylvinylether was monitored at m/e = 57 in series o, and at m/e = 100 in series ●).

Figure 3 Unimolecular Decomposition Rates (k_{uni}/s^{-1}) as a Function of Temperature for the Bond Fission in Benzylvinylether. (●, high flow rate series; o, low flow rate series; see text for details). The dashed line corresponds to E ± 1 kcal/mol at $\langle T \rangle$ = 750 K.

PRECEDING PAGE BLANK


k_{uni}
+ C_2H_4
10^2
10^1
10^0
10^{-1}
10^{-2}
k_{uni}/s^{-1}
$\log(k/s^{-1}) = 11.47 - \frac{43.40}{2.303\ RT}$
600
700
800
900
1000
1100
1200
T/K
TA-322522-20


10^3
10^2
10^1
10^0
10^{-1}
10^{-2}
k_{uni}/s^{-1}
k_{uni}
O
O
+
○ m/e 57
● m/e 100
$\log(k/s^{-1}) = 12.00 - \frac{38.40}{2.303\ RT}$
600
650
700
750
800
850
900
950
T/K
TA-322522-21


10^3
10^2
10^1
10^0
10^{-1}
10^{-2}
k_{uni}/s^{-1}
k_{uni}
E = 49.30 ± 1.00 T = 750 K
E = 48.15 ± 1.00 T = 300 K
$\log(k/s^{-1}) = 15.05 - \frac{49.30}{2.303\ RT}$
600 650 700 750 800 850 900 950
T/K
TA-322522-22

Appendix

In this section, details about the RRKM calculations shall be given. The reader is referred to Tables I-IV of the text which display the actual numerical values used in the calculations.

Ethylvinylether

A rather complete structural investigation of methylvinylether ($C_2H_3OCH_3$)[1] indicated the existence of nonbonded attractive interactions between the methyl and vinyl groups, a result recently obtained by ab initio calculations as well.[2] Calculating the entropy of methylvinylether at 300 K, following group additivity methods,[3] yields $S^o_{300}(CH_3OC_2H_3)$ = 73.50 e.u., whereas the result of an entropy calculation on the basis of the assigned frequencies experimental geometry (cis-planar conformation) of methylvinylether[1] reveals a value of 69.30 e.u., reflecting the nonbonded attractive interactions or higher degree of stiffness in that molecule.* About 3.0 e.u. of the total entropy difference of 4.20 e.u. can be accounted for by assigning substantial barriers to internal rotation to the O-vinyl internal rotation (3.3 kcal/mol) and O-methyl internal rotation (3.0 kcal/mol) in methylvinylether. The group additivity value for the entropy of ethylvinylether is 83.30 e.u. and was corrected by 3.0 entropy units to give 80.30 e.u. to account for the barriers to internal rotation. Except for the introduction of $CH_3^{\cdot}$ instead of $H^{\cdot}$, only

*A barrier to internal rotation of about 3.3 kcal/mol for the O-vinyl torsion results in the same entropy contribution as the experimentally observed torsion of frequency $\nu = 220 \pm 20$ cm^{-1} (reference 1).

minor corrections of the vibrational frequencies of methylvinylether had to be carried out in order to predict the frequencies for ethylvinylether to give a value of $S^0_{300}(C_2H_5OC_2H_3)$ = 80.30 e.u. The frequencies of the six-membered transition state for reaction (2) were then chosen in such a way to result in the experimentally observed Arrhenius A-factor of $10^{11.47}$ s^{-1} at $<T>$ = 900 K (the temperature dependence of log A is negligible, c.f., Table I). Basically, the three hindered internal rotations, together with some of the low-frequency bending modes of ethylvinylether were replaced by higher frequency out-of-plane ring bending modes, which were only slightly lower than the corresponding out-of-plane frequencies in benzene, in order to simulate the stiff six-membered ring transition state, where six electrons were redistributed similar to an aromatic hydrocarbon π-system. A list of the molecular parameters for the molecule and activation complex is presented in Table I of the text.

t-Butylvinylether

The published high-pressure Arrhenius A-factor for reaction (6)[4] was recognized to be too low together with too small a value for the activation energy, probably due to the rather restricted range of temperatures used in assessing the Arrhenius parameters. The A-factor was, therefore, obtained by making a correction of + .48 to log A = 11.47 for the corresponding reaction of ethylvinylether due to reaction path degeneracy of 3, thereby obtaining log A $\simeq$ 12.00 for reaction (6) at $<T>$ = 800 K. The concomitant assumption is that with respect to ethylvinylether, the lower frequency torsions due to the heavier masses in t-butylvinylether are balanced by lower ring puckering or ring out-of-plane deformation modes in the activated complex.[3] The group additivity value for t-butylvinylether (S^0_{300} = 96.40 e.u.)

AD-A056 022 SRI INTERNATIONAL MENLO PARK CA F/G 7/4
THE ABSOLUTE MEASUREMENT OF RATE CONSTANTS FOR SOME KEY REACTIO--ETC(U)
APR 78 D M GOLDEN, M ROSSI, G P SMITH F44620-75-C-0067
UNCLASSIFIED AFOSR-TR-78-1068 NL

2 OF 2
AD
A056 022



END
DATE
FILMED
8-78
DDC

was decreased by 3.0 e.u. to give 93.40 e.u. to account for (assumed) attractive nonbonded interactions analogous to the case of ethylvinylether. The frequencies of the molecule were chosen to correspond to S^{o}_{300} = 93.40 e.u., and the ones for the activated complex were determined in such a way to be compatible with log A = 12.00. Table II discloses the details of the molecule and activated complex parameters entering the RRKM calculation.

Benzylvinylether

The Arrhenius A-factor for reaction (9) was computed from the overall entropy change, ΔS^{o} (Table III), and the assumed rate constant for the recombination reaction (-9), $\log(k_{-9}/M^{-1}\ s^{-1}) = 10.00$. The assumption concerning the recombination reaction in the present study is, that it has no activation energy at T = 750 K ($E_r = 0$), so that one can identify the Arrhenius activation energy E_d for the bond fission process (9) with ΔE^{o} for the reaction. This yields the following A_d-factor at T = 750 K through relation (16):

$$R\ln\frac{10^{10}}{A_d} = -33.12 + 10.16^{*} \quad \therefore \log(A_d/s^{-1}) = 15.02 \qquad (16)$$

The value of 15.02 for log A_d compares well with the ones for the similar bond scission processes (17) and (18):

$$C_6H_5C_2H_5 \rightarrow C_7H_7^{\cdot} + \dot{C}H_3 \qquad \log(A_d/s^{-1}) = 14.60 \text{ at } \langle T\rangle = 950 \text{ K}^{5} \qquad (17)$$

$$C_6H_5C_3H_7 \rightarrow C_7H_7^{\cdot} + C_2H_5^{\cdot} \qquad \log(A_d/s^{-1}) = 14.90 \text{ at } \langle T\rangle = 950 \text{ K}^{5} \qquad (18)$$

---

* 10.16 represents the correction term $(R(1 + \ln R'T_m))$ for the change of standard states; R is the gas constant in units of cal $mol^{-1}\ K^{-1}$, and R' is in units of ℓ atm $mol^{-1}\ K^{-1}$.

The group additivity value for S^0_{300} of benzylvinylether was taken to be too large by ~3 cal K^{-1} mol^{-1} as in the case of methylvinylether for reasons of intramolecular interactions,[1] so that the molecular vibrational frequencies and moments of inertia were chosen to match $S^0_{300} = 99.80$, instead of $S^0_{300} = 103.60$.[6] The entropy of the activated complex was then chosen to be compatible with log $A_d = 15.02$. Table IV shows the details of the molecular and activated complex parameters for the RRKM calculation.

References to Appendix

1. P. Cahill, L. P. Gold, N. L. Owen, J. Chem. Phys., 48, 1620 (1968); N. L. Owen and H. M. Seip, Chem. Phys. Lett., 5, 1621 (1970).

2. F. Bernardi, N. D. Epiotis, R. Yates, and H. B. Schlegel, J. Amer. Chem. Soc., 98, 2385 (1976).

3. Estimated rate expression following the methods outlined in S. W. Benson, Thermochemical Kinetics, 2nd Ed., John Wiley and Sons, Inc., New York (1976).

4. T. O. Bamkole and E. U. Emovon, J. Chem. Soc., (B) 1968, 332.

5. G. L. Esteban, J. A. Kerr, and A. F. Trotman-Dickenson, J. Chem. Soc., 3873 (1963).

[Reprinted from the Journal of the American Chemical Society, 99, 8063 (1977).]
Copyright 1977 by the American Chemical Society and reprinted by permission of the copyright owner

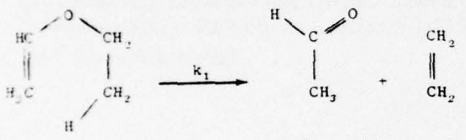
Chapter 4

Infrared Photodecomposition of Ethyl Vinyl Ether. A Chemical Probe of Multiphoton Dynamics

Sir:

Chemistry following multiphoton absorption[1] may, in general, involve collisionless *and* collision-induced processes.[2] The dynamics and time regimes associated with these processes remain to be well characterized experimentally. We report here the CO_2 TEA-laser photolysis of ethyl vinyl ether (EVE, **1**) and its relevance to these questions.

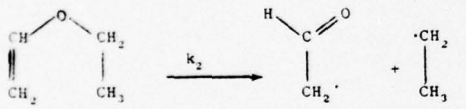
Conventional pyrolysis[3] of EVE yields ethylene and acetaldehyde by a retro-ene molecular elimination (eq 1).



$$\log[k_1/s^{-1}] = 11.6 - \frac{44,400}{2.303RT} \quad (1)$$

1

Decomposition with a focused laser yields not only these conventional products but also comparable amounts of ketene, ethane, and butane.[4] This suggests that a simple bond fission process[5] (eq 2) competes effectively with eq 1 upon multi-



$$\log[k_2/s^{-1}] = 15 - \frac{65,800}{2.303RT} \quad (2)$$

photon excitation.[6] Ketene is formed by subsequent disproportionation reactions of $\cdot CH_2CHO$ and the ratio $[CH_3CHO]/[CH_2CO]$ provides a measure of the relative rates of processes 1 and 2. This ratio, as a function of pressure, is as follows: 1.89 (440 Torr), 1.89 (280), 1.64 (230), 1.45 (25), 1.44 (20), 1.71 (11), 1.79 (10), 1.86 (10), 1.84 (5), and 1.75 (10 + 40 torr of He). Thus, $k_1 \simeq 0.37\ k_2$ over the pressure range studied. Irradiation with an unfocused beam yields only ethylene and acetaldehyde.

The two reactions compete at high energies since the reaction channel density for eq 2 exceeds that for eq 1 (as reflected in their A factors). A number of molecules will exhibit similar behavior if their lowest thermal path involves a cyclic transition state,[6] but EVE is especially interesting since the difference in activation energies for its two lowest energy channels is large, thereby increasing the dynamic range available for studying the energy distribution of reacting molecules.

Our experimental results can be considered in terms of the following steps: laser pumping, $A(E) \rightarrow A(E')\ \{k_p(I,E)\}$; collisional energy pooling or deactivation, $M + A(E') \rightarrow M + A(E'')$, $\{k_c\}$; and, reaction via channel i, $A(E) \rightarrow (\text{products})_i$, $\{k_i(E)\}$. Such a scheme calls attention to the various competitive processes, each of which may dominate under different experimental conditions.[7]

In our pressure range, ~1–100 collisions occur during the laser pulse. The observed lack of pressure dependence thus suggests that most the chemistry occurs after the pulse. Furthermore, assuming the applicability[7,9,10] of a quantum RRK model,[11] we find that $k_1(E)$ and $k_2(E)$ are comparable at $\sim 10^6$–$10^7\ s^{-1}$, which is $\lesssim$ collision frequency, implying that our results are predominantly collisional. Collisions between molecules in the irradiated region occur rapidly compared with escape and subsequent cooling, since the mean free path is small at our pressures. (Isotopic specificity may still obtain under these conditions since collisions with "cold" molecules are simply deactivating.) Therefore, in our experiments, the chemistry appears to be that of a collisionally (V–V) thermalized system. This is also consistent with recent experiments[10] which suggest that, at energy fluences of ~1 J cm^{-2}, although considerable excitation occurs, only a small fraction of excited molecules react. The low conversions typically observed in this regime are thus consistent with an energy distribution function that decreases monotonically above E_c, the threshold for reaction. Consequently, the collisional nature of this chemistry indicates the Arrhenius forms of k_1 and k_2 can be used in expressing the yield ratio, giving a temperature of ~1600 K. The temperature dependence of k_1/k_2 (for T = 300, 1000, 2000 K, $k_1/k_2 = (0.55 \times 10^{12}, 18.94, 8.68 \times 10^{-2})$ indicates the sensitivity of the branching ratio of EVE as a probe of excitation. The cleanliness of IR-laser photolysis relative to the high temperature pyrolysis[3] of EVE suggests this is an attractive alternative to conventional activation techniques. Evidence indicates that increasing fluence will raise the apparent "temperature"[11] so that eq 2 would compete more effectively with eq 1.

In summary, we have developed a sensitive chemical probe of energy distribution applicable to bulk and collisionless systems. Our results are consistent with recent studies[10,12] in terms of lifetimes and energy distribution functions. We are currently studying the intensity and buffer dependence of k_1/k_2

PRECEDING PAGE BLANK

and extending our experiments to include the collisionless regime by increasing fluence and decreasing pressure.

Acknowledgments. We thank Dr. Donald J. Eckstrom and Mr. Howard Young for technical assistance. The authors at Stanford University acknowledge the financial support of the National Science Foundation and the donors of the Petroleum Research Fund, administered by the American Chemical Society. The authors at SRI International acknowledge financial assistance provided by the Air Force Office of Scientific Research under Contract No. F44620-75-C-0067 with SRI International.

References and Notes

(1) (a) R. V. Ambartzumian and V. S. Letokkov, *Acc. Chem. Res.*, **10**, 71 (1977); (b) J. J. Ritter and S. M. Freund, *J. Chem. Soc., Chem. Commun.*, 811 (1976); (c) I. Glatt and A. Yogev, *J. Am. Chem. Soc.*, **98**, 7078 (1976); (d) A. Yogev and R. M. J. Benmair, *ibid.*, **97**, 4430 (1975).

(2) J. M. Preses, R. E. Weston, and G. W. Flynn, *Chem. Phys. Lett.*, **46**, 69 (1977).

(3) A. T. Blades and G. W. Murphy, *J. Am. Chem. Soc.*, **74**, 1039 (1952). At high temperatures, a variety of radical processes were found to intervene.

(4) Our excitation source was the SRI grating-tuned CO_2 TEA-laser operating on the 10.5 μm, P(14) line. Pulse energies were 0.3 J (measured with a calibrated thermocouple detector) and pulse widths were ~100 ns (measured with a Molectron J3 pyroelectric detector). The laser was run at a PRF of 0.5 Hz, and the output (beam diameter, ~2.5 cm) was focused with a spherical Al-coated mirror (focal length, 1 m) into a brass reaction cell (4 cm × 1 cm i.d.) fitted with KCl windows. Products were determined by flame ionization GC. Products were identified by their IR spectra and GC comparison with authentic samples. Photolyses were run for 200 pulses and the cell windows were replaced periodically as a check for heterogeneous effects.

(5) The Arrhenius parameters shown in eq 2 were estimated using methods described in S. W. Benson, "Thermochemical Kinetics", Wiley, New York, N.Y., 1976.
Similar effects are noted in the IR-laser photolysis of alkyl iodides.

(6) See W. Braun and W. Tsang, *Chem. Phys. Lett.*, **44**, 354 (1976).

(7) The average rate of a process i, $\langle k_i(E) \rangle$, can be formulated using a generalized Lindemann model.[9] The resulting expression depends on the rates of radiative and collisional activation and deactivation, decomposition, laser power, and pulse width. The time evolution of $k_i(E)$ depends on the relative rates of laser pumping, energy pooling, deactivation, and reaction and can be determined using a kinetic master equation. Work in this regard is in progress in our laboratories.

(8) W. Forst, "Theory of Unimolecular Reactions", Academic Press, New York, N.Y., 1973, Chapter 8.

(9) E. R. Grant, M. J. Coggiola, Y. T. Lee, P. A. Schulz, and Y. R. Shen, unpublished work.

(10) J. G. Black, E. Yablonovitch, N. Bloembergen, and S. Mukamel, *Phys. Rev. Lett.*, **38**, 1131 (1977).

(11) P. J. Robinson and K. A. Holbrook, "Unimolecular Reactions", Wiley, New York, N.Y., 1972.

(12) M. J. Coggiola, P. A. Schulz, Y. T. Lee, and Y. R. Shen, *Phys. Rev. Lett.*, **38**, 17 (1977).

Robert N. Rosenfeld, John I. Brauman*
Department of Chemistry, Stanford University
Stanford, California 94305

John R. Barker, David M. Golden*
Thermochemistry and Chemical Kinetics Group
SRI International, Menlo Park, California 94025
Received June 13, 1977

Chapter 5

APPLICATION OF RRKM THEORY TO THE REACTIONS $OH + NO_2 + N_2 \rightarrow HONO_2 + N_2$ (1) and $ClO + NO_2 + N_2 \rightarrow ClONO_2 + N_2$ (2); A MODIFIED GORIN MODEL TRANSITION STATE.

G. P. Smith and D. M. Golden
Thermochemistry and Chemical Kinetics Group
Stanford Research Institute, Menlo Park, California 94025

ABSTRACT

We have calculated rate constants as a function of both temperature and pressure for the title reactions using RRKM theory in conjunction with a modified Gorin transition state. The modification introduces a hindrance parameter which accounts for repulsive interactions between the rotating fragments.

At the highest stratospheric pressures ($\sim$ 50 torr) and at stratospheric temperature ($\sim 220^{\circ}K$), the extent of "fall-off" from first-order $[N_2]$ dependence is $\sim$ 70% for reaction (1) and $\sim$ 35% for reaction (2).

INTRODUCTION

Nitric acid formation via,

$$OH + NO_2 + N_2 \rightarrow HONO_2 + N_2 \qquad (1)$$

is an important stratospheric reaction which functions as a sink for ozone destroying HO_x and NO_x cycles.[1] Thus rate constants are available at several temperatures and nitrogen pressures.[2-5] At stratospheric pressures, reaction (1) is in the "fall-off" region, between the low-pressure termolecular limit and the high-pressure limit where bimolecular formation of metastable nitric acid is rate determining. Hence, reaction (1) is an excellent candidate for RRKM calculations[6] in order to: (a) see if the data can be fit within the confines of the theory, using reasonable model parameters; (b) provide a basis for extrapolation and interpolation of reliable reaction (1) data to other temperatures and pressures; and (c) pursue a priori criteria for the future selection of transition state parameters in simple bond fission reactions.

In furtherance of this last goal, we have adapted our successful model for reaction (1) to predict stratospheric rates of the analogous reaction:

$$ClO + NO_2 + N_2 \rightarrow ClONO_2 + N_2 \qquad (2)$$

This reaction is being extensively examined as a sink for ozone-destroying stratospheric chlorine species, which are introduced via chlorofluorocarbon propelled aerosols,[7] but very few experimental rate constants are currently available.[8]

PRECEDING PAGE BLANK

BACKGROUND

Recent advances in the understanding of unimolecular reactions have made it clear that a simple "fixed" transition state is an inadequate model for simple bond fission reactions. These advances have come from two directions, the microcanonical approach as exemplified by the work of Troe and coworkers,[9] and the canonical approach which we have favored.[10]

In the microcanonical view, Quack and Troe[9] have illustrated the problem by pointing out that individual open reaction channels may have maxima at various locations along a specified reaction coordinate. They have formulated their "Adiabatic Channel Model," taking this into account and using a single universal parameter to describe the potential surfaces for bond scission in a number of small polyatomic systems. (They have also recently presented[9c] a canonical model which in some ways is similar to that to be presented herein.)

In the canonical view,[10] we have postulated a transition state which can become "tighter" as the temperature increases. As a result of the decrease in position of the centrifugal maximum, the rotation of the product fragments is increasingly restricted. We thus introduce a hindrance parameter, η, to describe this tightness. If η is independent of temperature, we have a model which is equivalent to Reference 9c; if it is T dependent, we have introduced a second parameter.

The recombination rate k_1 can be deduced from the RRKM unimolecular decomposition rate k_{-1}, since $k_1 = K_{eq}k_{-1}$. RRKM theory[6] is a statistical theory which assumes fast random access by allowed internal states to molecular energy E^*, and a unique critical configuration along one coordinate, which is

PRECEDING PAGE BLANK

intermediate to all decompositions. Hence the important parameters for the calculation relate to the structure of this transition state. The rate is given by:

$$k_{uni} = \frac{Q_1^+ \, e^{-E_0/kT}}{hQ_1Q_2} \int \frac{G(E^+)e^{-E^+/kT} \, dE^+}{1 + Q_1^+ G(E^+)/hQ_1N(E^*)F\beta\omega} \qquad (3)$$

where E_0 is the critical energy, E^* is the total energy, and $E^+ = E^* - E_0$ is the maximum energy of the critical configuration; $G(E^+)$ is the sum of the states of the complex below energy E^+ and $N(E^*)$ is the density of molecular states; Q_1^+/Q_1 is the partition function ratio of the inactive modes (moments of adiabatic rotors), and Q_2 is the partition function for the active molecular modes; F is the Waage-Rabinovitch[11] centrifugal correction term for conservation of angular momentum among the adiabatic rotations, ω is the (Lennard-Jones) collision frequency of excited substrate with bath gas at pressure P, and β is the collisional efficiency for stabilization (sufficient energy removal). Our calculations used the Stein-Rabinovitch algorithm[12] to compute $G(E^+)$ and $N(E^*)$.

DETAILS OF THE CALCULATION

For our calculations, K_{eq} is computed from the JANAF Tables.[13] These same tables furnished the molecular frequencies for computing $N(E^*)$, and the dissociation energy of $HONO_2$ for computing E_0. We chose the top of the centrifugal barrier for a Lennard-Jones potential as the position of the critical configuration along the bond axis; we have[14]

$$Q_1^+/Q_1 = I^+/I = (r^+/r_0)^2 = (6D_e/RT)^{1/3} \qquad (4)$$

where r is the distance between the OH and NO_2 centers of mass and I^+ and I are moments of inertia in the transition state and molecule for the two-dimensional external rotation with axis perpendicular to the $HO-NO_2$ bond.

The collision frequency, ω, can be calculated by averaging the Lennard-Jones collision diameters, 5.2 Å for $HONO_2$ (estimated using the viscosity-derived hard sphere diameter[15] for NO_2Cl, since no critical data exists for $HONO_2$) with the value of 3.8 Å for N_2. Only the specification of frequencies in the critical configuration, to calculate $G(E^+)$, remains.

Previous RRKM calculations[16] for reaction (1) estimated the nitric acid transition state vibrational frequencies. This approach, however, is further complicated by the temperature dependence of these frequencies, since the critical bond stretching distance varies (see equation (4)). We have chosen a modified Gorin model[6,14] for the transition state. In the Gorin model, the internal modes of the transition state are simply the vibrations and rotations of the independent OH and NO_2 fragments (again, from the JANAF Tables[13]). Thus we have here five internal rotations, corresponding to the external rotations of the fragments. This effectively activates the external $HONO_2$ rotation about the $HO\text{---}NO_2$ bond axis, which is mostly an NO_2 rotation, and leaves only the other two external rotations inactive and adiabatic in the molecule (i.e., these modes do not share in the randomization of energy). Since the internal, fragment rotations are not actually free at the $OH\text{-}NO_2$ distance of the critical configuration, our modification introduces the aforementioned hindrance parameter, which decreases the entropy of internal rotation by decreasing the effective moment of inertia of the rotor. We thus decrease the number of available rotational states in accordance with the volume of rotational phase space excluded because of the other fragment's presence. Such a rotational model, as opposed to the usual vibrational ones, should be reasonable for recombination reactions with only centrifugal barriers, because they have loose, distant transition states.

In these calculations, the two-dimensional OH rotor and a two-dimensional NO_2 external rotation, chosen to exclude rotation about the bond axis, are each hindered. Thus, $k_\infty \propto I'_{OH} I'_{NO_2}$, where each $I' = \sqrt{1-\eta}$. Any model for estimating the hindrance of the OH rotor, for example, actually estimates a value for $\sqrt{1-\eta}$. The hindrance does not apply to the remaining, one-dimensional NO_2 rotor, which corresponds to the active molecular external rotation. This model, as applied to nitric acid, is illustrated in the appendix.

We thus have a model with two unknown parameters, the hindrance η and the collision efficiency β. There are some reasonable limiting criteria for the values and temperature dependences of these variables which are acceptable in attempting to fit the data. Previous experimental low-pressure rate constants indicate the relative efficiencies of various third bodies for a given recombination reaction.[16] For N_2, we expect $\beta \sim .3$ to $.5$. Furthermore, there is some low pressure, 296° data[4] which constrains the choice of β, as expected, to values near .5. Troe[17] has developed a theory relating k_0 and β to $\langle\Delta E\rangle$, the average energy transferred per collision. Since $\langle\Delta E\rangle$ is not expected to change much with temperature, the values of $\langle\Delta E\rangle$ derived from β used for the fitting should show only limited variation.

It is more difficult to set reasonable limits on η. By taking van der Waals radii for atomic sizes and constructing a mathematical "brick wall" half way between the transition state fragments, one value for the hindrance can be estimated by the solid angle excluded to each rotor by the wall. Such a model gives $\sim 45\%$ for 296°, but fails to include the effect of correlated motions among rotors. Furthermore, larger hindrances are required before one approaches the usual regime of loose vibrational transition states. For example, a 95% hindrance of the 2 two-dimensional internal rotors (78% each) would correspond in entropy to four 90-cm^{-1} vibrations (300°K). In view of the difficulty of choosing a priori values for η (or frequencies for the alternative

vibrational transition state model), the goal of investigating the behavior of η in this conceptually simple model by fitting data becomes apparent. Once the data are encoded in terms of this simple η parameter, a guarded transfer to similar systems may be considered. This η parameter is thus a simple empirical measure of "tightness" within the context of a Gorin type model. This Gorin model has the advantage that the lower heat capacity of the transition state, as compared to a vibrational model, is more in keeping with observation.

RESULTS

Figures 1 and 2 show the best RRKM matches to the data at 296°K, and other temperatures between 220° and 550°. A good fit, within experimental error, is obtained, although a 15% variation in β or $(1 - \eta)$ generally still fits the data. This, then, is roughly the uncertainty in our RRKM extrapolation of the falloff region data to the high pressure (k_∞) and low-pressure (k_0) rate constants. We note that our values at times do not agree with those extrapolated by Anastasi and Smith[2] using Troe's[18] Kassel integral method.

Table I lists the fitting parameters used for Anastasi and Smith's[2] data at 220°-550°K, and Glänzer and Troe's data[19] for nitric acid decomposition at 1000°K. The 1000° η and β are consistent with extrapolation of the lower temperature trends. The fit is less accurate, but the data, and hence the fitting parameters, are more uncertain.

Table I also gives values for $\langle\Delta E\rangle$ averaging 1.4 kcal/mole. The value of $\langle\Delta E\rangle \sim 1.4$ is typical of nitrogen energy removal rates from small molecules such as CH_3CN.[17] Although considerable latitude exists in the choices of $\langle\Delta E\rangle$, the table indicates $\langle\Delta E\rangle$ may decline slightly with temperature. (It should also be noted that values of β are strongly dependent on the exact calculation of the "strong collision rate constant."[17] Using Troe's method we calculate that at 296°K, $\beta \approx .37$ as opposed to .64, as reported in Table I. This difference is due to an approximate correction for anharmonicity and a more refined treatment of the torsional motion, and changes $\langle\Delta E\rangle$ from $\sim$ 2 kcal/mole to $\sim$ 0.6 kcal/mole.)

The hindrance reaches unexpedtedly high values at moderate temperatures, although increasing with temperature as predicted (since r^+ (eq. 4) decreases with temperature, internal rotations become more hindered). This suggests

PRECEDING PAGE BLANK

Table I

RRKM HINDERED GORIN MODEL PARAMETERS

T/°K	$r^+/\text{Å}$	I^+/I	β	(N_2) $\langle\Delta E\rangle$/kcal	% hindrance	$k_\infty/10^{-12}$ cm^{-3} s	$k_0/10^{30}$ cm^{-6} s	Decomposition E_a^∞ (kcal mol^{-1})	Decomposition log A^∞/s^{-1}
			Nitric Acid Recombination Fit						
220	5.25	8.80	.73	2.3	65	36.4	9.7	48.82	16.85
	6.40	13.2	.58	1.1	77	36.4	9.7	48.82	16.85
238	5.20	8.60	.61	1.3	80	21.1	6.5	48.89	16.66
265	5.10	8.30	.47	.9	80	21.3	3.9	48.97	16.71
			.63	1.7	85	16.2	5.2	48.97	16.59
296	5.00	8.00	.48	1.0	76	26.1	3.1	49.04	16.83
			.64	2.0	80	21.8	4.2	49.04	16.74
358	4.85	7.55	.51	1.4	86	16.2	2.1	49.14	16.64
450	4.70	7.00	.37	1.0	96	5.0	.84	49.18	16.10
550	4.55	6.55	.39	1.3	97	3.8	.51	49.13	15.92
1000	4.10	5.30	.11	.4(Ar)	99	1.26	.019	48.18	15.08
				Decomposition		3.2×10^4 cm^3/s	4.7×10^{-16} cm^6/s		
			Chlorine Nitrate Recombination Model						
220	6.60	9.90	1.39		60	26.0	.50	25.52	17.35
298	6.40	8.90	.83		80	14.5	.15	25.49	16.98

that the netherland between hindered rotations and torsional vibrations occurs at distances longer than our original model envisioned. (A 99% hindered rotation might more properly be viewed as a vibration.) The table also indicates some temperature-to-temperature irregularities in the variation of β and η, due perhaps to the sparsity of the data and possible errors at some temperatures.

The 220° entry in the table also illustrates an identical fit using different parameters. If η is lowered, I^+/I must be treated as a new variable and decreased to maintain the same entropy, or A-factor $k \propto (1 - \eta)(I^+/I)]$. However, since the F-factor (equation 3) also depends on I^+/I, β must be increased to balance the I^+/I decrease. Such adjustments cannot attain more reasonable high-temperature hindrance values and still retain reasonable I^+/I and β values.

The table also contains two alternate fits for 296°, which depend somewhat upon one's interpretation of the low-pressure data. Howard and Evenson[4] interpret their data in terms of an underlying bimolecular wall reaction. It is suggested from our calculations, however, that their experiments are not in the low-pressure limit, although both experiments and calculation are nearly linear in this region. Thus, great care must be used in interpreting low pressure results. We can fit the data, adjusted for their wall reaction (Figure 1, β = .48), or assuming no wall reaction (β = .64), although the former model fits the data of reference 3 better.

Finally, Figure 3 utilizes our fit of the data and the standard profile of the atmosphere[20] to calculate (roughly) the effective bimolecular rate constant for reaction (1) as a function of altitude.

EXTRAPOLATION OF THE MODEL TO $ClONO_2$

Since only a few rate constant measurements,[8] all below 10 torr, have been reported for reaction (2), the necessary inquiry into the degree of fall-off from third-order kinetics at higher stratospheric pressures suggests an RRKM calculation. The model and parameters chosen should be consistent with the successful reaction (1) fitting. In this way the hindrance concept and the data fitting approach permit an educated choice for the reaction (2) transition state.

For our reaction (2) calculations, ΔG_f^o (for calculating K_{eq}), the frequencies, and the moments of inertia for the $ClONO_2$ molecule were derived from Miller et al.,[21a] using D_0^o = 24.8 kcal/mole.[21b] The corresponding JANAF values[13] were used for the fragments. The critical distance is calculated from (4) as before.

A Lennard-Jones collision diameter of $\sim$ 5.6 Å was estimated by adjusting the nitric acid value for the larger Cl atom size. Since true low-pressure rate constants are available for reaction (2), the collisional efficiency is a completely empirical value. The three data sets[8] are in close agreement, and we have used the values of Zahniser, Chang, and Kaufman[8b] in determining β. The "efficiency" is thus .83 at 298° and 1.4 at 220°. While this temperature dependence is consistent with that using He as a third body,[8b] and with the reaction (1) fit, the magnitude is surprisingly large. Such a large increase in β or the collision diameter upon slight alteration of the excited molecular species would be very surprising. Application of Troe's[17] method to $ClONO_2$-N_2 collisions at 298°K indicates that β might be lowered to 0.69 as a result of anharmonicity corrections and the effect of treating the internal rotation as a torsion. But, this

PRECEDING PAGE BLANK

would still mean that $\langle\Delta E\rangle \sim 2.8$ kcal/mole (compared to .6 kcal/mole using Troe's method for $HONO_2$). The 220°K value of $\beta = 1.39$ simply reflects some of the general uncertainty in computing the strong collision rate constant. It should also be kept in mind that if E_0 were slightly higher (1-2 kcal/mole), the difference in β and $\langle\Delta E\rangle$ between HNO_3-N_2 and $ClONO_2$-N_2 would disappear.

The hindrance parameter was estimated in the following manner. We applied our simple "brick wall" van der Waals model to the $ClONO_2$ transition state at r^+, to obtain a predicted hindrance. Next, we determined the distance r^+ in $HONO_2$ which predicts the same value of η. This $HONO_2$ transition state separation, r^+, corresponds to a specific temperature, given by equation (4). An actual hindrance, η', was used to fit the $HONO_2$ data at this temperature. We used this same η' to predict the $ClONO_2$ rates. (This procedure must, of course, be repeated for each $ClONO_2$ temperature, i.e., r^+.) The larger $ClONO_2$ r^+(weaker bond, looser transition state) and the repulsion of the more bulky chlorine atom generally balanced one another, and the hindrances for reactions (1) and (2) at similar temperatures are close. High pressure data is required for a more accurate determination of η.

Finally, we must choose an effective, active, external moment of inertia for the $ClONO_2$ molecule, a problem not evident for $HONO_2$ because OH, unlike OCl, could be approximated as a point mass. If θ is the angle between the axis of the active rotation and the principal axis R_A, the effective active moment is given by $I = I_A \cos^2\theta + I_B \sin^2\theta$. The effective adiabatic moment (2D) will then equal the total $ClONO_2$ moment (3D) divided by the effective active moment (1D). Two logical choices for the active axis are: (1) An axis through the center of mass and parallel to the dissociating bond, or (2) an axis parallel to the active, in-plane, Cl-O axis of rotation. This

second choice insures a strict correlation between the active external molecular rotation and the active fragment rotations in the transition state. We have investigated both possibilities. Note that now I^+/I does not equal $(r^+/r_0)^2$.

Figure 4 shows the percent deviation from third-order low-pressure behavior by the effective bimolecular rate constant for recombination, as a function of pressure. The results are insensitive to the choice of active rotor model. Furthermore, the degree of fall-off is relatively unchanged by use of a different collisional efficiency. Using Leu, Lin, and DeMore's value ($k_0 = 7.0 \times 10^{-31}$ cm^6 s^{-1}; $\beta = 1.9$)[8a] at 220°, $\Delta k/k_0$ at 50 torr only increases by 4%. Of course, inaccuracies in the low-pressure rate constant will be reflected in kind at higher pressures, but the extent of fall-off will not be appreciably affected. The fall-off is somewhat sensitive to η. A significantly lower value of η than that used is unlikely, since k_∞ is already comparable to the large $HONO_2$ values. Higher η means a lower k_∞ and a lower pressure commencement of the fall-off. Thus, for η = 70% at 220°, $\Delta k/k_0$ at 50 torr rises by ~ 6%. Hence the rates derived from our fall-off model can be viewed as the maximum possible rates. Note in comparison to reaction (1), the degree of fall-off is smaller, but still significant at lower stratospheric pressures. The lower bond energy of $ClO-NO_2$ means a greater specific rate constant for decomposition (lesser for recombination) so a higher pressure is required to insure all activated molecules will suffer a stabilizing collision before refragmenting. Zellner[22] has also recently done falloff calculations for $ClONO_2$. Although he used a different value for k_∞, the degree of falloff was similar to the current results.

Figure 3 includes a similar rough rate vs. altitude plot for reaction (2) based on our model results.

CONCLUSIONS

Our calculations indicate one should take the fall-off into account in stratospheric modeling calculations concerning the role of reaction (2) in trapping active chlorine, which may destroy the stratospheric layer of protective ozone. However, one should not use the fall-off of reaction (1), as the NAS report did.[23] We believe our rates are reasonable, maximum values (minimum fall-off, maximum k_∞), and thus would predict the maximum healing effect of reaction (2). Certainly future higher pressure rate constants for reaction (2) will test this point, and the ability to use such models with statistical theories to predict rate constants.

Perhaps, future experiments and modified Gorin model RRKM fits will someday permit a more accurate and systematic method for the a priori selection of hindrance values. The results here indicate that the potential surface for $HONO_2$ decomposition cannot be fit with a single parameter. This has also been shown in reference 8c, and future work may illustrate such behavior for a variety of decompositions.

ACNOWLEDGEMENTS

This work was supported by the AFOSR under Contract F44620-75-C-0067 with SRI.

The authors wish to thank Dr. M. Lev-On for her work on the RRKM program.

PRECEDING PAGE BLANK

REFERENCES

(Chapter 5)

1. H. S. Johnston, Ann. Rev. Phys. Chem., 26, 315 (1975).

2. C. Anastasi and I.W.M. Smith, J.C.S. Faraday II, 72, 1459 (1976).

3. J. G. Anderson, J. J. Margitan, and F. Kaufman, J. Chem. Phys., 60, 3310 (1974).

4. C. J. Howard and K. M. Evenson, J. Chem. Phys., 61, 1943 (1974).

5. See, also, R. Atkinson, R. A. Perry, and J. N. Pitts, Jr., J. Chem. Phys., 65, 306 (1976) and G. W. Harris and R. P. Wayne, J. Chem. Soc., Faraday Trans. I, 71, 610 (1975) which are consistent with references 2-4.

6. W. Forst, Theory of Unimolecular Reactions, Academic Press, New York, 1973.

7. F. S. Rowland, J. E. Spencer, and M. J. Molina, J. Phys. Chem., 80, 2710 (1976).

8. (a) M. T. Leu, C. L. Lin, W. B. DeMore, J. Phys. Chem., 81, 190 (1977);

   (b) M. S. Zahniser, J. S. Chang, and F. Kaufman, J. Chem. Phys., 67, 997 (1977).

   (c) J. W. Birks, B. Shoemaker, T. J. Leik, R. A. Bordess and L. J. Hart, J. Chem. Phys., 66, 459 (1977).

9. (a) M. Quack and J. Troe, Ber. Bunsenges. Phys. Chem., 79, 170 (1975);

   (b) Ibid., Reaction Kinetics, Vol. II, P. G. Ashmore, ed., Specialist Periodical Reports, Chem. Soc., London, 1977. In press.

   (c) M. Quack and J. Troe, Ber. Bunsenges. Phys. Chem., 81, 000 (1977). In press.

10. S. W. Benson and D. M. Golden in Vol. VII of Physical Chemistry; An Advanced Treatise, edited by H. Eyring, D. Henderson, and W. Jost, Academic Press, New York, 1975.

11. E. V. Waage and B. S. Rabinovitch, Chem. Rev., 70, 377 (1974).

12. S. E. Stein and B. S. Rabinovitch, J. Chem. Phys., 58, 2438 (1972).

PRECEDING PAGE BLANK

13. JANAF Thermochemical Tables, NBS RDS-NBS 37, Government Printing Office, Washington, D.C., 1970.

14. S. W. Benson, Thermochemical Kinetics, John Wiley and Sons, Inc., New York, N. Y., 1976 (2nd ed.).

15. M. Volpe and H. S. Johnston, J. Amer. Chem. Soc., 78, 3903 (1956).

16. W. Tsang, Int. J. Chem. Kinetics, 5, 947 (1973); C. Morley and I.W.M. Smith, J. Chem. Soc., Faraday II, 68, 1016 (1972).

17. J. Troe, Ber. Bunsenges. Phys. Chem., 77, 665 (1973); J. Troe, J. Chem. Phys., 66, 4745 (1977).

18. J. Troe, Ber. Bunsenges, Phys. Chem., 78, 478 (1974).

19. K. Glanzer and J. Troe, Ber. Bunsenges. Phys. Chem., 78, 71 (1974).

20. Handbook of Chemistry and Physics, Chemical Rubber Company, Cleveland, Ohio, 1967, p. F139.

21. (a) R. H. Miller, D. L. Bernitt, I. C. Hisatune, Spect. Acta, 23A, 223 (1967);

(b) H. D. Knauth, H. Martin, and W. Stockmann, Z. Naturforsch., 29a, 200 (1974).

22. R. Zellner, Z. Naturforsch., 32a, 648 (1977).

23. Halocarbons: Effect on Stratospheric Ozone, National Academy of Sciences, Washington, D.C., 1977.

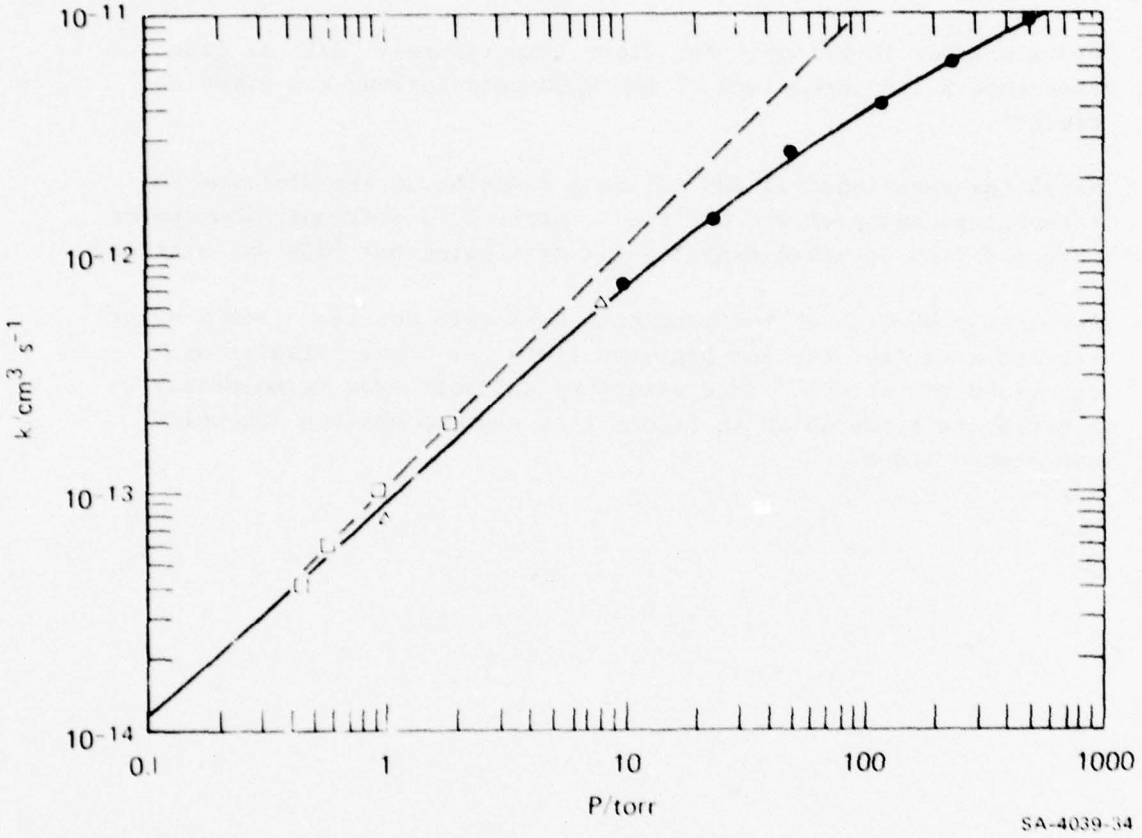
FIGURE CAPTIONS

1. Effective bimolecular rate constants for nitric acid recombination versus pressure at 296°K. Experimental points are from the data of references 2 (●), 3 (Δ), and 4 (□). A wall reaction was assumed for the reference 4 data. The solid line is the β = .48 RRKM fit (parameters in Table I). The dashed line represents termolecular behavior, characteristic of low pressures.

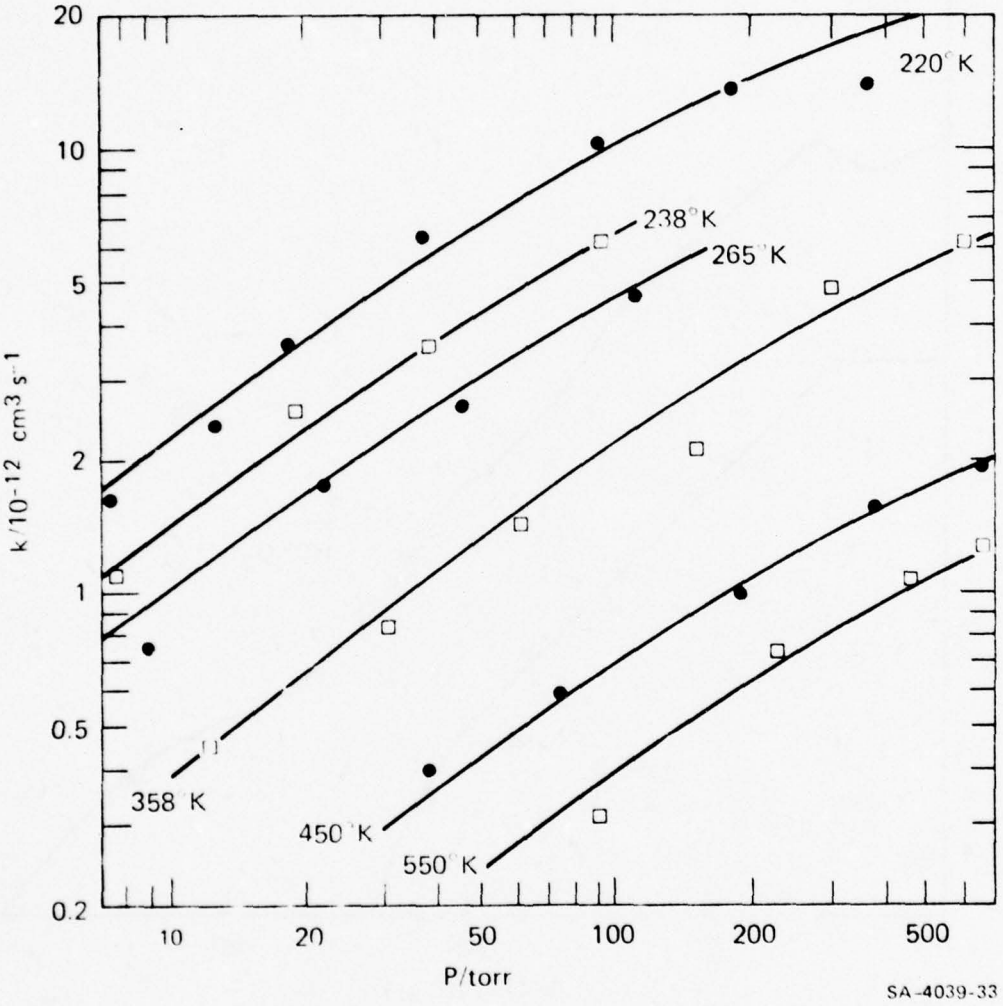
2. Plots similar to Figure 1 for other temperatures. Data is from reference 2 and parameters of the RRKM calculations are given in Table I.

3. Rates for reactions (1) and (2) as a function of the atmospheric temperature and pressure profile. Derived by extrapolation and/or interpolation of known experimental data using our RRKM calculations.

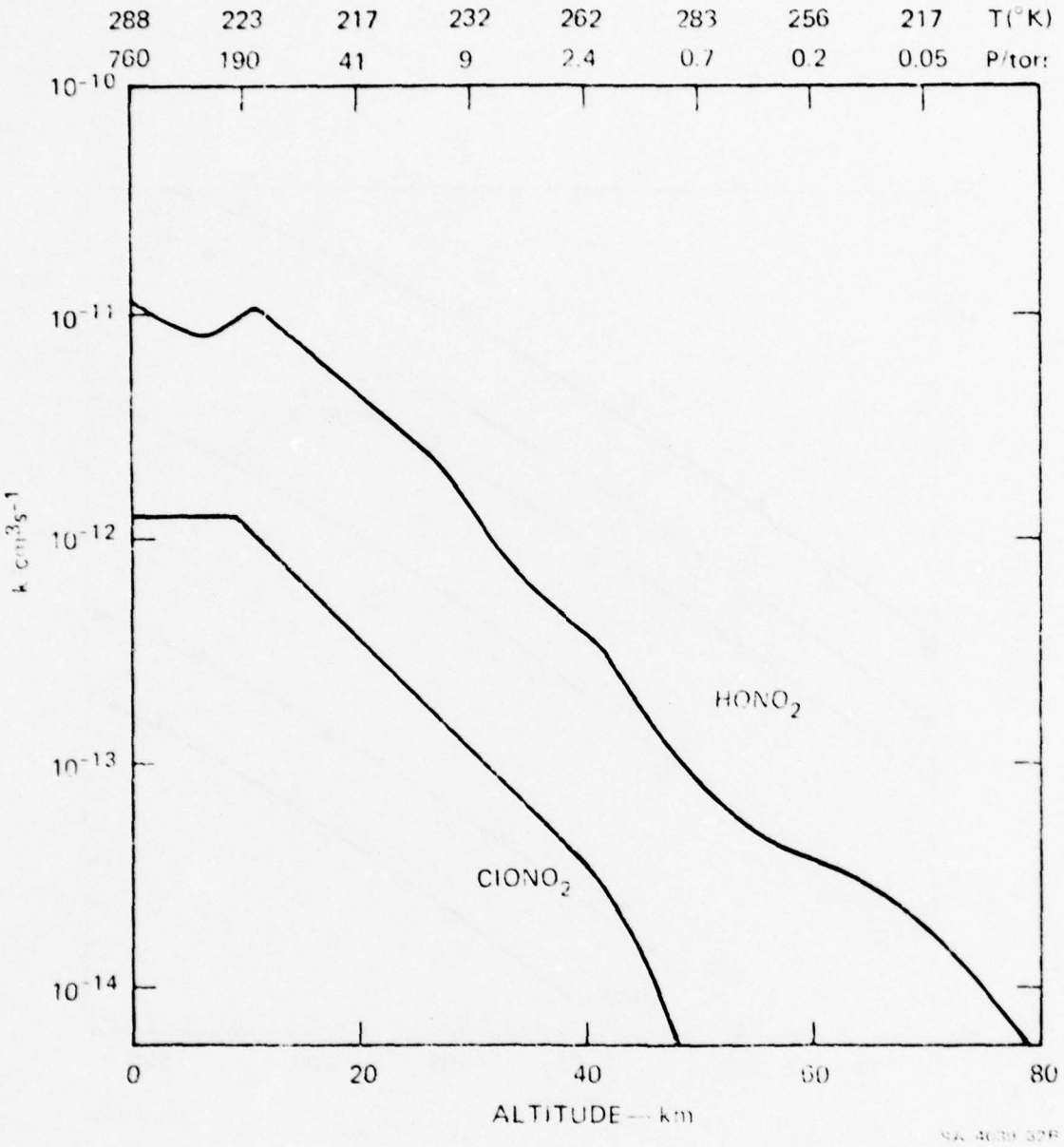
4. Percentage decline of the predicted RRKM rate constant from a value extrapolated from the low-pressure limit for three calculations described in Table I. This extent of fall-off from termolecular behavior is represented in Figure 1 by the gap between the solid and dashed lines.



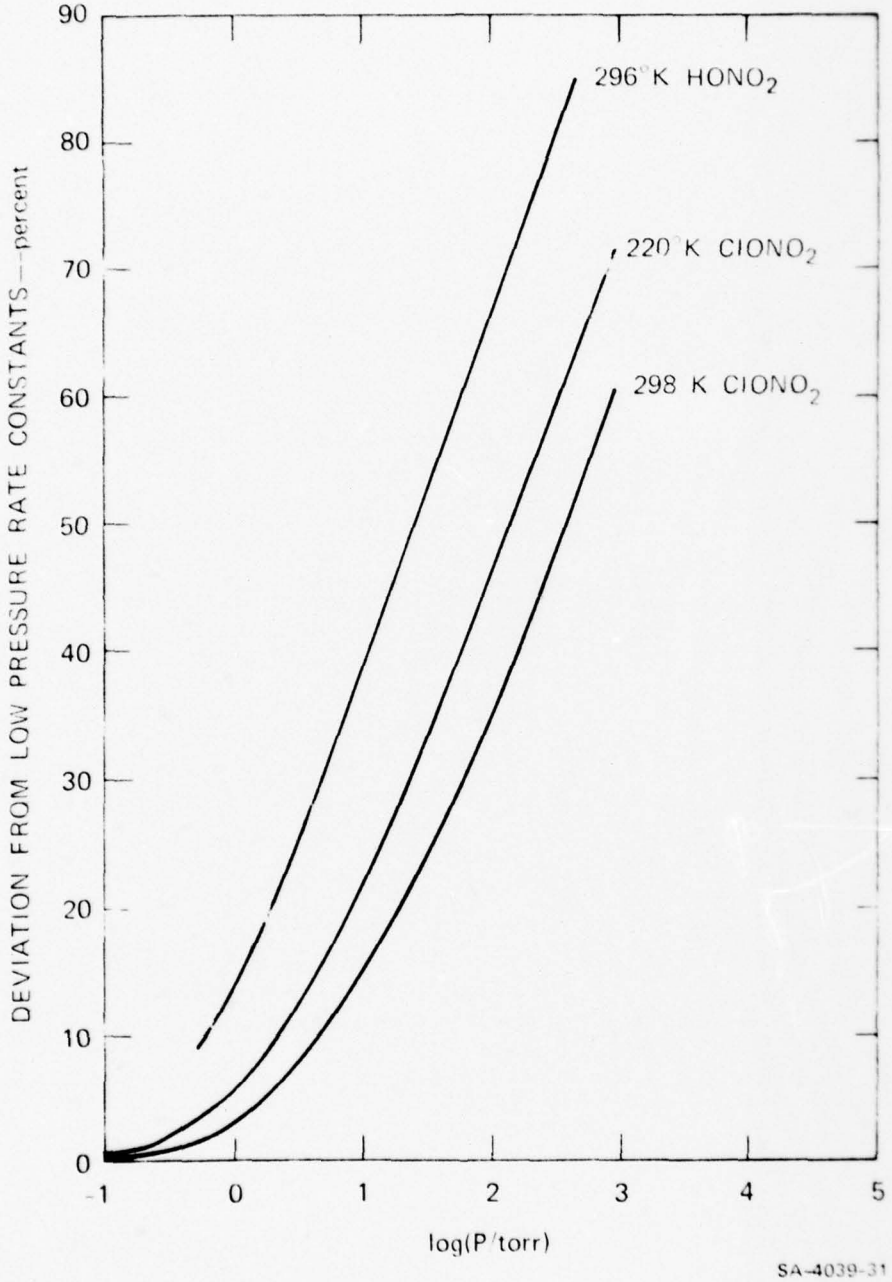
HO + NO$_2$ RECOMBINATION RATE CONSTANT AT 296°K



HO + NO_2 RECOMBINATION RATE CONSTANTS



EFFECTIVE BIMOLECULAR RECOMBINATION RATE VS. ALTITUDE



DEGREE OF FALLOFF

Appendix

PARAMETERS FOR NITRIC ACID $G(E^+)$ AND $N(E^*)$ CALCULATION

Molecule; $N(E^*)$

Vibrational frequencies: 3650, 1710, 1330(2), 880, 760, 680, 580, 465

Moments of inertia (external): Active - 64.3×10^{-40}

Inactive - 97.3×10^{-40} (2)

Transition State; $G(E^+)$

Vibrational frequencies: OH part - 3730

NO_2 part - 1620, 1320, 750

Moments of inertia: Active

OH part - 1.45×10^{-40} (2) for 0% hindrance, or
$.92 \times 10^{-40}$ (2) for 60% hindrance

NO_2 part - 64.3×10^{-40} (= external rotation)
15.45×10^{-40}(2) for 0% hindrance, or
9.77×10^{-40}(2) for 60% hindrance

Inactive, external, $97.3 \times 10^{-40} \times I^+/I$ (2)

PRECEDING PAGE BLANK

Chapter 6

A MODIFIED GORIN TRANSITION STATE IN BOND SCISSION REACTIONS. AN APPLICATION TO ETHANE DISSOCIATION.[‡]

G. P. Smith, M. Lev-On,[*] and D. M. Golden
Thermochemistry and Chemical Kinetics Group
SRI International, Menlo Park, California 94025

[‡] This work was supported, in part, by Contract No. F44620-F-75-C-0067 with the Air Force Office of Scientific Research.

[*] Present address: Environmental Sciences Division, Israel Institute for Biological Research, Ness-Ziona, P.O.B. 19, Israel.

PRECEDING PAGE BLANK

ABSTRACT

RRKM calculations are presented for the thermal dissociation of ethane and the reverse recombination reaction of methyl radicals. The transition state employed includes several hindered rotations, and matches the experimental high-pressure data between 300°K and 1400°K using a single temperature dependent hindrance parameter. The experimentally observed rate constants in the pressure falloff are also calculated using values for the average energy transferred in deactivating collisions, in general accord with previous results. The modified Gorin model is also consistent with chemical activation results, provided the methylene singlet-triplet splitting is less than 9 kcal/mole. Comparisons are made with other theoretical attempts to characterize the ethane system.

PRECEDING PAGE BLANK

I INTRODUCTION

In order to quantitatively understand the mechanism for a complex thermal chemical process, it is necessary to be able to describe the elementary thermal rate constants as a function of temperature and pressure. In general, it has been found that the framework offered by the simple transition state theory[1] is sufficient. This generalization is found wanting only for simple bond scission reactions leading to free radicals in which electronic rearrangement is minimal. Thus, in the system $C_2H_6 \rightleftarrows 2CH_3$ to be discussed herein, a simple fixed transition state will not describe the temperature dependence of the rate data adequately. We thus choose a transition state including several hindered rotations, with the structure of the transition state and consequently the extent of hindrance varying with temperature.

Using the thermodynamic notation to which transition state theory lends itself, the problem may be simply restated by pointing out that the molecular frequencies necessarily assigned to match the data in simple bond scission processes require values of $\Delta C_p^{\ddagger}$ which in turn predict large increases in both $\Delta S^{\ddagger}$ (A-factor) and $\Delta H^{\ddagger}$ (activation energy) over easily accessible temperature ranges (ca. 300-1300°K), in contrast to observations. Quack and Troe[2] have reviewed many simpler systems where fixed vibrational transition states are also inadequate. However, there is very little indication of such a problem for reactions characterized by extensive electronic rearrangement in the incipient radicals, such as, but-1-ene $\rightleftarrows CH_3$ + allyl,[3] ethylbenzene $\rightleftarrows CH_3$ + benzyl,[4] and hexa-1,4-diene $\rightleftarrows$ 2 allyl.[5] These systems showing extensive electronic rearrangement in the incipient radical may be characterized by fixed transition states with diminished heat capacity as a result of the increasing restriction to internal rotations. Thus, transition state theory does not predict large temperature variations in these cases, in accord with most observations.

PRECEDING PAGE BLANK

Simple bond scission processes occur often, and we attempt herein to extend the simple approach which we have recently utilized in dealing with the reactions $HO + NO_2 \rightleftarrows [illegible]_2$,[6] $ClO + NO_2 \rightleftarrows ClONO_2$,[6] $HO_2 + NO_2 \rightleftarrows HOONO_2$,[7] and certain ion-molecule reactions involving the formation of proton-bound dimers of amines,[8] H_2O, and H_2S,[9] to the title reaction. Our future plans include the extension to other alkane decompositions, considering the importance of these processes to the combustion and pyrolysis of hydrocarbons, as well as to ion-molecule reactions involving species of interest in atmospheric and interstellar chemistry.

The relevance of nonthermal experiments, such as chemical activation,[10,11] to the model presented here will be discussed along with some comments on current uncertainties in $\Delta H_f^0(CH_3)$ and $\Delta H_f^0(CH_2[^1A])$.

II BACKGROUND

The considerable body of experimental results on the ethane system has been reviewed by Waage and Rabinovitch[12] with more recent results summarized by Glanzer, Quack and Troe.[13] Thus the related recombination and decomposition reactions are good candidates for theoretical study,[12,14,17] as simple prototypes of important processes in hydrocarbon combustion. Such attempts provide a probe of current assumptions regarding the behavior of highly excited polyatomic molecules, and an extrapolation technique for predicting rates under different conditions or for similar systems.

High pressure data is available over a wide temperature range. There is considerable spread in the reported values for the high-pressure recombination rate constant at 300-400°K, but the recent results of Parkes, Paul, and Quinn[18] confirm the concensus value of $\sim 4 \times 10^{-11}$ cm^3 s^{-1}. The experiments of

Glänzer et al.[13] indicate a slightly lower rate at 1400°K. Ethane decomposition rates have been measured at 800-1000°K by Lin and Back,[8,19] and by Clark and Quinn,[20] and can be inverted via the equilibrium constant to give recombination rates.

Several other pertinent observations have been made on the ethane system. Both Clark and Quinn[20] and Glänzer et al.,[13] have also measured rate constants for perdeuteroethane. Experimental uncertainties, however, preclude the use of the temperature dependence of the isotopic rate ratio as a sensitive test of theoretical calculations. Kennedy and Frey[10] and Simons and coworkers[11] have studied the pressure dependence of ethane decomposition prepared by singlet methylene insertion into methane (chemical activation). Any model which fits the thermal recombination data should hopefully also be able to predict these rates given a good value for $\Delta H(CH_2(^1A_1))$. Finally, pressure dependent rate studies in the falloff region have been reported,[12] many of which are old (and scattered) or over a limited range of pressures. For a representative test of our model over a wide temperature and pressure range, we have considered the experimental pressure dependence reported by Glänzer et al.[13](1400°K), Lin and Back[19] (decomposition 913°K), and Casas et al.[21] (370°K).

Several efforts have been made to fit these results with RRKM calculations, as summarized by Waage and Rabinovitch[12] and Hase.[15] The choice of a proper critical configuration is crucial, and most authors have chosen a fixed vibrational transition state to attempt fitting a wide range of data. It is now clear[15-17] that only only variable transition state models fit the observed temperature dependence.

Within the generally accepted statistical assumption imposed by practicality two broad approaches to the high-pressure rate constant are possible: the statistical adiabatic channel theory of Quack and Troe[14] which counts the number

of individual open reaction channels whose maxima lie at various positions along a specified reaction coordinate; or alternatively, our[6] canonical approach to transition state theory with provisions for a tighter critical configuration at higher temperatures. We reason that the centrifugal maximum closely describes the C-C distance in the transition state and that since this distance decreases with increasing temperature,[22] the transition state characteristics are also temperature dependent. We describe the hindered Gorin[23] model which emerges in terms of a hindrance parameter which measures the effective "tightness" of the transition state as a function of C-C distance and thus, temperature (see details below).

Quack and Troe[14a] have applied their statistical adiabatic channel (SAC) model to the ethane system, successfully reproducing the temperature dependence of the high-pressure rate constant, although the absolute numbers are slightly too high. They have not discussed pressure dependence or chemical activation. We (and they[14b]) feel that SAC will always remain too difficult to apply to large molecules of practical interest. Quack and Troe have suggested[14b] a simpler empirical interpolation technique to avoid this problem. They suggest that a one-parameter extrapolation from partition functions of reactant to those of products will suffice. In the molecules they consider, the parameter which they call γ has a single value, but this is surely questionable in the face of data on systems leading to stabilized radicals, such as mentioned in the introduction. Thus, these two canonical approaches will probably turn out to be very similar in the sense that both require a system-independent interpolation parameter to maximize free energy. (A canonical model never really addresses itself to the minimization of state density which is a microcanonical requirement; thus, the free energy chosen might not correspond to the "best" critical configuration, but the computed rate constants are not very sensitive to minor structural variations of the activated complex.) Theoretical predictions in the falloff region also require equal consideration of the low-pressure rate constant, a factor too often given only cursory attention. Troe[24] and van den Bergh[25] have applied Troe's recent low-pressure theory,[24] which predicts a collisional deactivation efficiency (β) from the average energy transferred, $\langle \Delta E \rangle$, to ethane. This formulation will be followed here.

III DETAILS OF THE CALCULATIONS

The RRKM Model

The relevant reactions for the thermal decomposition of ethane are:

$$C_2H_6^* \xrightarrow{k(E^+)} 2CH_3 \qquad (1)$$

$$C_2H_6^* + M \rightleftarrows C_2H_6 + M \qquad (2)$$

where the excited ethane molecules are those in the Boltzmann tail above the dissociation limit (E_0). According to the statistical RRKM theory,[26] the decomposition rate is given by:

$$k_{uni} = \frac{Q_1^+ e^{-E_0/kT}}{hQ_1Q_2} \int_0^\infty \frac{P(E^+)e^{-E^+/kT}\,dE^+}{1 + Q_1^+ P(E^+)/hQ_1N(E^*)F\beta\omega} \qquad (3)$$

wher $E^+ = E^* - E_0$ is the maximum energy of the critical configuration. The sum of the states of the complex below energy E^+, $P(E^+)$, depends on the structure chosen for this transition state. Here, $N(E^*)$ is the density of molecular states, Q_2 is the partition function of the active molecular modes, Q_1^+/Q_1 is the partition function ratio of the inactive modes (I^+/I, the moments of the adiabatic external rotors), and F is the Waage-Rabinovitch centrifugal correction term[17] for conservation of angular momentum for the adiabatic rotations. In using the ethane bond energy at 0^oK for E_0, we effectively assume no intrinsic barrier for the recombination step (− 1). The collision frequency ω of excited ethane with the bath gas M at pressure P (reaction 2) is calculated from the Lennard-Jones collision cross section at temperature T. The collisional efficiency for stabilization, β, is calculable from the average energy transferred (exponential model) in reaction (2), $\langle \Delta E \rangle$, by Troe's formula:[6]

$$\beta/(1 - \sqrt{\beta}) = \langle \Delta E \rangle / F_E kT \qquad (4)$$

where the usually small F_E term which corrects for the nonlinearity of the vibrational state density near E_0 is given by[24]

$$F_E = \sum_{i=0}^{s-1} \frac{(s-1)!}{(s-1-i)!} \left(\frac{kT}{E_0 + \alpha E_z}\right)^i \qquad (5)$$

where E_z is the zero point energy and the empirical $\alpha \sim 1$. The recombination rate constant, k_r, can be computed from k_{uni} via the equilibrium constant, K_{eq}. Furthermore, the dependence on E_0 cancels out.

The Transition State

For our model (see Table I) of the critical configuration, we choose the top of the centrifugal barrier for a Lennard-Jones potential as the separation distance along the bond axis:

$$Q_1^+/Q_1 = I^+/I = (r^+/r_0)^2 = (6D_e/RT)^{1/3} \qquad (6)$$

where $D_e = D_0 + \Sigma h\nu(\text{complex}) - \Sigma h\nu(\text{molecule})$.

A modified Gorin model[6,23] is used for the transition state. The internal modes are the vibrations and rotations of two methyl radicals. The six transition state internal rotations correlate to four molecular rocking modes, the torsional vibration, and the ethane external rotation about the C-C bond axis. This thus leaves only two external ethane rotations inactive and adiabatic. These rotational modes do not share in the random distribution of molecular energy. [This treatment conserves the angular momentum of the inactive rotors, but does not strictly conserve the total angular momentum. Note, however, that the active external rotor has the largest rotational spacing of the three, and hence the lowest average quanta of angular momentum.]

The four methyl transition state rotors corresponding to ethane rocking vibrations are not actually free to rotate at the C-C distances described above. The modified Gorin model hence represents these degrees of

Table I

PARAMETERS

Lennard-Jones Collision Diameters (Å):[31]

C_2H_6	4.4
Ar	3.5
$i\text{-}C_3H_7\text{-}CO\text{-}CH_3$	(5.3) estimated
$i\text{-}C_4H_{10}$	5.3
CH_4	3.8

Equilibrium Constants:

K_1	838°K	1.31×10^4 cm^{-3}
	913°K	1.07×10^6 cm^{-3}
	1000°K	7.75×10^7 cm^{-3}

Molecule:

ν = 2977(4), 2954, 2896, 1469(4), 1383(2), 1190(2), 995, 822(2), 260 cm^{-1}

$I = 11.7 \times 10^{-40}$ gm cm^2

Inactive $I = 40 \times 10^{-40}(2)$ gm cm^2

Transition State:[29]

ν = 3184(4), 3002(2), 1383(4), 580(2) cm^{-1}

$I = 11.7 \times 10^{-40}$, 29.3×10^{-40} gm cm^2

0% hindrance: $29.3 \times 10^{-40}(4)$ gm cm^2

50% hindrance: $20.7 \times 10^{-40}(4)$ gm cm^2

Inactive $I = 40 \times 10^{-40} \times I^+/I$ (2) gm cm^2

freedom as hindered rotations. This is perhaps a more reasonable picture for the "loose" transition states typical of simple bond scission reactions than the usual very low-frequency vibrational model. This hindrance is accomplished in the calculation by decreasing the effective moments of inertia, I_H, of the two two-dimensional methyl rotors:

$$Q_2^+ \alpha (I_H)_1 (I_H)_2 \tag{7a}$$

$$I_H = I_{CH_3} (1 - \eta)^{1/2} \tag{7b}$$

where η is the hindrance parameter and Q_2^+ is the partition function for the active modes in the transition state, to which the high pressure k_{uni}^{∞} is proportional. This effectively decreases the number of available rotational states by excluding each rotating radical from the volume occupied by the other, and thus η should rise with temperature, as r^+ drops (see equation 6). [We note that in one sense the interfragment distance alone does not entirely represent the reaction coordinate ($r^+ \neq q^+$), since the four other modes which vary with temperature may also contribute. However, for purposes of the RRKM calculation, the C-C bond stretch is used as the critical mode.]

Ethane frequencies and moments of inertia from the NSRDS table[27] were used, while methyl radical values were taken from the JANAF tables.[28] From photoionization measurements[29,30] of $\Delta H_f(CH_3)$, E_0 = 87.7 kcal/mole was chosen. From this information, K_{eq} was calculated (matching tabulated values)[44,28] and Q_1, Q_2, $P(E^+)$, and $N(E^*)$ were computed. The Lennard-Jones cross section on which ω depends was derived from ethane viscosity data,[24] and suitably averaged with like values for the bath gases.[31] Table I lists some of the parameters for the calculations. Thus, we are left with two adjustable parameters at each temperature to fit the wide range of data. While $<\Delta E>$, which determines the low-pressure (step 2) rate constant, k_0, is expected to be temperature independent, η which determines the high-pressure (step 1) rate constant k_∞, is not, as mentioned earlier. (Thus, if $\eta = a + bT$, we would have three constants to characterize the system.) In any event, these two parameters have simple

physical meanings, and any data fitting attempt is restricted to a range of $\langle \Delta E \rangle$ and η values reasonable for the system.

Chemical Activation

In chemical activation studies, $C_2H_6^*$ is prepared nearly monoenergetically by insertion of $CH_2(^1A_1)$ into CH_4. The measured quantity, to be matched theoretically, is the ratio of decomposition to stabilization rates, i.e., the relative yields of products from reactions (1) and (2), D/S. Since the rate of (2), i.e., S, is pressure dependent, the "dimensionless" quantity by which results are reported, analogous to k_{uni}, is $\omega D/S$, where ω is calculated (roughly) by the previously described method. If we consider deactivation by a stepladder model, the number of steps $n = (E^* - E_0)/\langle \Delta E \rangle$, D in the high pressure limit is just an average of $k(E^+)$ over n steps, and $(\omega D/S)_\infty = \sum_{i=1}^{n} k(E_i^+)$. In the low-pressure limit, according to Robinson and Holbrook,[26] $(\omega D/S)_0 = \omega^{(1-n)} \prod_{i=1}^{n} k(E_i^+)$. In the falloff, the fraction collisionally deexcited to the next step, $\omega/\left(\omega + k(E_i^+)\right)$, must be calculated at each step, and $\omega D/S$ can be derived from $S/(D + S) = \prod_{i=1}^{n} \left(\omega/(\omega + k(E_i^+))\right)$. We note that $k(E_i^+)$ is easily determined from the RRKM computation, $k(E^+) = P(E^+)/hN(E^*)$. The parameters for such a calculation are ω, calculated from Lennard-Jones viscosity diameters; $\langle \Delta E \rangle$, determined by fitting the ethane decomposition data; and E^*, which depends on the value chosen for $\Delta H_f(CH_2(^1A_1))$, and on the amount of CH_2 vibrational energy from the photolytic generation not removed before insertion. Simon's and Curry's value[32] gives $E^* \geq 101.4$ kcal/mole, from the measurements of McCulloh and Dibeler[30b] and Zittel et al.,[33] $E^* \geq 115.5$ kcal/mole.

A small correction term must be added to the transition state energy:[15] $E^+ = \Delta H_R^{298} - E_0 + \Delta E_{rot}$. The activated ethane after formation has $E_{rot} = RT \sim .6$ kcal/mole average rotational energy in the two adiabatic external rotors. Since

angular momentum must be conserved going to the transition state, $IE_{rot} = I^+E^+_{rot}$ and $\Delta E_{rot} = RT(1 - \frac{I}{I^+}) \sim .5$ kcal/mole becomes available to the other modes in the transition state. This correction for average angular momentum is akin to the Waage-Rabinovitch correction[34] employed in the thermal case.

The fact that we have not chosen the critical configuration in such a way as to assure that it corresponds to a minimum in the density of states ($N(E^*)$) will introduce some uncertainty here. However, the uncertainties in all the input factors are considerably greater. One can vary the critical configuration in such a way as to maintain the same value of $\Delta G^{\ddagger}_{max}$ while varying $\Delta S^{\ddagger}$ (i.e., state density) and $\Delta H^{\ddagger}$ within reasonable bounds.

IV RESULTS AND DISCUSSION

High-Pressure Rate Constants (Hindrance)

Figure 1 shows some experimental values of the high-pressure limit of the bimolecular rate constant for the recombination of methyl radicals k_∞ as a function of temperature. The points between 800 and 1000°K are derived from ethane decomposition using the equilibrium constant.[28,29] The results show considerable scatter and would have shown more had we included some older measurements. Also illustrated are the predictions of statistical adiabatic channel theory,[14] which appear slightly too high, and our choice of a rough, empirical fit to the data. Our line follows the perceived slight decline of k_∞ with temperature.

This fit of the data corresponds to a modified Gorin model transition state, as outlined previously, with a hindrance η varying from 63% at 300°K to 81% at 1400°K. Furthermore, this hindrance varies linearly with r^+, the radical separation distance in the transition state, given as a function of temperature by equation (6). Hence we have

$$\eta = 144 - 17r^+ = 144 - 212\ T^{-1/6} \qquad (8)$$

and the entire fit of the data is accomplished by two parameters

within a physically simple model. Interestingly enough, the two constants of equation (8) can be related through the constraint that $\eta = 100\%$ at $r^+ = 2.6$ Å, which is just twice the nonbonded H-atom interaction distance[22]; that is, the flat methyl radicals cannot rotate at all at this distance. This would mean that η at any one temperature is sufficient for predicting η at any other temperature. (A value of η near 100% would indicate that the four degrees of freedom which we are treating as rotations should be treated as vibrations.)

By the same token this simple van der Waals model would indicate that $\eta = 0\%$ for $r^+ \geq 4.8$ Å, where the methyl radicals fail to repel each other even in a C-H- - - H-C arrangement (1.1 Å C-H distance + 2 x 1.3 Å H van der Waals radius + 1.1 Å H-C distance = 4.8 Å). Yet at 300°K where $r^+ = 4.8$ Å, $\eta = 63\%$, not 0%. Thus, as in the nitric acid case previously explored,[6] the hindrance is larger than might be expected and more slowly decreasing with r^+, although the ethane values are more reasonable and systematic. These higher hindrance values indicate that additional, attractive forces are important in restricting or coupling the motions of the rotors. The differences between the behavior of η in nitric acid and ethane suggest that the nature of the potential surfaces at these large separations vary between systems with significant effects. Clearly, a larger body of data must be fit with this modified Gorin model before it is justified by the observation of systematic behavior and available as a predictive tool.

If we accept the values of C-C distance which correspond to the minimum in state density, from reference 16, we may calculate η', which is the value of η required to reproduce k_∞ considering these somewhat smaller distances. We find that at 400 K, $\eta' = 56\%$ compared with $\eta = 66\%$ and at 860°K, $\eta' = 70\%$ compared with $\eta = 76\%$. Changes of this nature make no significant change in

k_{uni} over practical ranges of interest and account for our decision to forego the complicated minimization calculation which they would require.

The values of η' are somewhat closer to the van der Waals model. It is possible that future work may show the use of a microcanonical η' parameter, a function of r or E, with the minimum density of states criterion could prove more comfortable physically. Our η is a canonical parameter, a function of r^+ or T, and our model an easy to calculate canonical one.

Shaw[35] has recently compared the forward and reverse rate constants over a wide temperature range for the reaction $CH_3 + H_2 \rightleftharpoons CH_4 + H$. The methyl radical heat of formation can be derived from the temperature dependence of the equilibrium constant $K_E = k_F/k_R$. This leads to an ethane bond energy of 85.3 kcal/mole (0^oK), 2.4 kcal below the generally accepted value. In our model, η is fixed by the recombination data at 300^oK and 1400^oK and is independent of the bond energy. η (913^oK) should lie between η (300^oK) and η (1400^oK). Thus, the ethane decomposition data[19] at 913^o-1000^oK provides an added test of the bond energy via our RRKM model. Using the lower bond energy (instead of 87.7 kcal/mole as in Figure 1) in the ethane equilibrium constant, the 1000^oK methyl recombination high-pressure rate constant obtained by inverting the measured ethane decomposition rate constant is 7×10^{-11} cm^3/s. This can be accommodated within our smoothly varying model only if (1) a combined 50% error exists in the recombination (300^oK) and dissociation (1000^oK) rates,

which is unlikely considering the extent of work done on these systems, or (2) the 1400°K recombination measurement[13] is incorrect and k_∞ rises with temperature (i.e., the hindrance increases less strongly with temperature). We do note, however, that a 1.5 kcal/mole drop in the ethane bond energy only raises the 1000°K recombination rate constants to 4×10^{-11} cm^3/s which is accommodated by our model, given reasonably generous estimates of experimental errors. An error this size in the ethane bond energy derived from the dissociative photoionization threshold measurements[29,30b] might be accounted for by kinetic energy release for $CH_4^+ \rightarrow CH_3^+ + H$ near the threshold.[36] The value of 86.7 ±.8 kcal/mole for $D_0^0(CH_3-CH_3)$ derived from Benson and coworkers' recent measurements[37] on the equilibrium $CH_3 + HCl \rightleftarrows CH_4 + Cl$ is also consistent with the Lin and Back ethane decomposition-methyl radical recombination results. Finally, the 838°K ethane decomposition rate constant of Clark and Quinn[20] lies closer to our fit, and consequently is not consistent with significantly lower ethane bond energies. (A change of 1.2 kcal/mole doubles the recombination rate constant.)

Pressure Dependence ($< \Delta E >$)

We have used an RRKM program[38] to fit the pressure dependence of the rate constant for several recent, representative experiments which spanned a large pressure range. Here η is fixed by equation (8), and the collisional efficiency β, which determines the low-pressure rate constant k_0, is calculated from $< \Delta E >$ by Troe's formulation.[24] Values of $< \Delta E >$ consistent with previous determinations would thus indicate a match of theory and experiment.

The data and fits in Figure 2 and the parameters in Table II are given for the 1400°K recombination experiment in Argon by Glänzer et al.,[13] the 913°K decomposition results of Lin and Back in ethane,[19] and the 370K recombination results of Casas et al. in isopropylmethyl ketone and other gases.[21] Excellent fits, suitable for extrapolation with care to other pressures, are obtained. Van den Bergh[25] has done similar fits for the data of Glänzer et al.[13] The energy transfer values are, in general, in accord with past values[39] of .2 to .7 kcal mole^{-1} in Ar and 1.2 to 4.4 kcal mole^{-1} in C_2H_6, but the anomalously low value in isopropylmethyl ketone (370°K) indicates possible experimental problems. The theoretical framework provides a good diagnostic of experimental results.

Table II

MODEL PARAMETERS FOR ETHANE DECOMPOSITION
(Energies in kcal/mole)

T(°K)	r^+(Å)	I^+/I	η	$< \Delta E >$	β	$\log[A/s^{-1}]$	E_a
300	4.8	9.6	63			17.12	89.56
370	4.6	9.0	66	1.0	.41	17.23	89.89
450	4.45	8.4	67			17.37	90.16
910	3.95	6.6	77	2.3	.38	17.12	90.13
1400	3.7	5.7	82	.3(Ar)	.06	16.69	88.57

Chemical Activation

Growcock et al.[11] and Frey and Kennedy[10] have performed chemical activation studies on ethane decomposition. The results give values for $\omega D/S$ of 5.1×10^9 and 7.9×10^9, respectively. To calculate theoretical values of $\omega D/S$ by RRKM theory according to the formulas of section II, we need values for E^*, $\langle \Delta E \rangle$, ω, and $k(E^+)$. The Lennard-Jones collision frequency, ω, was calculated for the experimental gas mixtures from the parameters listed in Table I. The experimental values of $\omega D/S$ given above are based on these values of ω, which differ slightly from those used by the authors. Two different values were considered for the excitation energy E^*. These values are minima, since CH_2^* vibrational excitation just prior to insertion was assumed to be low. We note, however, that Growcock et al.[11] claim a 13 kcal vibrational excitation. A low value of 99 kcal/mole for $\Delta H_f(CH_2^*)$ taken from Simon and Curry's[32] interpretation of chemical experiments gives $E^* \geq 101.4$ kcal/mole. The more direct physical measurements of references 30 and 33 combine to give a high value of $E^* \geq 115.5$ kcal/mole. Welge[40] recently observed singlet methylene from the N_2 laser photolysis (337 nm) of ketene. This supports a low value for the singlet-triplet splitting and for E^*. Recent theoretical results[41] give a splitting of 11 kcal/mole ($E^* \geq 105.5$ kcal/mole). The most critical parameter in calculating $\omega D/S$ is $\langle \Delta E \rangle$, since the amount of energy transferred per collision determines the number of collisions, , necessary for stabilization, i.e., the time available for decomposition. Since the bath gas in the chemical activation experiments was predominantly ethane, we have used the value of 2.3 kcal/mole for $\langle \Delta E \rangle$ derived previously from the fit of the falloff data for thermal ethane decomposition at 913°K. For chemical activation, however, the bath gas temperature is lower (300°K) and the excitation energies of the activated molecules are much higher. There is little definitive evidence on how $\langle \Delta E \rangle$ varies with either of these parameters.[39,42]

Secondly, we have chosen the formalism of Troe[24] which regards $<\Delta E>$ as a constant, over that of Tardy and Rabinovitch[42] which considers $<\Delta E>$ down, the average energy transferred in deactivating collisions, as the important parameter. Since the Troe method[24] appears to be independent of the energy transfer model used, $<\Delta E>$ derived from an exponential model for the 913°K thermal system can be transferred to a stepladder model for the chemical activation system. Furthermore, since $<\Delta E> \gg RT$, $<\Delta E> \cong <\Delta E>_{down}$. One might expect that any variation of $<\Delta E>$ with excitation level would produce larger $<\Delta E>$ at higher E^*. This would increase theoretical estimates of the stabilization rates S and decrease $\omega D/S$. For the two values of E^*, n = 6 and 12.

Values of $k(E^+)$ are computed directly by our RRKM program, with T = 300°K and η = 63%, as given by equation (8) and as shown in Figure 3. They are calculated before application of the rotational energy correction discussed in section II, and are compared with the J = 0 statistical adiabatic channel values.[14] Our model predicts slightly lower values of $k(E^+)$ at the lower E^+ values sampled most in thermal systems (giving lower thermal k_{uni}), but higher $k(E^+)$ at the high E^+ values sampled via chemical activation. If it is the modified Gorin model which improperly perceives the potential surface and critical configuration (one hopes future sophisticated experiments will tell), then the decomposition rate D, hence the theoretical $\omega D/S$ must once again be reduced.

The theory predicts minimum high pressure values for $\omega D/S$ of 1.6×10^9 s^{-1} and 4.5×10^{10} s^{-1} for the low and high values of $\Delta H_f^0(CH_2^*)$, respectively. The experiments of Growcock et al.,[11] which extend further into the high pressure limit than Kennedy and Frey's work,[10] give a value of 5.1×10^9 s^{-1}. Increasing the value used for $<\Delta E>$ will lower the theoretical numbers, but

even in the strong collision limit, the high $\Delta H_f^0(CH_2^*)$ value for $\omega D/S$ is still 1.8×10^{10} s^{-1}. Our theoretical model fits the experimental result if $E^* = 105$ kcal/mole, i.e., for a methylene singlet-triplet splitting ≤ 9 kcal/mole (and our values of ΔH_f^0 for CH_3 and CH_2), in rough agreement with the recent experimental[40] and theoretical[41] values. Thus our model is not consistent with the higher value for $\Delta H_f(CH_2^*)$.

This is more clearly illustrated in Figure 4, which shows several attempted fits to Kennedy and Frey's pressure-dependent data.[10] The deviation from the high-pressure limit, as illustrated by a rapidly increasing slope, is very apparent in this range for the high value of E^*. Predicted values in the falloff region are quite sensitive to parameter variation. For example, a change in the value used for $<\Delta E>$ requires an almost equal change in E^*. (However, this then lowers the high-pressure value of $\omega D/S$.) Our fit is consistent with the similar model of Kennedy and Frey,[10] which used $<\Delta E> = 2.3$ kcal/mole, $E^* = 107$ kcal/mole, a larger ω and a vibrational transition state (different k(E)). Although the Figure 4 falloff fit appears to be a very sensitive way to determine E^*, an examination of uncertainties reveals otherwise. Despite our transfer of the $<\Delta E>$ value from our thermal ethane decomposition fit, a 1-kcal error is reasonable and gives a like uncertainty to E^*. Our differences with Kennedy and Frey over ω indicate a 10% uncertainty, which could change E^* by .5 kcal. Uncertainty in the position of the high-pressure experimental intercept in Figure 4 permits an adequate fit with another 1-kcal variation in E^*. The use of a vibrational frequency for the ethane torsional motion results in an underestimation[43] of $\omega D/S$ of up to 25%. Thus the data and our fit tentatively support the lower value for the methylene singlet-triplet splitting, and a range of higher values, but not the 19.5 kcal $mole^{-1}$ value of reference 33. While this does not consider the possibility of a much larger

$< \Delta E >$ at high excitation energies, or possible overestimation of k(E) by the Gorin model, a combined error of ~ 400% is required to support the high value of $\Delta H_f(CH_2^*)$. Clearly, however, without a conclusive determination of E^*, this particular system cannot utilize the pressure dependence of $\omega D/S$ to test the RRKM theory, k(E), or examine behavior of $< \Delta E >$ at higher excitation energies.

The authors of SAC theory did not attempt to fit the chemical activation data. We note, however, that k(E, J = 0) is an upper limit[14] to k(E,J). Since SAC theory predicts lower k(E) values than the Gorin model at the higher energies sampled by chemical activation, SAC values of $\omega D/S$ will be lower. Thus, for E^* = 105 kcal/mole, $E - E_0$ = 17 kcal/mole, the Gorin value for k(E) corresponds to the SAC value of $k(E')$ for an energy E' of 22 kcal/mole above the decomposition limit (see Figure 3). Thus, a rough SAC fit of the chemical activation results requires a higher value for the CH_2 singlet triplet splitting, approximately 14 kcal/mole. This is higher than recent values,[40,41] assuming little CH_2^* vibrational excitation, but well within all the uncertainties discussed above.

V Conclusions

Hase,[16] and Olson and Gardiner[17] have recently attempted to predict the ethane data with a minimum density of states criteria for locating the critical configuration, using other temperature-dependent transition state models. These models portray the hindered transition state rotors as methyl rocking vibrations whose frequencies vary with temperature (or r^+) or as free rotors with potential barriers to rotation whose barrier height varies with temperature. The simple functional forms used by the authors for the frequency or barrier variation fail to fit the experimental methyl radical rate constant temperature variation.

Physically, more complex models for the parameter variations would be required to fit the data. Furthermore, since the barrier-to-internal-rotation model represents the internal rotations as free rotors at the high energies sampled by chemical activation, this theory predicts significantly higher k(E) and D/S values[17] than our hindered Gorin model. To summarize, the vibration, barrier, and Gorin models represent the transition state methyl rocking mode by parabolic, cosine, and square well[45] potentials, respectively, and it is still uncertain which form and resulting k(E) is the most accurate and easily applied one.[45]

A brief comparison of the hindered Gorin RRKM model with the one-parameter partition function interpolation procedure[14] adopted by Quack and Troe as an approximation to their statistical adiabatic channel (SAC) theory is of interest. Noting the difference in the k(E) plot (Figure 3), any temperature dependent transition states constructed to reproduce the results of reference 14 must differ from the hindered Gorin one. Alternatively, any potential surface interpolation between reactant and product state densities which reproduces the Gorin model k(E)'s must differ somewhat from the interpolation chosen by Quack and Troe to approximate the SAC results. The correct transition state, the correct interpolation, and which formalism is more convenient and applicable, remain undecided.

The use of a hindered Gorin transition state in this work successfully fits the data for ethane decomposition and methyl recombination, using values for η and ΔE consistent with the physical model and previous results. These fits provide a convenient method for extrapolating the rates to other, unmeasured, temperatures and pressures. In contrast to most vibrational models, the transition state here is characterized by a single temperature-dependent parameter,

hindrance. The large entropies required of the hindered rotations would correspond to vibrational frequencies below 100 cm^{-1}, and treatment of the temperature dependence would be harder to visualize. The convenient hindered Gorin representation is physically reasonable and meaningful for loose transition states, and provides a compact method for codifying data. More experience with the model, however, is necessary before a priori predictions of the hindrance and estimates of rate constants become practicable. We plan to extend this work to other alkane systems in the near future.

Secondly, we note the considerable uncertainties upon which these theoretical endeavors rest. Besides the scatter of experimental values, thermochemical uncertainties, and approximate collision cross sections, $<\Delta E>$, and its temperature variation can only be loosely estimated. Furthermore, it is not established that the Gorin-RRKM model, or any other, gives a true representation of the sum of states at the critical configuration. Any conclusions to be drawn from interpretation of the chemical activation results remain shrouded in the previously discussed uncertainties.

Further research, aimed at a more microscopic level than the general systems fit here, should provide more accurate parameters for such calculations, test the Gorin model form for k(E), and determine the validity of the statistical assumption upon which RRKM and transition state theory depend.

ACKNOWLEDGEMENTS

The authors thank Professor H. M. Frey, Dr. G. K. Kennedy, and Dr. D. B. Olson, and Professor W. C. Gardiner, Jr., for preprints of their work prior to publication, and Dr. R. Shaw, Dr. A. J. Colussi, Professor S. W. Benson, and Professor K. Welge for discussions of their recent results.

REFERENCES

(Chapter 6)

1. D. L. Bunker and M. Pattengill, J. Chem. Phys., 48, 772 (1968).

2. M. Quack and J. Troe in Gas Kinetics and Energy Transfer, Specialist Periodical Reports, Chemical Society, London, Vol. 2, p. 175.

3. A. B. Trenwith, Trans. Faraday Soc., 66, 2805 (1970).

4. D. F. McMillen, P. K. Trevor, and D. M. Golden, to be published.

5. M. Rossi and D. M. Golden, to be published.

6. G. P. Smith and D. M. Golden, Int. J. Chem. Kinetics, in press.

7. A. C. Baldwin and D. M. Golden, J. Phys. Chem., submitted.

8. W. N. Olmstead, M. Lev-On, D. M. Golden, and J. I. Brauman, J. Amer. Chem. Soc., 99, 992 (1977).

9. J. Jacinski, R. N. Rosenfeld, J. I. Brauman, and D. M. Golden, to be published.

10. H. M. Frey and G. K. Kennedy, to be published.

11. F. B. Growcock, W. L. Hase, and J. W. Simons, Int. J. Chem. Kinetics, 5, 77 (1973).

12. E. V. Waage and B. S. Rabinovitch, Int. J. Chem. Kinetics, 3, 105 (1971).

13. K. Glänzer, M. Quack, and J. Troe, Chem. Phys. Letters, 39, 304 (1976).

14a. M. Quack and J. Troe, Ber. Bunsenges, Physik. Chem., 78, 240 (1974).
b. M. Quack and J. Troe, Ber. Bunsenges, Physik. Chem., 81, 329 (1977).

15. W. L. Hase, J. Chem. Phys., 57, 730 (1972).

16. W. L. Hase, J. Chem. Phys., 64, 2442 (1976).

17. D. B. Olson and W. C. Gardiner, Jr., Int. J. Chem. Kinetics, to be published.

18. D. A. Parkes, D. M. Paul, and C. P. Quinn, J. Chem. Soc. Faraday Trans. I, 72, 1935 (1976).

PRECEDING PAGE BLANK
PRECEDING PAGE BLANK

19. M. C. Lin and M. H. Back, Can. J. Chem., 44, 2357 (1966).

20. J. A. Clark and C. P. Quinn, J. Chem. Soc., Faraday Trans. I, 72, 706 (1976).

21. F. Casas, C. Previtali, J. Grotewald, and E. A. Lissi, J. Chem. Soc., A (1970) 1001.

22. S. W. Benson, Thermochemical Kinetics, 2nd Ed. (John Wiley and Sons, Inc., New York, 1976).

23. E. Gorin, Cata Physicochem., URSS, 9, 691 (1938).

24. J. Troe, J. Chem. Phys., 66, 4745 (1977).

25. H. E. Van den Bergh, Chem. Phys. Letters, 43, 201 (1976).

26. P. J. Robinson and K. A. Holbrook, Unimolecular Reactions, Wiley-Interscience, New York (1972).

27. Tables of Molecular Vibrational Frequencies, NSRDS-NBS39, Government Printing Office, Washington, D.C., 1972.

28. JANAF Thermochemical Tables, NSRDS-NBS37, Government Printing Office, Washington, D.C. 1970.

29. W. A. Chupka, J. Chem. Phys., 48, 2337 (1968).

30. (a) W. A. Chupka and C. Livshitz, J. Chem. Phys., 48, 1109 (1968).
(b) K. E. McCulloh and V. H. Dibeler, J. Chem. Phys., 64, 4445 (1976).

31. R. C. Reid and T. K. Sherwood, The Properties of Gases and Liquids, McGraw-Hill, New York, 1968, p. 632.

32. J. W. Simons and R. Curry, Chem. Phys. Letters, 38, 171 (1976).

33. P. F. Zittel, G. B. Ellison, S. V. O'Neil, E. Herbst, W. C. Lineberger, and W. P. Reinhardt, J. Amer. Chem. Soc., 98, 3731 (1976).

34. E. V. Waage and B. S. Rabinovitch, Chem. Rev., 70, 377 (1970).

35. R. Shaw, private communication.

36. R. Stockbauer, J. Chem. Phys., 58, 3800 (1973).

37. A. J. Colussi and S. W. Benson, private communication.

38. S. E. Stein and B. S. Rabinovitch, J. Chem. Phys., 58, 2438 (1973).

39. J. Troe, Ber. Bunsenges. Phys. Chem., 77, 665 (1973); S. H. Luu and J. Troe, Ber. Bunsenges, Phys. Chem., 78, 766 (1974); H. Van den Bergh, N. Benoit-Guyot; and J. Troe, Int. J. Chem. Kinetics, 9,223 (1977).

40. K. Welge, private communication.

41. L. B. Harding and W. A. Goddard, J. Chem. Phys., 67, 1777 (1977).

42. D. C. Tardy and B. S. Rabinovitch, Chem. Rev., 77, 369 (1977).

43. S. E. Stein and B. S. Rabinovitch, J. Chem. Phys., 60, 908 (1974).

44. D. R. Stull, E. F. Westrum, and G. C. Sinke, The Chemical Thermodynamics of Organic Compounds, John Wiley and Sons, Inc., New York, 1969, p. 244.

45. The width of the square well is proportional to $(1 - \eta)^{1/4}$.

FIGURE CAPTIONS

1 High-Pressure Methyl Radical Recombination Rate Constants at Various Temperatures

□ Experiments of Reference 18; • Reference 13; ▲ Derived from the ethane dissociation experiments of Reference 19 and Reference 20, using the equilibrium constants in Table I; ---SAC Theory of Reference 14; —— modified Gorin model of this work. The ◆ points represent the inverted ethane dissociation data for a bond energy D_0^0 = 86.2 kcal/mole.

2 Pressure Dependence of Rate Constants

Theory using parameters of Tables I and II.

• Experiment: (A) Ratio of bimolecular methyl radical recombination rate constant to the high-pressure rate constant at 370°K vs. isopropylmethyl ketone pressure from Reference 21.

(B) Ethane decomposition unimolecular rate constant at 913°K vs. ethane pressure from Reference 19.

(C) Bimolecular methyl radical recombination rate constant at 1400°K vs. Ar pressure from Reference 13.

3 Ethane Decomposition Rate k(E) as a Function of Excess Molecular Energy $E-E_0$.

X is the 300°K transition state of the modified Gorin model with no correction for angular momentum; • is the J = 0 statistical adiabatic channel result of Reference 14.

4 Pressure Dependence of the Relative Yields for Reactions (1)(decomposition) and (2)(stabilization) for Chemical Activation. Points are the data of Reference 10. Ordinate scale is equivalent to D/S times an experimental intercept value. The theoretical curves are from our stepladder deactivation, modified Gorin transition state model, using the following parameters:

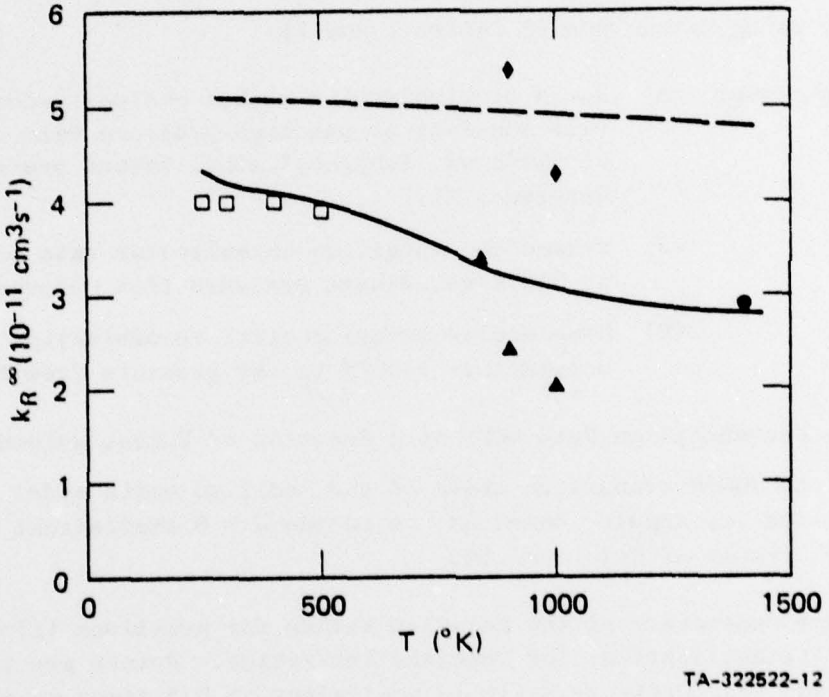
(A) E^* = 101.4 kcal/mole (low CH_2 singlet-triplet splitting), $\langle \Delta E \rangle$ = 2.3 kcal/mole;

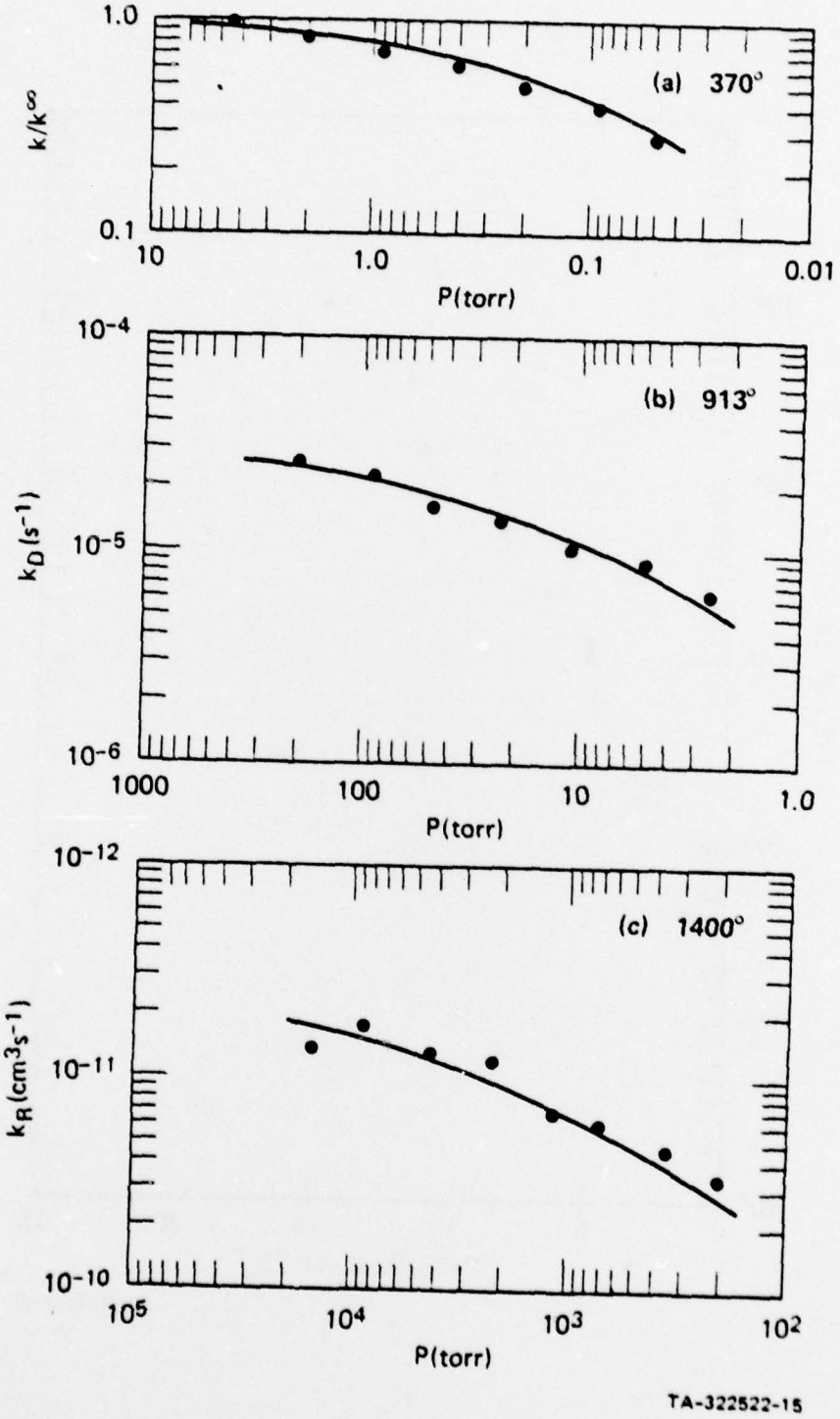
(B) E^* = 115.5 kcal/mole (high splitting), $\langle \Delta E \rangle$ = 2.3 kcal/mole;

(C) E^* = 105 kcal/mole, $\langle \Delta E \rangle$ = 2.3 kcal/mole;

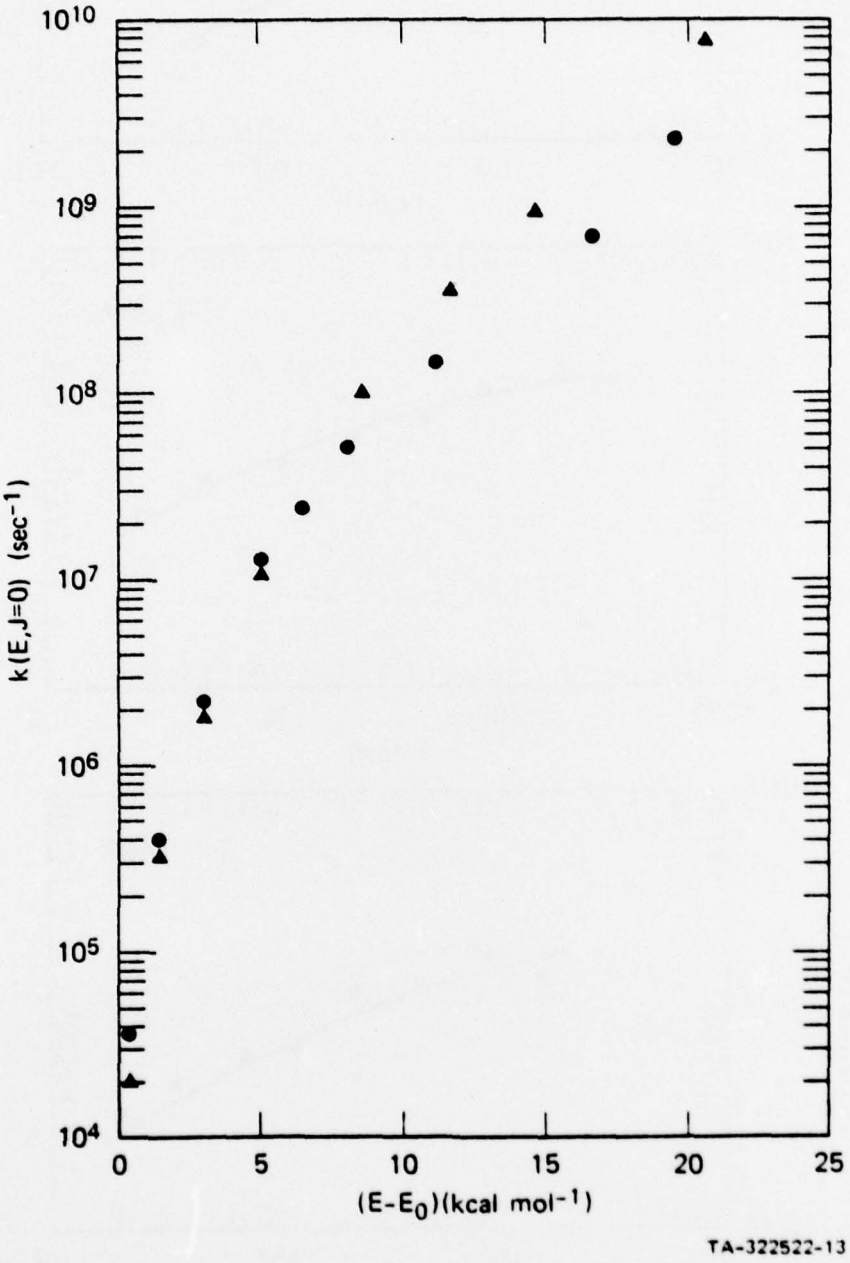
(D) E^* = 106 kcal/mole, $\langle \Delta E \rangle$ = 4.6 kcal/mole.

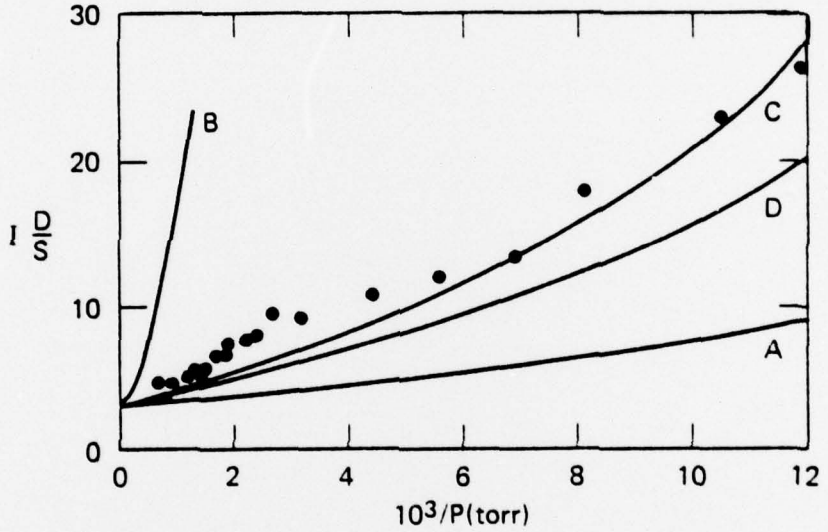
PRECEDING PAGE BLANK


6
5
4
3
2
1
0
0
500
1000
1500
T (°K)
$k_R^{\infty}(10^{-11}\ cm^3s^{-1})$
TA-322522-12


1.0
0.1
k/k∞
(a) 370°
10
1.0
0.1
0.01
P(torr)
10⁻⁴
10⁻⁵
10⁻⁶
k_D(s⁻¹)
(b) 913°
1000
100
10
1.0
P(torr)
10⁻¹²
10⁻¹¹
10⁻¹⁰
k_R(cm³s⁻¹)
(c) 1400°
10⁵
10⁴
10³
10²
P(torr)

TA-322522-15


10^{10}
10^{9}
10^{8}
10^{7}
10^{6}
10^{5}
10^{4}
k(E,J=0) (sec^{-1})
0
5
10
15
20
25
(E-E$_0$)(kcal mol^{-1})
TA-322522-13



TA-322522-14

UNCLASSIFIED

SECURITY CLASSIFICATION OF THIS PAGE (When Data Entered)

REPORT DOCUMENTATION PAGE		READ INSTRUCTIONS BEFORE COMPLETING FORM
1. REPORT NUMBER	2. GOVT ACCESSION NO.	3. RECIPIENT'S CATALOG NUMBER
4. TITLE (and Subtitle) THE ABSOLUTE MEASUREMENT OF RATE CONSTANTS FOR SOME KEY REACTIONS INVOLVING FREE RADICALS		5. TYPE OF REPORT & PERIOD COVERED FINAL: 1 January 1975 thru 28 February 1978 6. PERFORMING ORG. REPORT NUMBER
7. AUTHOR(s) David M. Golden, Michel J. Rossi, Gregory P. Smith, Karan E. Lewis, Sidney W. Benson, Miriam Lev-On, Stephen E. Stein, and Friedhelm Zabel		8. CONTRACT OR GRANT NUMBER(s) F44620-75-C-0067
9. PERFORMING ORGANIZATION NAME AND ADDRESS SRI International (formerly Stanford Research Institute) 333 Ravenswood Avenue Menlo Park, California 94025		10. PROGRAM ELEMENT, PROJECT, TASK AREA & WORK UNIT NUMBERS Gas-Phase Kinetics
11. CONTROLLING OFFICE NAME AND ADDRESS Director of Chemical Sciences--AFOSR Bolling AFB, DC 20332		12. REPORT DATE April 1978 13. NUMBER OF PAGES 174
14. MONITORING AGENCY NAME & ADDRESS(if different from Controlling Office)		15. SECURITY CLASS. (of this report) Unclassified 15a. DECLASSIFICATION/DOWNGRADING SCHEDULE

16. DISTRIBUTION STATEMENT (of this Report)

Approved for public release; distribution unlimited.

17. DISTRIBUTION STATEMENT (of the abstract entered in Block 20, if different from Report)

Approved for public release; distribution unlimited.

18. SUPPLEMENTARY NOTES

19. KEY WORDS (Continue on reverse side if necessary and identify by block number)

Gas-phase Kinetics
Allyl, Benzyl, and Acetonyl Radical, Heat of Formation of
Biallyl Pyrolysis; Allyl Combination
Reaction of OH with NO_2
Ion-Molecule Reactions, Theory of
Reaction of ClO with NO_2
Radical-Radical Reactions, Theory of
Multiphoton Processes
Very Low-Pressure Pyrolysis
Free Radical Recombination

20. ABSTRACT (Continue on reverse side if necessary and identify by block number)

Progress has been made in several areas of experimental and theoretical importance to the understanding of rate parameters in reactions important to combustion. We combined simple physical models with experiments devised to test these models with the objective of increasing our ability to estimate rate constants with an accuracy useful at a chemical level.

PRECEDING PAGE BLANK

DD FORM 1 JAN 73 1473 EDITION OF 1 NOV 65 IS OBSOLETE

UNCLASSIFIED

SECURITY CLASSIFICATION OF THIS PAGE (When Data Entered)

We have devised experimental approaches to the study of both the thermochemistry and thermal kinetics of free radical reations. In the course of this contract we have established thermochemical values for acetonyl radicals, allyl radicals, and benzyl radicals using our newly developed techniques of modulated molecular beam sampling, very low-pressure pyrolysis. The same techniques have also yielded rate constants for allyl combination and for allyl and benzyl with HI.

We have begun a study of infrared multiphoton chemistry from the prospective of gas kineticists interested in testing theories of reactivity using non-thermal energization techniques. In a complimentary study, we have studied the thermal reactions relevent to our study of the laser-induced decomposition of ethylvinyl-ether.

We have developed and applied models for understanding radical-radical interactions, as well as ion-molecule processes. Our use of a modified Gorin model has enabled us to understand the pressure and temperature dependence of these processes.